NRL Memorandum Report 1941

ARPA Coupling Program on Stress-Corrosion Cracking

(Seventh Quarterly Report)

Sponsored by

Advanced Research Projects Agency
ARPA Order No. 878

October 1968

NAVAL RESEARCH LABORATORY
Washington, D.C.

CONTENTS

This research was supported by the Advanced Research Projects Agency of the Department of Defense, NRL Problem No. M04-08, and was monitored by the Naval Research Laboratory under Contract Nos. Nonr 610(09), Nonr-760(31), N00014-66-C0365, and Nonr-991(15).

ABSTRACT

A progress report of the research investigations being carried out on the problem of stress-corrosion cracking of high strength materials under ARPA Order 878 is presented. Work at Carnegie-Mellon University, Lehigh University, Georgia Institute of Technology, The Boeing Company, and the Naval Research Laboratory concerning test techniques, materials characterization, physical metallurgy, surface studies, and corrosion fatigue is described. The report is divided into three main sections covering work on high strength titanium, steel, and aluminum.

STATUS

This is a progress report; work is continuing.

AUTHORIZATION

NRL Problems 61M04-08
63M01-08
ARPA Order 878 and
RR 007-08-44-5512

INTRODUCTION

In order to learn how to improve high strength structural alloys with respect to their resistance to stress-corrosion cracking (SCC) the Advanced Research Projects Agency of the Department of Defense has established under ARPA Order 878 a broadly based interdisciplinary attack upon the problem of SCC in high strength titanium alloys, steels, and aluminum alloys. The project is composed of sectors located in The Boeing Company, Carnegie-Mellon University, Lehigh University, Georgia Institute of Technology, and the Naval Research Laboratory. In addition to having its own research activity, NRL has the responsibility for keeping the entire technical program attuned to DoD needs.

The complex phenomenon of SCC can be divided into four elements as follows: (1) the stress field, (2) the metallic phase, (3) the corrodent phase, and (4) the interface (with or without corrosion-product films) between metal and corrodent. Because of the obvious complexities of the phenomenon (and perhaps additional complexities not yet obvious), an interdisciplinary approach is essential. Scientists prominent in the fields of surface physics and surface chemistry have been enlisted in the project in order to bring the tools of these new sub-disciplines to complement those of traditional electro-chemistry/thermodynamics in order to design new advances in the practical problem.

The reporting system has been modified as follows: Detailed technical progress from project units will be published twice each year. The technical progress report will be organized into three main sections: Titanium, Steel, and Aluminum. Further division within each section will generally be made first according to material classification, such as commercial alloys or simplified research alloys, and second according to research discipline, such as physical metallurgy or surface physics. Submissions for these progress reports will be forwarded to section editors who, in turn, will submit the edited sections to NRL for publication as an NRL report. These sections must be kept brief to be

manageable, and the project personnel are enjoined to publish the research details in the standard technical journals as a means of most effectively injecting the output of the program into the technological mainstream. The remaining two quarterly reports will contain (1) abstracts of newly published reports and manuscripts of project sponsored work, (2) a chronological listing of the titles of all ARPA generated reports, and (3) selected abstracts of reports and journal articles from outside the ARPA program in the area of stress-corrosion cracking. Each quarterly will contain a diary of events section.

A. TITANIUM

1. Introduction

This section describes the research activities in the titanium alloy system. Two main categories have been identified as "commercial alloys" and "simplified research alloys," respectively. Because of the rapidly developing titanium technology, it is not always easy to discriminate between "commercial" and developmental alloys, and no rigid distinction is made here. A major portion of the commercial alloys prepared and procured by contractual funds is processed through a macroscopic "characterization" phase to establish and catalog the apparent threshold stress intensity for stress-corrosion crack propagation (or arrest) and to determine test-method optimization for titanium alloys.

Fundamental studies in physical metallurgy and crystal mechanics are being conducted on commercial and experimental alloys to relate the effects of solid-state transformations, dislocation substructure, texture, etc., to susceptibility to stress-corrosion cracking and to elucidate the stress-corrosion mechanism. Commercial alpha, alpha-beta, and beta titanium alloys are being investigated. Complementary surface studies are presently restricted to simplified research alloys of titanium.

Experimental "project alloys" have either been already procured or are on order for the titanium alloy system. They have been specifically chosen to represent the basic alloy chemistries of commercial alloys and to provide alloys of sufficient strength and adequate microstructural simplicity to lend themselves to a thorough study by all the disciplines in the program. It should be recognized, however, that simplified research alloys are not produced in large quantities and, therefore, cannot be extensively tested for characterization in numerous environments. Data from related studies on commercial alloys should aid in choosing appropriate environments.

2. Commercial Alloys

(i) Test Techniques

It is the opinion of users of high-strength alloys that, for the foreseeable future, we may not be able to completely eliminate susceptibility to stress-corrosion cracking (SCC) without unacceptably degrading other important properties such as strength, toughness, and fabricability. Therefore, we need to learn how to safely use materials that are moderately susceptible. The objective of this phase of the study is to develop laboratory methods of generating stress-corrosion data that can be used by the designer to predict the behavior of large complicated engineering structures. The absence of such methods and the inability to collate data generated at different laboratories by existing techniques constitute a serious gap between the required and existing knowledge of the field of stress-corrosion testing.

Before providing the guidelines for stress-corrosion testing, many experiments must be conducted to justify the technological, practical, and fiscal basis of a recommended procedure. The following has been accomplished:

- Experiments with a wedge-force-loaded specimen at Boeing (1) have demonstrated the inability of increasing net-section stress to rationalize decreasing stress-corrosion crack

growth in a titanium alloy. This experiment indicated that the stress-intensity factor controlled the rate of subcritical stress-corrosion crack growth and also that a true lower limit of stress-intensity factor (K_{Iscc}) existed for crack initiation in corrosive environments.

- The SCC characteristics of Ti-8Al-1Mo-1V sheet in methyl alcohol were also determined at Boeing using a wedge-force-loading technique. A center-notched, longitudinal panel 0.160 in. by 9 in. by 24 in. was prepared from Ti-8Al-1Mo-1V sheet and fatigue precracked using wedge-force cyclical loading. From available information, it was estimated that K_{Iscc} in methyl alcohol for this alloy is about 21 ksi$\sqrt{in}$. A test load was selected that would cause the crack to propagate at a stress intensity K of 31 ksi$\sqrt{in}$. Because of the decreasing K-versus-crack-length relationship peculiar to wedge force loading of this particular type of panel, it was anticipated that crack growth would be arrested at a length of approximately 2 in. (K = 22 ksi$\sqrt{in}$.) However, the anticipated arrest did not occur, and a K value at the crack tip decreased to 17 ksi$\sqrt{in}$. before the crack became unstable and the panel failed. Charpy specimens were prepared from the broken halves of the panel, and a K_{Iscc} value of 22 ksi$\sqrt{in}$. was obtained from subsequent tests. A second wedge-force panel was fabricated and tested, whereby successive arrests were obtained at K values of 14.0, 15.7, 17.1, 17.9, and 19.8 ksi$\sqrt{in}$. During these tests, it was observed that the crack sometimes extended further on one side than on the other. This nonsymmetry probably introduced errors into the analysis that could account for the disparity in K_{Iscc} values indicated by the wedge-force tests with those of the Charpy tests.

- Experiments at NRL (2) confirmed that the behavior of materials in large structures in service can be predicted from observations of small specimens tested in the laboratory. In these tests, K_{Iscc} values obtained on small cantilever-beam specimens were similar to those obtained on large surface-cracked specimens of a titanium alloy. This comparison involved two different methods of stressing, two different crack geometries, and a major difference in specimen size.

- A successful comparison of data generated at two different laboratories has also been achieved (3). Single-edge cracked specimens of Ti-8Al-1Mo-1V mill-annealed plate were evaluated by cantilever bending at NRL and by four-point loading at Boeing. In addition, the experiment was further varied at Boeing by adding on aqueous environment before and after loading. The K_{Iscc} values obtained by NRL and Boeing were similar. The electrolyte/loading sequence was repeated for Ti-4Al-3Mo-1V, which is tougher and less susceptible than mill-annealed Ti-8Al-1Mo-1V. Again, similar K_{Iscc} values were obtained. A further series of tests on commercially pure titanium, which is very tough but susceptible to SCC, indicated lower values for K_{Iscc} when the specimens were loaded in the presence of the electrolyte. Recently, a similar trend has been noticed in alpha and alpha-beta commercial titanium alloys (see (ii) Characterization). Thus, it has been recommended that the specimen always be loaded in the presence of an aqueous environment.

- The effect of thickness on the SCC characteristics of mill-annealed Ti-6Al-4V alloy has been investigated at Boeing to establish: (1) the minimum thickness required to obtain a plane-strain threshold stress intensity K_{Iscc} and (2) the specific relationship between K_{Iscc} and thickness. Single-edge cracked specimens (1.5 in. by 7.5 in. by thickness) were prepared by machining 1-inch thick plate to size. The thicknesses investigated are 1.0, 0.75, 0.50, 0.25, 0.125, and 0.050 inch. Specimens 0.125 in. and thicker were bend tested, whereas

specimens 0.125 in. and thinner were tension tested. Tests of 0.125-in.-thick specimens provided a basis for comparison of bend and tension loading modes. Although it was not planned for in the program, enough material was available to obtain K_{Ic} values in the bend tests (thicknesses from 0.125 to 1.0 in.). K_{Ic} values of 60 ksi $\sqrt{\text{in.}}$ were obtained for the 0.25- and 0.125-in.-thick specimens. These results indicate a value between 1.5 and 3.0 for C in the expression for the plane-strain K_{Ic} validity requirement,

$$\text{thickness} \geqslant C \left[\frac{K_{Ic}}{Y.S.}\right]^2$$

No transition was observed in K_{Iscc} values; K_{Iscc} values of about 20 ksi $\sqrt{\text{in.}}$ were obtained for all thicknesses. However, good agreement was obtained when the tension test data were compared with the bend test data. It was concluded that the transition from plane-strain to plane-stress conditions existed at some thickness less than 0.050 in. The data are presented in Table A-1. It is planned to evaluate 0.025-in.-thick material and to generate similar data for a material with higher K_{Ic} and K_{Iscc} properties. This information will be used to aid in establishing validity requirements for a specification on stress-corrosion testing of titanium alloys.

- Boeing has also completed an investigation of the influence of fatigue precracking stress level on the K_{Iscc} of mill-annealed Ti-8Al-1Mo-1V and Ti-6Al-4V. Notched bend specimens of 0.5-in. thickness were fabricated from each material and fatigue cracked at stresses corresponding to K levels of 20, 30, 40, 50, 60, 70, and 80% of K_{Ic}. Five specimens from each precracking stress level were used. No effect on K_{Iscc} was observed in either material, although some scatter was observed in the data (Table A-2). Future tests are planned to determine whether the precracking stress level affects alloys with higher K_{Iscc} (50 to 70 ksi $\sqrt{\text{in.}}$) properties. As in the thickness evaluation described above, these tests will provide part of the information needed to establish the validity requirements for a proposed test specification.

- Experiments at NRL and Boeing have verified that, although stress-corrosion cracks can propagate at a stress intensity lower than K_{Ic}, this does not mean that fracture toughness is reduced by the corrosive environment. Rather, as the crack grows, the instantaneous value of stress-intensity factor increases (under constant load or moment) until it attains the critical value for fast fracture.

- Terminal fracture of titanium alloys containing stress-corrosion cracks has been investigated at Boeing (4). The length of stress-corrosion cracks was measured in 55 precracked specimens of Ti-6Al-4V and Ti-4Al-3Mo-1V that had previously been sustain loaded in 3.5% sodium chloride solution. The fracture toughness index $K_{I\delta}$ of the residual ligament was calculated for each specimen. ($K_{I\delta}$ is fracture toughness calculated from the length of an environmental crack after failure in a conventional sustained-load SCC test on a fatigue-precracked notched bend specimen.) The data compared well with the mean K_{Ic} values observed from tests in an air environment. The ratio $K_{I\delta}$:K_{Ic} was within 0.85 to 1.14, except for approximately 10% of the specimens that had higher ratios. The rather wide distribution of values was attributed to the inherent scatter in K_{Ic} and to the irregular shape of many stress-corrosion crack fronts, which prevented measurement of an effective critical crack length.

Table A-1

Effect of Thickness of Mill Annealed Ti-6Al-4V* on K_{Iscc} and K_{Ic}

	Thickness (in.)						
	0.98	0.70	0.50	0.25	0.125	0.125**	0.050**
K_{Ic} (ksi $\sqrt{in.}$)	57.9	60.0	61.3	90.5	93.2		
K_{Iscc} (ksi $\sqrt{in.}$)	21	19	21	17	22	22	19

*Mechanical properties
UTS = 155.6 ksi
Y.S. = 147.9 ksi
Elong. = 13%
R.A. = 34.5%

**Single-edge, notched, tension specimens; the remainder were precracked bend specimens.

Table A-2

Effect of Precracking Stress Level on the K_{Iscc} of Mill-Annealed Ti-8Al-1Mo-1V* and Ti-6Al-4V**

	%K_{Ic}						
	20	30	40	50	60	70	80
Ti-8Al-1Mo-1V (K_{Iscc} in ksi $\sqrt{in.}$)	30	28	29	25	29	28	23
Ti-6Al-4V (K_{Iscc} in ksi $\sqrt{in.}$)	24	21	26	26	28	24	24

*Ti-8Al-1Mo-1V:
UTS = 151.7 ksi
Y.S. = 146.9 ksi
Elong. = 15%
R.A. = 38%
K_{Ic} = 37.3 ksi $\sqrt{in.}$

**Ti-6Al-4V:
UTS = 153.0 ksi
Y.S. = 142.6 ksi
Elong. = 15%
R.A. = 36%
K_{Ic} = 53.6 ksi $\sqrt{in.}$

- The influence of crack length on the $K_{I\delta}$:K_{Ic} ratio was also examined. This revealed a trend for the $K_{I\delta}$:K_{Ic} ratio to exceed 1.0 when the crack-length-to-specimen-width ratio is greater than 0.4. This is contrary to the results reported by Brown and Srawley (5) for specimens containing fatigue cracks of various lengths. In view of these conflicting results, this trend should be treated with caution and requires further investigation.

- A technique for determining the rate of crack propagation in corrosive environments has been developed at Boeing (6). Grids were prepared either by vacuum deposition or by selectively etching metal from a foil. The grid is placed on the surface of the specimen across the anticipated crack path and is electrically insulated by oxide films from both metal and corrodent. The electrical resistance of the grid is monitored to indicate severing of the individual elements.

Future participation in the development of SCC testing procedures will involve strong interaction with ASTM (Committee G1 on Corrosion of Metals) and the Structures and Materials Panel of the Advisory Group for Aerospace Research and Development (AGARD) of NATO. Membership and participation in these key committees is the best way of persuading industry to adopt SCC test procedures. In addition, it is the most effective way of disseminating ideas throughout the technological community and of providing the benefits of critical discussion by qualified people in industry, government agencies, and universities.

(ii) Characterization

Salt water SCC resistance has been determined by NRL for a large number of titanium alloys representative of commercial production (7). These characteristics were compiled as part of an NRL program to determine the underlying principles of SCC in metals and to establish procedures for improving the SCC resistance of these metals.

The SCC resistance was determined using a precracked, cantilevered, bend specimen with analysis by fracture mechanics techniques. Test results presented for the spectrum of alloys and weldments studied indicated that no correlation with mechanical properties existed, which makes precise prediction of SCC properties of particular alloys difficult, if not impossible.

The titanium characterization program at Boeing has examined the effect of composition, thermal treatment, and thermomechanical treatment on the stress-corrosion behavior of titanium alloys at room temperature in an attempt to relate this behavior to microstructure. Characterization data for alpha alloys Ti-50A (O_2 = 1200 ppm), Ti-70 (O_2 = 3800 ppm), Ti-5Al-2.5Sn, and Ti-5Al-5Sn-5Zr and alpha-beta alloys Ti-2.5Al-11Sn-4Mo-0.2Si (IMI 680), Ti-4Al-3Mo-1V, Ti-4Al-4Mo-2Sn-0.5Si (Hylite 50), Ti-5Al-3Mo-1V-2Sn, Ti-6Al-4V, Ti-6Al-2Mo, Ti-6Al-6V-2Sn, Ti-6Al-5Zr-1W-0.2Si (IMI 684), Ti-7Al-2.5Mo, Ti-7Al-4Mo, and Ti-8Al-1Mo-1V in various heat treatment conditions are given in Tables A-3 and A-4. Values of K_{Iscc} were obtained on specimens that were four-point loaded in bending in 3.5% sodium chloride solution. These data are discussed in (iii) Physical Metallurgy.

At NRL, the effects of hydrogen content on subcritical crack growth for two Ti-8Al-1Mo-1V heats in air, hexane, salt water, and methanol were determined by cantilever-beam testing techniques. The hydrogen content was controlled by vacuum annealing.

Table A-3

Strength, Toughness, and Stress-Corrosion Properties
of Alpha Titanium Alloys

Alloy	Condition	UTS (ksi)	0.2% Y.S. (ksi)	K_{Ic} (ksi $\sqrt{in.}$)	K_{Iscc}* (ksi $\sqrt{in.}$)
Ti-50A	1300°F/½ hr/AC	65.8	42.5	60	60
Ti-70	1300°F/½ hr/AC	102.2	84.3	114	54 (86)
	1400°F/½ hr/AC	101.3	83.6	121	38 (84)
	1500°F/½ hr/AC	102.0	83.2	123	33 (92)
	1500°F/20 hr/AC	99.7	79.6	111	33 (33)
	1500°F/½ hr/WQ	106.5	84.6	126	34 (34)
	1500°F/½ hr/WQ + 1050°F/½ hr/AC	103.2	82.5	113	39 (75)
	1500°F/½ hr/WQ + 1050°F/20 hr/AC	101.1	82.2	113	33 (89)
	1700°F/½ hr/WQ	100.9	76.5	105	70 (90)
	1700°F/½ hr/WQ + 1050°F/½ hr/AC	101.8	77.2	96	48 (82)
	30% CR	129.1	115.2	82	33 (46)
	30% CR + 925°F/½ hr/AC	111.4	98.6	116	50
	30% CR + 1200°F/½ hr/AC	103.7	88.0	92	55
	30% CR + 1500°F/½ hr/AC	102.4	85.5	91	38
	60% CR	136.5	121.4	45	40

Table A-3 (Continued)

Alloy	Condition	UTS (ksi)	0.2% Y.S. (ksi)	K_{Ic} (ksi $\sqrt{in.}$)	K_{Iscc}* (ksi $\sqrt{in.}$)
	30% HR at 1100°F	108.8	94.4	115	34
	30% HR at 1500°F	107.1	87.6	104	35
	30% HR at 1700°F	111.8	86.9	93	54
Ti 5Al-2.5Sn	1400°F/2 hr/AC	138.2	129.2	72	26
	1650°F/1 hr/AC	134.2	126.5	88	30
	1650°F/10 hr/AC	132.1	125.1	90	32
	1650°F/100 hr/AC (in Argon)	130.3	118.7	92	27
	As rcvd + 1100°F/8 hr/FC to 932°F/120 hr	139.8	130.5	46	21
	1650°F/1 hr/WQ	135.4	124.2	103	27
	1850°F/1 hr/WQ	140.1	127.8	116	31
	2000°F/½ hr/WQ	140.0	126.6	119	37
	1850°F/1 hr/WQ + 1250°F/8 hr/AC	139.4	129.3	83	23
	30% CR + 1100°F/8 hr/FC to 932°F/120 hr/AC	158.0	145.4	43	19
	30% CR + 1400°F/1 hr/AC	140.9	129.1	86	36
	30% CR + 1650°F/1 hr/AC	136.6	124.5	115	24
	30% CR	166.2	151.2	60	38
Ti-5Al-5Sn-5Zr	1650°F/½ hr/AC	128.2	116.5	83	50
	1650°F/½ hr/WQ	126.9	109.7	101	67

Table A-3 (Concluded)

Alloy	Condition	UTS (ksi)	0.2% Y.S. (ksi)	K_{Ic} (ksi $\sqrt{in.}$)	K_{Iscc}* (ksi $\sqrt{in.}$)
	1750°F/½ hr/WQ	128.5	109.9	131	81
	1850°F/½ hr/WQ	136.6	114.1	102	55
	1650°F/½ hr/AC + 1100°F/8 hr/AC	128.0	119.2	83	34
	1750°F/½ hr/WQ + 1250°F/8 hr/AC	127.9	116.7	78	51
	1650°F/½ hr/AC + 1100°F/8 hr/FC to 932°F/120 hr	130.0	120.5	54	28
	30% CR + 1400°F/1 hr/AC	131.0	119.9	111	51
	30% CR + 1650°F/1 hr/AC	125.7	111.9	89	37
	30% CR	152.6	134.8	74	47
	30% HR @ 1650°F	138.9	127.2	112	41
	30% CR + 1100°F/8 hr/AC	141.4	131.6	92	41

* Threshold for loading in 3.5% sodium chloride solution, except values in parentheses, which are for loading in air followed by addition of salt solution.

AC = air cooled; WQ = water quenched; CR = cold rolled; HR = hot rolled

Table A-4

Strength, Toughness, and Stress-Corrosion Resistance
of Alpha-Beta Titanium Alloys

Alloy	Condition	UTS (ksi)	0.2% Y.S. (ksi)	K_{Ic} (ksi $\sqrt{in.}$)	K_{Iscc}* (ksi $\sqrt{in.}$)
Ti-2.25Al-11Sn-4Mo-0.2Si (IMI 680)	2100° F Forge + 1500° F/½ hr/WQ + 930° F/24 hr/AC	190.5	166.1	44	28
Ti-4Al-3Mo-1V (8)	1250° F/8 hr/AC	127.0	125.7	116	104
	1875° F/1 hr/AC + 1725° F/1 hr/WQ + 1150° F/8 hr/AC	154.8	137.2	96	77
Ti 4Al-4Mo-2Sn-0.5Si (Hylite 50)	1650° F/½ hr/WQ	169.4	136.0	56	44
	1800° F/½ hr/WQ	212.0	182.3	49	43
	1650° F/½ hr/AC + 932° F/24 hr/AC	168.5	157.5	55	27
	1650° F/½ hr/AC + 1100° F/24 hr/AC	162.7	153.7	44	23
	1650° F/½ hr/AC + 1300° F/24 hr/AC	150.7	145.6	42	22
	1500° F/½ hr/WQ + 1100° F/24 hr/AC	157.2	150.4	45	19
	1650° F/½ hr/WQ + 1100° F/24 hr/AC	175.6	164.7	31	19
	1800° F/½ hr/AC + 1650° F/½ hr/WQ + 1100° F/24 hr/AC	172.6	156.8	62	31
	1800° F/½ hr/AC + 1650° F/½ hr/AC + 932° F/24 hr/AC	167.2	145.7	97	50
	1650° F/½ hr/AC + 20% CR + 932° F/24 hr/AC	190.7	178.5	52	24

Table A-4 (Continued)

Alloy	Condition	UTS (ksi)	0.2% Y.S. (ksi)	K_{Ic} (ksi $\sqrt{in.}$)	K_{Iscc}* (ksi $\sqrt{in.}$)
	1650°F/½ hr/AC + 20% HR @ 932°F + 932°F/24 hr/AC	195.5	179.8	47	20
	1650°F/½ hr/AC + 800°F/24 hr/AC + 932°F/16 hr/AC	176.5	160.5	75	26
	20% CR + 1650°F/ 20 min/AC + 932°F/ 24 hr/AC	175.9	175.2	72	36
Ti-5Al-3Mo-1V-2Sn (9)	1875°F/½ hr/AC + 1725°F/½ hr/WQ + 1100°F/8 hr/AC	167.3	147.0	70	52
	1650°F/30 min/AC + 1300°F/8 hr/AC	130.6	126.3	80	80
Ti-6Al-2Mo (9)	1975°F/½ hr/AC + 1825°F/½ hr/WQ + 1200°F/4 hr/AC	153.5	138.6	94	63
	1700°F/½ hr/AC + 1300°F/8 hr/AC	127.8	118.6	92	55
Ti-6Al-4V (8)	1900°F/½ hr/AC + 1725°F/½ hr/WQ + 1250°F/8 hr/AC	155.3	142.2	87	58
	1300°F/2 hr/AC	152.8	144.1	61	34
Ti-6Al-6V-2Sn (10)	1800°F/½ hr/AC + 1625°F/1 hr/WQ + 1200°F/4 hr/AC	166.1	152.9	72	45
	1300°F/2 hr/AC	157.6	150.7	59	37
Ti-6Al-5Zr-1W-0.2Si (11) (IMI 684)	1913°F/45 min/WQ + 932°F/24 hr/AC	154.0	135.0 (0.1% proof stress)	75	34
Ti-7Al-2.5Mo	50% HR (1750°F)	147.5	135.5	65	45
	1675°F/½ hr/WQ	137.8	106.0	95	80
	1800°F/½ hr/WQ	161.1	133.1	93	73
	1650°F/½ hr/AC	139.6	127.1	96	65

Table A-4 (Concluded)

Alloy	Condition	UTS (ksi)	0.2% Y.S. (ksi)	K_{Ic} (ksi$\sqrt{in.}$)	K_{Iscc}* (ksi$\sqrt{in.}$)
	1650°F/½ hr/FC to 932°F/120 hr/AC	135.9	122.6	74	44
	1800°F/½ hr/WQ + 1100°F/8 hr/AC	166.6	151.9	52	37
	1500°F/4 hr/WQ + 700°F/120 hr/AC	141.6	117.2	59	40
	1900°F/½ hr/AC + 1800°F/½ hr/WQ + 1100°F/8 hr/AC	158.4	134.8	72	43
	30% CR + 1400°F/½ hr/FC	156.1	150.9	43	37
	30% CR + 1650°F/½ hr/FC	139.9	133.4	71	37
	30% CR	160.9	143.1	83.4	61
Ti-7Al-4Mo (10)	1925°F/½ hr/AC + 1650°F/½ hr/WQ + 1250°F/4 hr/AC	157.6	143.4	68	44
	1750°F/½ hr/AC + 1400°F/4 hr/FC	154.0	145.1	32	23
Ti-8Al-1Mo-1V	1450°F/8 hr/FC	148.4	140.9	46	18

* Threshold for loading in 3.5% sodium chloride solution, except values in parentheses, which are for loading in air followed by addition of salt solution.

AC = air cooled; FC = furnace cooled; WQ = water quenched; CR = cold rolled; HR = hot rolled

The results for one of the heats (R-7) are shown in Fig. A-1. The cantilever-beam specimens, 0.27 in. thick and side grooved to a depth of 0.010 in. on each side, produced fractures of WR orientation. With a reduction in hydrogen content, the value of K_{1H} required for slow crack growth in dry air increased and approached the values of K_{1x} and $K_{1\delta}$, the parameters that describe the inherent fracture strength of the alloy. The values of K_{1scc} in salt water, methanol, and hexane were not increased by a reduction of hydrogen content.

The results were somewhat different for the second heat (R-26), as shown in Fig. A-2. The specimens of this alloy were from a sheet cross-rolled to a 0.125-in. thickness and were not side grooved. The specimens containing 50 ppm hydrogen were not in the mill-annealed condition but had been heated to 1150°F for half an hour. This alloy appears to be nearly immune to stress-corrosion cracking in hexane, whatever the hydrogen content. It is tempting to attribute this immunity to the thinness of the alloy. However, it appears that the R-26 alloy had a more favorable distribution of beta phase and a finer grain size due to tests at temperatures below the beta transus.

Stress-corrosion cracking characteristics of a Ti-7Al-2Cb-1Ta alloy (Y.S. = 103 ksi) were measured in the TR orientation (in the rolling plane and in the rolling direction) using self-stressed cantilever-beam specimens. Preliminary indications show that K_{1scc} for this orientation is significantly higher than in the WR or RW orientation. In these measurements, K_{1scc} in 3.5% sodium chloride solution was 47 ksi $\sqrt{\text{in.}}$, whereas it was 31 ksi $\sqrt{\text{in.}}$ in the other orientations.

The electrochemical potential and the pH of the solution at the crack tip were measured using the same techniques described for aluminum alloys in Sec. C. The most negative potential recorded during the experiments was -0.8 volts using a silver/silver chloride reference electrode. This value was measured while the specimen was being loaded. It represents a decrease in potential of over 0.5 volt from the uncracked specimen measurement. Areas in the crack tip region of the same specimen contained solutions with a pH as low as 1.8. The measurement was made using a bromocresol green indicator, which distinctly changed from blue to yellow.

(iii) Physical Metallurgy

Boeing has now completed an initial study of four alpha alloys: a low interstitial grade of commercially pure titanium (Ti-50A, 0_2 = 1200 ppm), a high interstitial grade of commercially pure titanium (Ti-70, 0_2 = 3800 ppm), Ti-5Al-2.5Sn, and Ti-5Al-5Sn-5Zr.

In the as-received (mill-annealed) heat-treat condition, only the Ti-50A alloy is immune to SCC (Table A-3). Immunity is evidenced by a lack of crack growth in salt solution and by the relationship of K_{1c} to K_{1scc}. The degree of susceptibility of the other alpha alloys is dependent upon several factors, including: (1) grain orientation; (2) composition, order, and dislocation structure; (3) grain size and morphology; and (4) transformation behavior of the beta phase, if present.

Oxygen is responsible for much of the strength difference between Ti-50A (0.2% yield = 42.5 ksi) and Ti-70 (0.2% yield = 84.3 ksi) in the mill-annealed condition. A portion of the strength increase, approximately 10 ksi, is due to the high percent of iron in Ti-70 (0.38% in Ti-70 compared with 0.10% in Ti-50A), which stabilized 3 volume percent of beta.

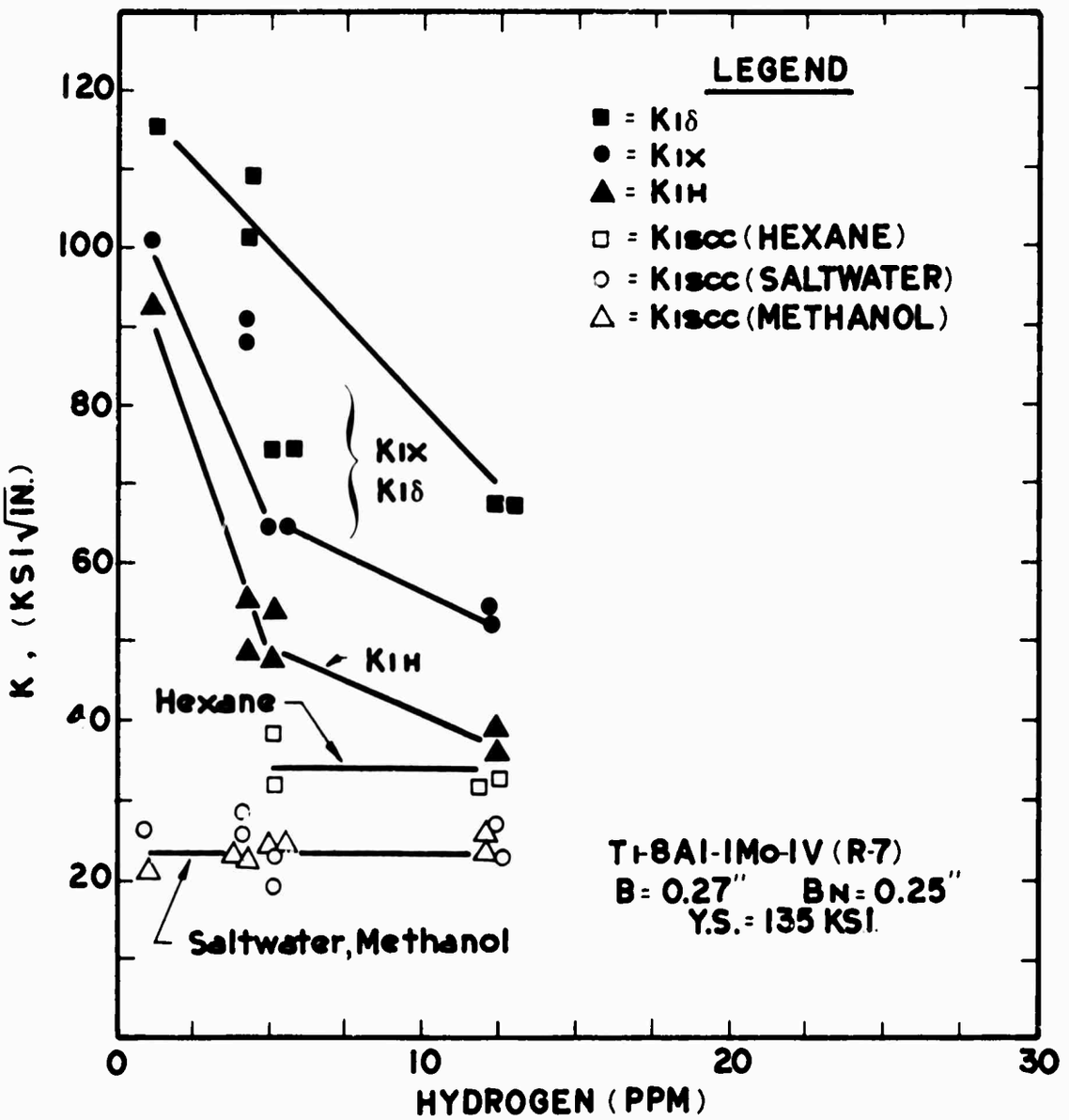

Fig. A-1 - Effect of hydrogen content of Ti-8Al-1Mo-1V (R-7) on fracture toughness and resistance to slow crack growth in air, hexane, salt water, and methanol

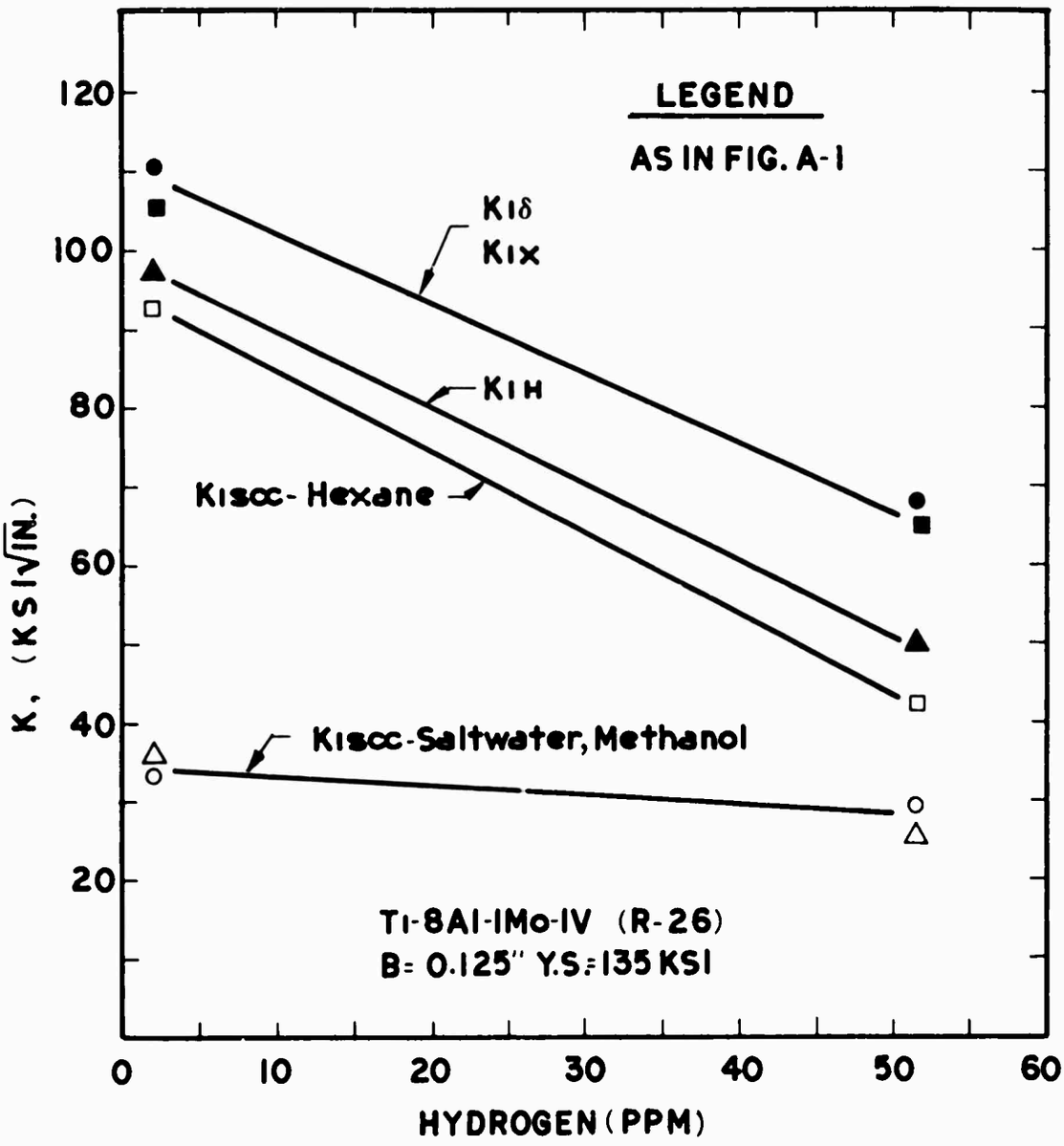

Fig. A-2 - Effect of hydrogen content of Ti-8Al-1Mo-1V (R-26) on fracture toughness and resistance to slow crack growth in air, hexane, salt water, and methanol

In addition to strengthening, the increased oxygen in Ti-70 modified the deformation behavior of the alpha phase so that slip is restricted to a single set of planes, predominately $\{10\bar{1}0\}$. The resulting dislocation structure after 3% to 4% deformation by rolling is shown in the electron micrograph in Fig. A-3(a). Slip on the $\{10\bar{1}0\}$, $\{10\bar{1}1\}$, and (0001) planes in Ti-50A produced dislocation tangles after the same amount of deformation (Fig. A-3(b)). Operation of these slip systems in Ti-50A is consistent with the results of Churchman (12) who found the critical resolved shear stress for slip on each system to be nearly equal for oxygen levels near 1000 ppm. For a lower oxygen level (100 ppm), slip is preferred on the $\{10\bar{1}0\}$ $<11\bar{2}0>$ system (12). The results of this investigation suggest that prismatic slip is also preferred at high oxygen levels ($\sim$ 3800 ppm).

Addition of aluminum, tin, and zirconium to an immune, commercially pure base (Ti-50A type) also promoted stress corrosion susceptibility by restricting slip. Thin-foil studies showed that slip in Ti-5Al-2.5Sn and Ti-5Al-5Sn-5Zr is predominantly coplanar. Figure A-4(a) illustrates coplanar $\{10\bar{1}0\}$ slip in disordered Ti-5Al-5Sn-5Zr that has been deformed 4.0% in tension. Formation of ordered domains of $Ti_3(Al, Sn)$ in this alloy appeared to reduce the number of operative $\{10\bar{1}0\}$ slip planes and the slip-band thickness. See Fig. A-4(b). Decreased slip-band thickness is believed to reduce the probability of dislocation-source activation across a grain boundary and to intensify the dislocation pileup stress (13, 14). As expected from the dislocation structures, susceptibility was least pronounced for the disordered solid solution and increased with amount of order in the alpha phase.

Transformation of an unstable beta phase in Ti-70 and Ti-5Al-2.5Sn strongly influenced the mechanical properties of these alloys. In many cases, beta transformations were more pronounced than structural changes in the alpha phase that were being related to SCC. A trace of iron (0.39%) is responsible for the presence of the beta phase. X-ray analysis detected approximately 3 and 1.5 volume percent beta in the mill-annealed condition of Ti-70 and Ti-5Al-2.5Sn, respectively.

Thin-foil studies showed that unstable beta precipitated omega and/or alpha phases, depending on the conditions of heat treatment. Extremely fine omega ($\sim$ 25 Å diameter) was formed in Ti-70 during air cooling from 1200° and 1300°F. Because the particles were too small for direct imaging with the electron microscope, they were detected from diffuse spots in the electron diffraction patterns. Diffuse omega was also detected in the beta phase in most heat-treat conditions of Ti-5Al-2.5Sn. Its presence in alpha-quenched Ti-5Al-2.5Sn reduced K_{Iscc} below the level for the beta-quenched condition, even though the effective grain size was larger for the beta-quenched condition. Diffused omega phase is believed to promote stress-corrosion susceptibility by nucleating cracks in the beta phase. Pronounced tensile embrittlement has also been attributed to a fine dispersion of omega in the beta phase (15).

A higher solution temperature reduced the iron content of beta and allowed more extensive transformation during cooling. In Ti-70, approximately 50 volume percent omega phase (100 Å diameter) was formed in the beta phase during cooling from 1500°F. This additional omega phase reduced stress-corrosion resistance as shown in Fig. A-5. Solution treatment at 1700°F transformed the beta phase to martensite and improved K_{Iscc} to the highest level measured for this alloy.

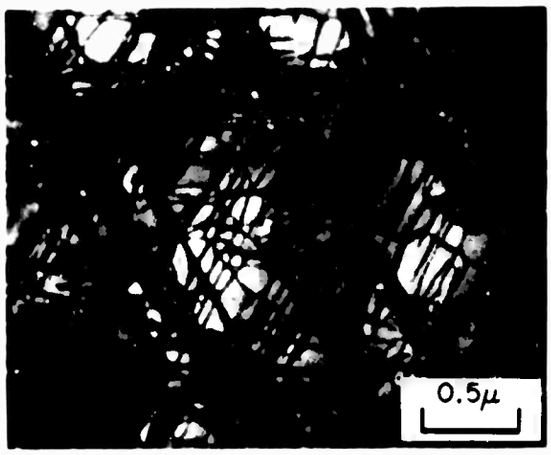

(a)

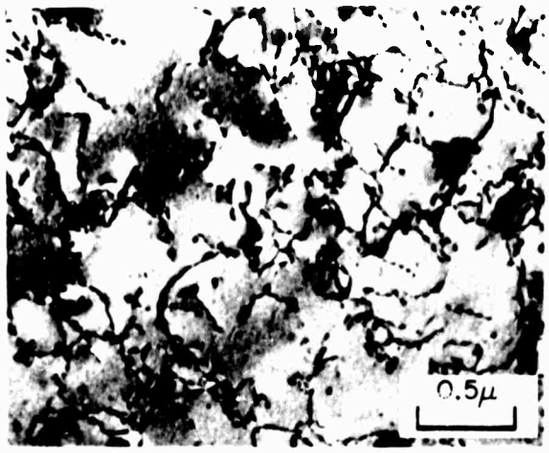

(b)

Fig. A3 - Dislocation arrangements in (a) Ti-70 (0.38 wt % oxygen) and (b) Ti-50A (0.12 wt % oxygen) after 3% to 4% deformation by rolling ($[0001]_\alpha$ zone axes).

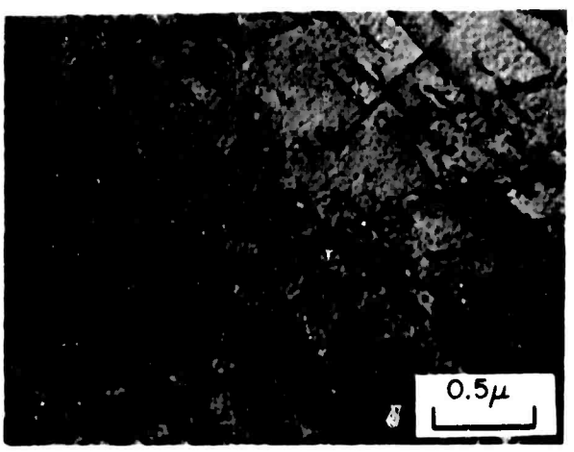

(a)

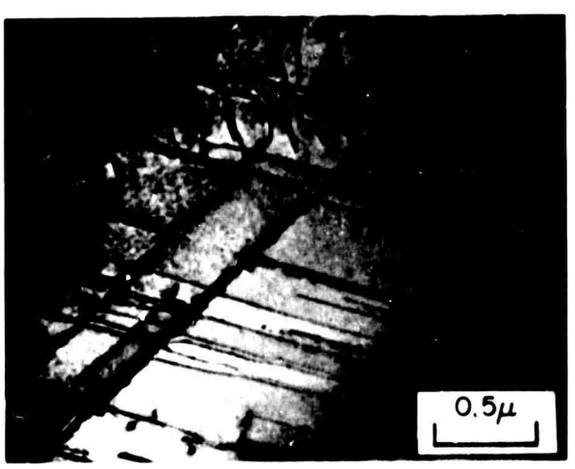

(b)

Fig. A-4 - Effect of order on coplanar slip in Ti-5Al-5Sn-5Zr deformed 4% in tension ($[0001]_\alpha$ zone axes). (a) Disordered - 1650° F/1/2 hr/WQ; (b) Ordered - 1650° F/1/2 hr/AC + 1100° F/8 hr/FC to 932° F/120 hr/AC.

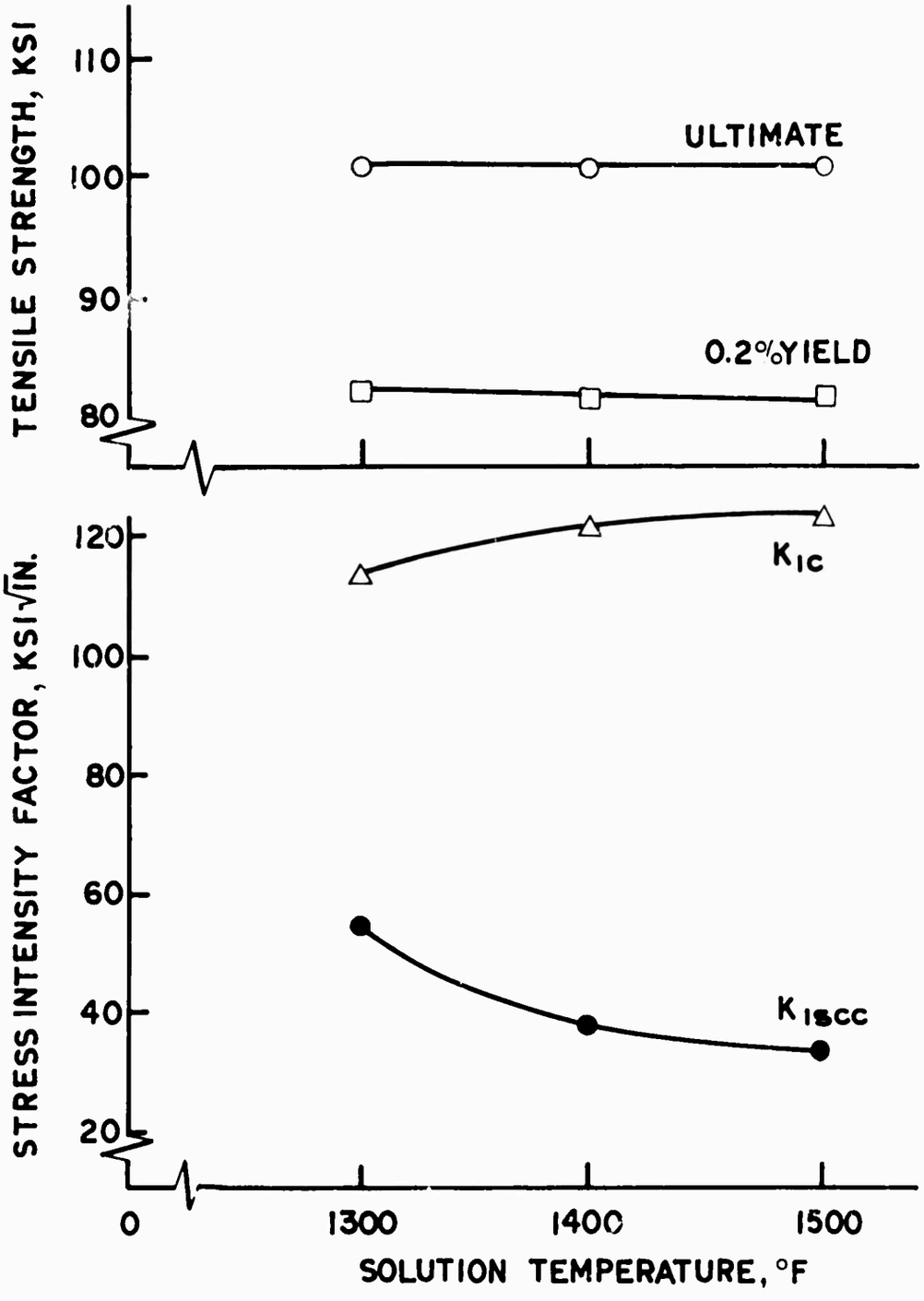

Fig. A-5 - Effect of solution temperature on the properties of Ti-70: solution heat treated 1/2 hr and air cooled

Isothermal aging at temperatures above the maximum temperature of omega stability (approximately 700°F) decomposed the omega phase and precipitated alpha phase in the beta phase by a cellular mechanism. Annealing cold-rolled Ti-70 containing diffused omega phase at 925°F for 30 minutes precipitated alpha particles (∼ 500 Å diameter) and relatively large alpha plates (5000 Å long). These transformations improved the K_{Iscc} from 33 ksi $\sqrt{in.}$ to 50 ksi $\sqrt{in.}$ Transforming larger omega particles (100 Å diameter) present in a 1500°F water-quenched condition by annealing at 1050°F for 30 minutes similarly improved the K_{Iscc} from 34 ksi $\sqrt{in.}$ to 75 ksi $\sqrt{in.}$ However, further annealing at 1050°F for 20 hours reduced the K_{Iscc} to the level measured for the 1500°F water-quenched condition. This behavior suggests that a large-volume fraction of alpha phase can embrittle the beta phase as effectively as the omega phase. In Ti-5Al-2.5Sn, transformation of diffused omega phase to the alpha phase reduced the K_{Iscc} from 26 ksi $\sqrt{in.}$ to 19 to 21 ksi $\sqrt{in.}$

A characterization program has now been completed by Boeing on 11 alpha-beta alloys: Ti-2.25Al-11Sn-4Mo-0.2Si (IMI 680), Ti-4Al-3Mo-1V, Ti-4Al-4Mo-2Sn-0.5Si (Hylite 50), Ti-5Al-3Mo-1V-2Sn, Ti-6Al-4V, Ti-6Al-2Mo, Ti-6Al-6V-2Sn, Ti-6Al-5Zr-1W-0.2Si (IMI 684), Ti-7Al-2.5Mo, Ti-7Al-4Mo, and Ti-8Al-1Mo-1V. Mill-annealed properties are compared with those of the alpha alloys in Fig. A-6. This figure shows that the addition of beta stabilizing elements increased alloy strength and often improved stress-corrosion resistance. Stress-corrosion resistance improved with increased volume percent beta phase, which is stabilized by molybdenum or vanadium, as shown in Fig. A-7. Similar beta-STA heat-treat conditions* were selected for each alloy included in Fig. A-7. Beta has been shown to reduce stress-corrosion susceptibility by arresting stress-corrosion cracks that propagate readily through the alpha phase (14, 16, 17).

In addition to the effect of volume percent beta on stress-corrosion resistance, Fig. A-7 shows that aluminum content above approximately 6% promotes susceptibility. This was attributed to ordering and increased planarity of slip in Ti-5Al-5Sn-5Zr (see previous comments on alpha alloys). Ordered domains also increased susceptibility in the alpha-beta alloy Ti-7Al-2.5Mo. The K_{Iscc} decreased from 80 ksi $\sqrt{in.}$ in the disordered condition, to 65 ksi $\sqrt{in.}$ in a partially ordered condition, to 44 ksi $\sqrt{in.}$ in a more fully ordered condition.

Although beta has been shown to act in a ductile manner in SCC, tests on Ti-6Al-6V-2Sn and Ti-4Al-4Mo-2Sn-0.5Si (Hylite 50) suggest that beta eutectoid stabilizers, Fe + Cu and Si, reduce stress-corrosion resistance. Ti-6Al-6V-2Sn containing 0.7 weight percent Fe and 0.7 weight percent Cu was more susceptible (K_{Iscc}/K_{Ic} = 0.63) than alloys containing only isomorphous stabilizers based on volume percent beta (15%) and aluminum and tin content (Fig. A-7). In addition, Ti-4Al-4Mo-2Sn-0.5Si exhibits greater susceptibility (K_{Iscc}/K_{Ic} = 0.5) than two similar alloys, Ti-4Al-3Mo-1V and Ti-5Al-3Mo-1V-2Sn, that do not contain silicon (Fig. A-7). The detrimental effect of Cu and Si is believed to result from formation of intermetallic compounds Ti_2Cu or Ti_5Si_3. These intermetallics should act as brittle inclusions, i.e. fracture at low strain, in an analogous manner to omega and alpha phases in Ti-70 and Ti-5Al-2.5Sn.

Ti-4Al-4Mo-2Sn-0.5Si was aged at temperatures between 932° and 1300°F to determine the effect of transformed beta-phase morphology, including Ti_5Si_3 particle size, on mechanical properties. A similar study (17) conducted on Ti-4Al-3Mo-1V showed that increasing aging

*Beta annealed, solution treated (beta transus temperature ± 75°F/WQ), and aged (1100°F - 1250°F/4hrs/AC)

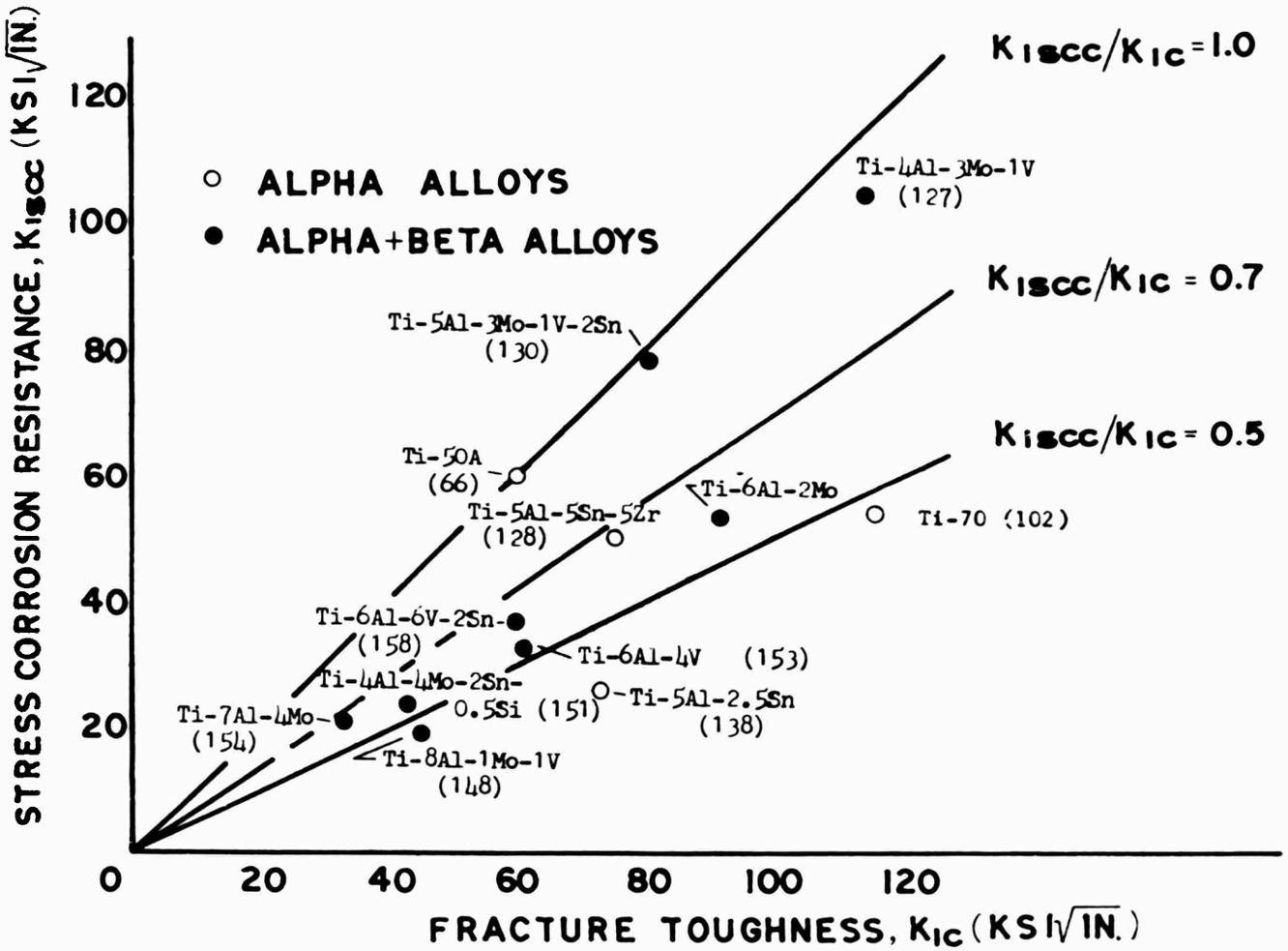

Fig. A-6 - Mill-annealed properties of alpha and alpha-beta titanium alloys (ultimate tensile strength in ksi is shown in parentheses).

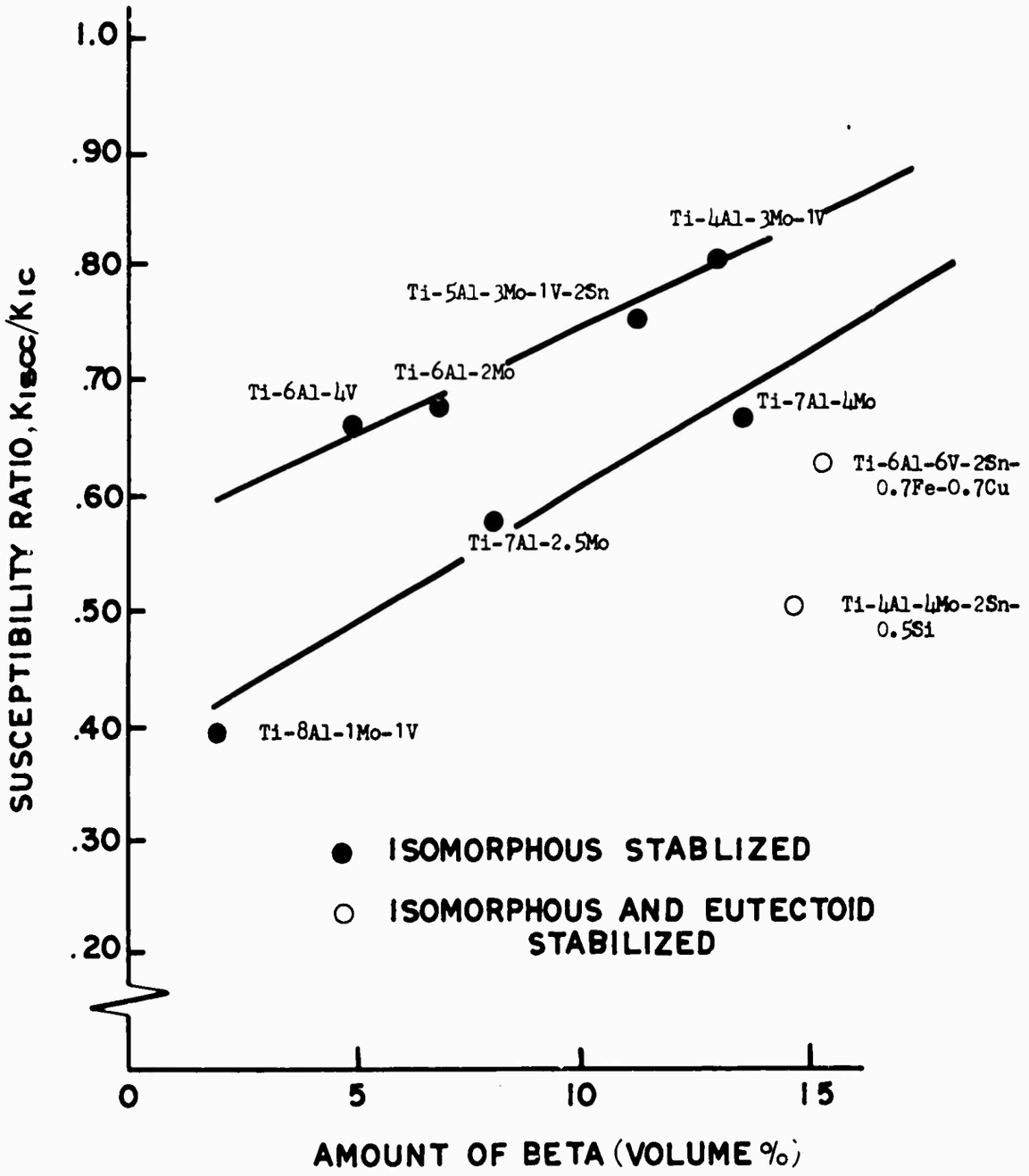

Fig. A-7 - Effect of beta phase on stress-corrosion susceptibility, beta-STA heat treatment.

temperature coarsened alpha and beta phases in the transformed region, reduced strength, but markedly improved K_{Ic} and K_{Iscc}. In Ti-4Al-4Mo-2Sn-0 5Si, higher aging temperatures also coarsened the transformed structure but reduced K_{Ic} and K_{Iscc} as well as strength (Fig. A-8). Increased Ti_5Si_3 particle size is believed to cause the reduction in fracture properties.

Plastic deformation was combined with heat treatment in an attempt to improve the properties of Hylite 50 by refining primary alpha and the transformed structure. It was shown that 20% rolling prior to aging increased 0 2% yield strength by 20 ksi without significantly changing K_{Ic} or K_{Iscc}. Both a reduced particle size and an increased dislocation density are believed to contribute to the improved properties A reduction in particle size by "duplex aging" increased strength and stress-corrosion resistance slightly but markedly improved fracture toughness. Increased dislocation density improved strength, toughness, and stress-corrosion resistance in Ti-7Al-2.5Mo.

In recent studies at Boeing, an attempt has been made to compare and contrast the SCC of a commercial alpha-beta alloy in methanol and in 3.5% sodium chloride solution. Work by Meyn (18) has shown that fracture in methanol occurs by a cleavage very similar to cleavage in salt solutions. Work by Beck (19) also showed characteristics similar to salt solutions in that, as Ti-8Al-1Mo-1V is given higher temperature solution treatments, it became less susceptible to cracking in methanol. The material became virtually immune when quenched from the beta phase field to produce an all-martensite structure. Optical metallography was performed in the present st''dy and, as would be expected, cracks tended to stop at the beta-phase particles (point . in Fig. A-9). This apparent immunity of the beta phase and martensite phase transformed from the beta is consistent with the change in susceptibility with heat treatment in the alpha-beta phase field similar to cracking in salt solution (16, 18, 19).

Ti-8Al-1Mo-1V plate, exhibiting pronounced preferred orientation of basal planes normal to the plate surface and parallel to the rolling direction, was available from a previous study (16). Standard precracked Charpy specimens were fabricated from this material and tested in reagent-grade methanol according to a procedure described in Ref 16. No control was exercised over the water or chloride content of the methanol

Initial tests were conducted on specimens in which the preferred (0001) planes were *parallel* to the main fracture path (designated transverse-longitudinal specimens) The data are reported in Fig. A-10 where the stress-intensity ratio K_{Ii}/K_{Ic} as a function of time to failure is an indication of the severity of cracking (17) These results demonstrate that cracking is more severe in methanol (curve A) than in sodium chloride solution (curve B) This is consistent with the data from tensile tests (0.005 min^{-1} strain rates) performed on unnotched specimens of mill-annealed Ti-8Al-1Mo-1V in that premature failure occurred after 2% plastic strain in methanol, but no effect was seen in the sodium chloride solution.

The cracks shown in Fig. A-9 occurred approximately normal to the long dimension of the alpha grains. As determined previously (16) by electron microscopy, this corresponds to the (0001) preferred orientation in these elongated alpha grains. It is reasonable to conclude then that fracture in methanol occurs on or near the (0001) planes similar to cracking in salt solution (the $(10\bar{1}7)$ or $(10\bar{1}8)$ in salt solution as determined by Blackburn (20)).

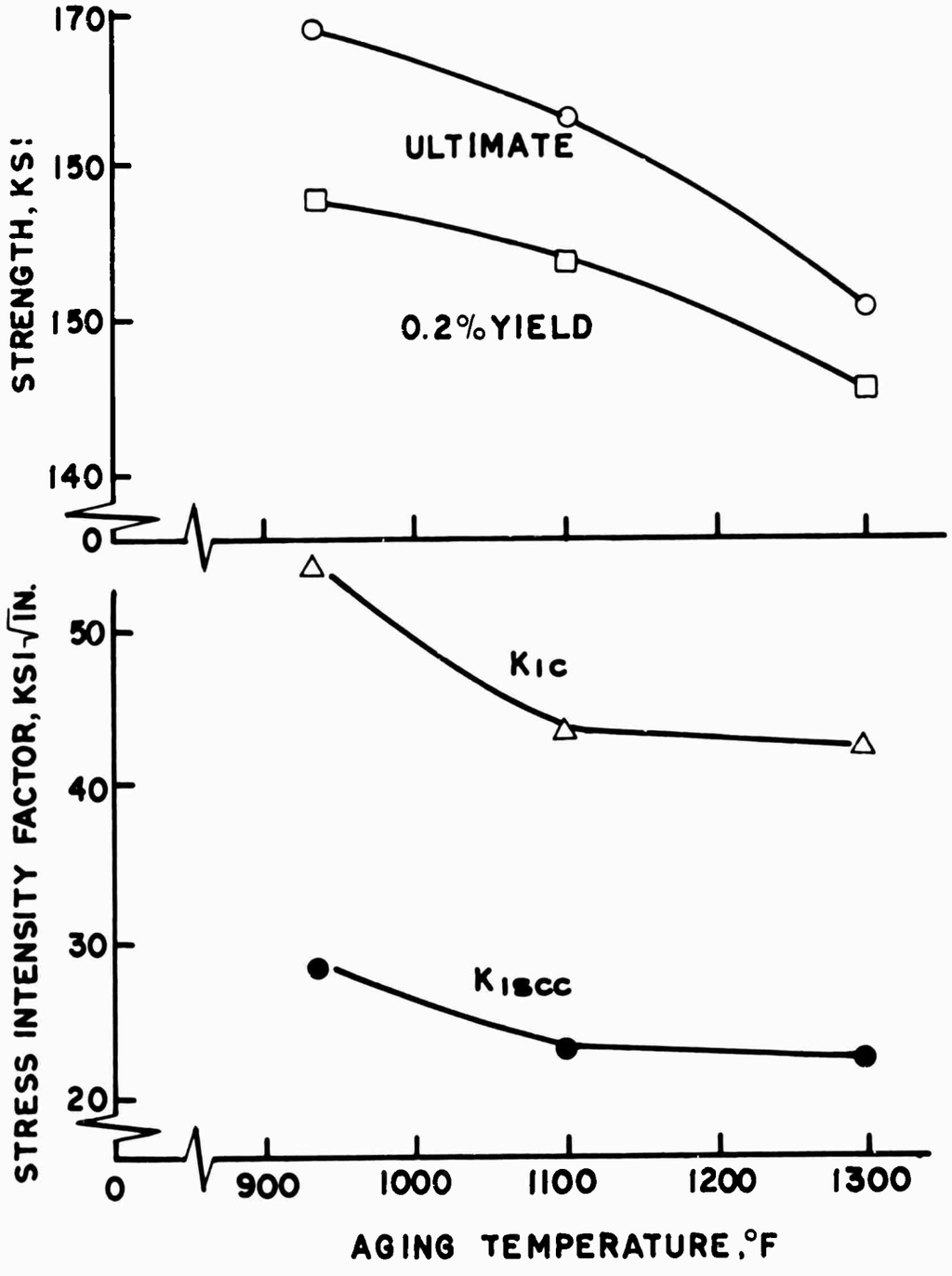

Fig. A-8 - Effect of aging temperature on the properties of Hylite 50: solution heat treated 1650° F/1/2 hr/AC prior to aging for 24 hr at temperature shown.

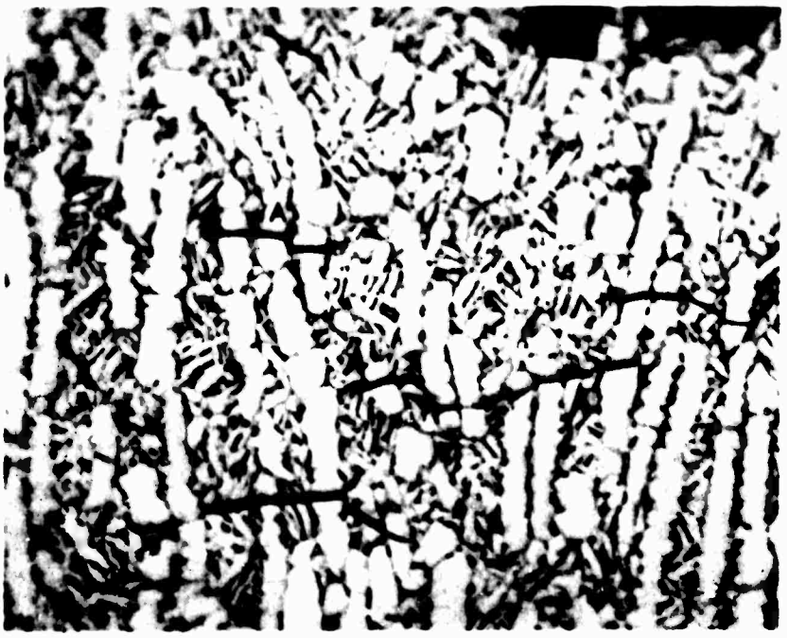

Fig. A-9 - Methanol cracking in Ti-8A1-1Mo-1V: crack arrest by beta phase at A; longitudinal view; fracture face above. × 1000

If fracture in methanol could occur on planes other than near the (0001), this might explain why cracking in this environment is more severe than cracking in sodium chloride solution. To examine this possibility, further tests were conducted on specimens in which the preferred (0001) planes were *normal* to the direction of the main fracture (designated longitudinal-transverse specimens), i.e. the $(11\bar{2}0)$ or $(1\bar{1}00)$ planes would be the most favorable for cracking. Data for these specimens in Fig. A-10 (curve C) show that failure does not occur below the baseline K_{Ic} (critical stress-intensity factor). A fracture face from a specimen in this orientation is shown in Fig. A-11. The crack propagated from the fatigue crack at A in a predominantly ductile manner (B) until stress conditions were favorable at C for cleavage near the preferred basal planes, even though they were unfavorably oriented to aid propagation in the main cracking direction. From the test results and the observed fracture morphology, it is apparent that ductile failure occurs in preference to cleavage on nonbasal planes in methanol, exhibiting the same behavior as in sodium chloride solution (16).

The difference in shape of curves A and B in Fig. A-10 is considered significant and outside the limits of experimental error. Titanium alloys more susceptible in sodium chloride solution than Ti-8Al-1Mo-1V have a cracking curve similar to D (with the same specimen geometry and loading conditions). Since the crack-path characteristics are similar, the lower curve (A) in Fig. A-10 indicates that cleavage in the alpha grains occurs at a lower stress (or strain) level in methanol than in sodium chloride solution. The difference in shape between curves A and B implies that some step in the cleavage process occurs slower in methanol than in sodium chloride solutions.

A further study of the crystallography of fracture in commercial titanium alloys is continuing at NRL. The fracture surfaces of specimens of titanium alloys that exhibited subcritical crack growth in a wide variety of environments, including aqueous solutions, alcohols, hydrocarbon gases, carbon tetrachloride, and dry air were examined by means of electron fractography and X-ray diffraction. The principal alloy studied was Ti-8Al-1Mo-1V in mill-annealed and vacuum-annealed and furnace-cooled conditions. Additionally, Ti-7Al-2Cb-1Ta, Ti-5Al-2.5Sn, and a coarse-grained Ti-0.35O alloy were investigated. The dominant and characteristic fracture mode was always cleavage, becoming mixed with an ever-increasing proportion of ductile mechanical fracture as the applied K_I level increased. The cleavage plane in all the aluminum-containing alloys was oriented at 15 deg from the (0001) of the alpha phase. The cleavage plane in the Ti-0.35O alloy ranged in orientation from 15 to 26 deg from (0001). No indices could be assigned to the 15+deg cleavage plane because of uncertainty as to which zone it lay in.

The fracture surfaces of alloy specimens susceptible to stress-corrosion cracking, when fatigue tested at low enough frequencies and with $K_{I_{max}}$ (during the peak of the cycle) about equal to or higher than $K_{I_{scc}}$, also show a cleavage mode that appears to be identical with that found for subcritical cracking under sustained loads. Such alloys, when fatigue tested at amplitudes well below $K_{I_{scc}}$ and when crack propagation rates are quite low, exhibit a type of cleavage that is somewhat similar. However, more than one cleavage plane appears to exist: the orientations are 0 deg, 8 to 10 deg, and 15 deg from (0001).

Three commercially available beta alloys are presently under study on the program. Carnegie-Mellon is investigating Ti-1Al-8V-5Fe, and Boeing is investigating Beta III and monitoring studies at the University of Washington on Ti-13V-11Cr-3Al. The combined objective of these programs is to relate the physical metallurgy of these metastable beta alloys to their stress-corrosion resistance.

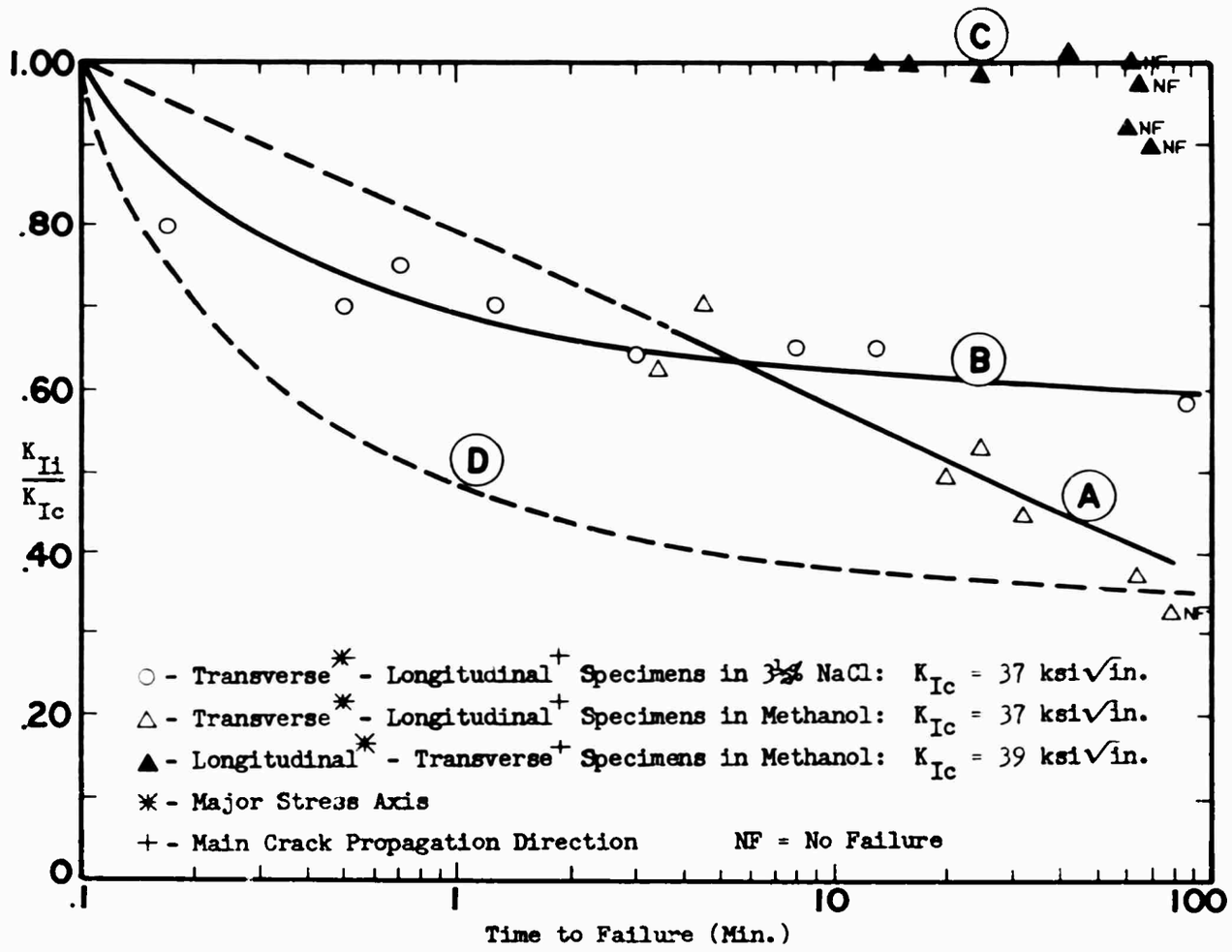

Fig. A-10 - Susceptibility of Ti-8Al-1Mo-1V in methanol and salt solution

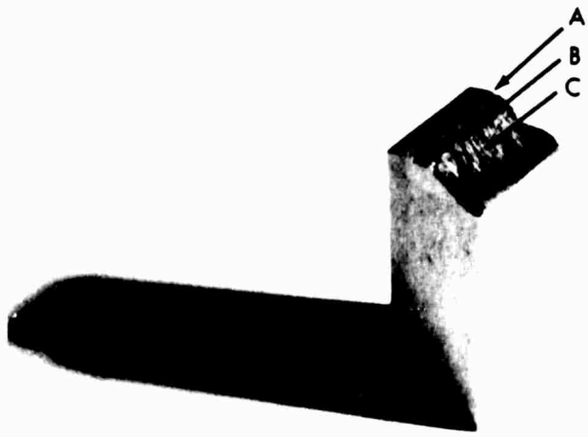

Fig. A-11 - Fracture face of longitudinal-transverse specimen failed in methanol: fatigue crack at A; ductile at B; cleavage near preferred basal planes at C.

Beta III is a compound-free beta alloy developed by the Crucible Steel Company and has the composition Ti-11.5Mo-5.5Zr-4.5Sn. Molybdenum is a strong beta stabilizer, and zirconium and tin are neutral strengtheners. The reaction is very sluggish in this pseudo-isomorphous system, and 100% beta can be retained at room temperature on water quenching.

Beta III deforms by multiple-order mechanical twinning. This observation is in agreement with some recent work by Blackburn and Williams (21) on binary Ti-Mo alloys. Figure A-12 shows first-order twins formed on a polished surface after 2% uniform elongation. At these low strains, the twins are straight sided for a considerable portion of their length and are similar to those observed by Jaffe and his coworkers (22) in Ti-Mn alloys. At intermediate strains (4% to 6% uniform elongation), the twins assume a lenticular shape that contains several variants of internal striations (Figs. A-13 and A-14). Upon cursory examination, it is easy to see why similar features have been mistaken for martensite plates. At high strains (10% to 15% uniform elongation), the twins exhibit accommodation kinking and serration of their interfaces, as shown in Fig. A-15.

Transmission electron microscopy has been used to further delineate the finer details of the twinning mode of deformation in Beta III. Figure A-16 shows a bright-field micrograph of a twin formed during 1% to 2% uniform elongation. Note again the straight-sided interface. The relatively high dislocation density within the first-order twins is illustrated in the dark-field micrograph (Fig. A-17) on imaging a twin reflection. Compare these latter observations with the twins produced after a 5% uniform elongation in which two or more twinning systems are present. Note the severe bending (Fig. A-18), and serration (Fig. A-19) of the interface.

Trace analysis has shown that the twins formed after 1% to 2% deformation have a habit plane near $\{112\}\beta$, which is consistent with the common $\{112\} < 111 >$ twinning system normally operating in body-centered cubic materials. Accommodation kinking and distortion of the primary interface complicates trace analysis at higher strains. In the absence of prior strain, the aging characteristics of Beta III can be divided into two parts (Fig. A-20):

1. For aging temperatures below 800°F, omega formation is responsible for strengthening. Aging commences without an incubation period, and a high degree of strengthening is exhibited.

2. Above 800°F, alpha precipitation is the strengthening mechanism, and classical age-hardening characteristics are exhibited.

The omega morphology is ellipsoidal and typical of binary Ti-Mo alloys. Figure A-21 is a dark-field micrograph imaging on a $(10\bar{1}0)\omega$ reflection in a $[311]\beta$ zone. The alpha morphology is typically Widmanstätten, as shown in Fig. A-22. The effect of deformation and aging is shown in Figs. A-23, A-24, and A-25. At all the aging temperatures investigated, the marked initial strain hardening is not maintained with increasing aging time and decreases to minimum at peak hardness. Experiments are now being performed to determine the fracture resistance (K_{Ic} and K_{Iscc}) in specimens (1) strain hardened, (2) omega strengthened, and (3) alpha strengthened at the same initial grain size and the same processed yield strength.

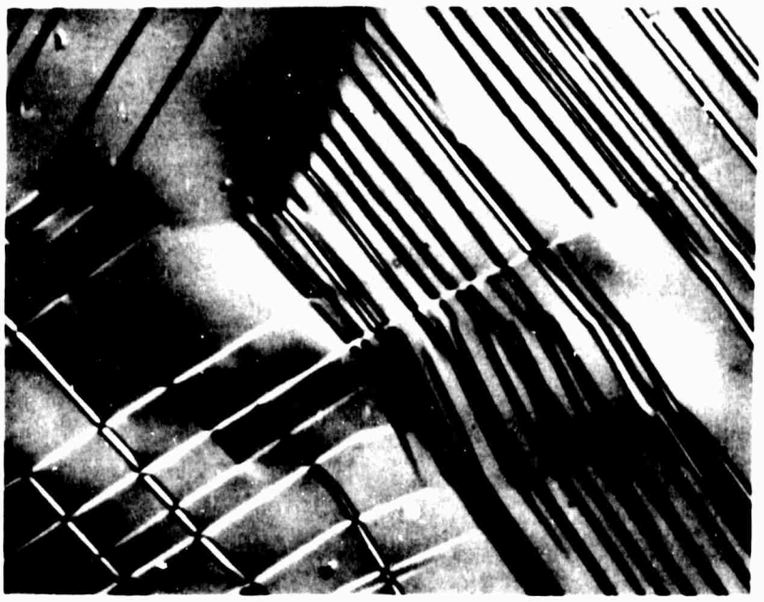

Fig. A-12 - First-order twins formed during 2% uniform elongation; Normarski interference contrast. × 750

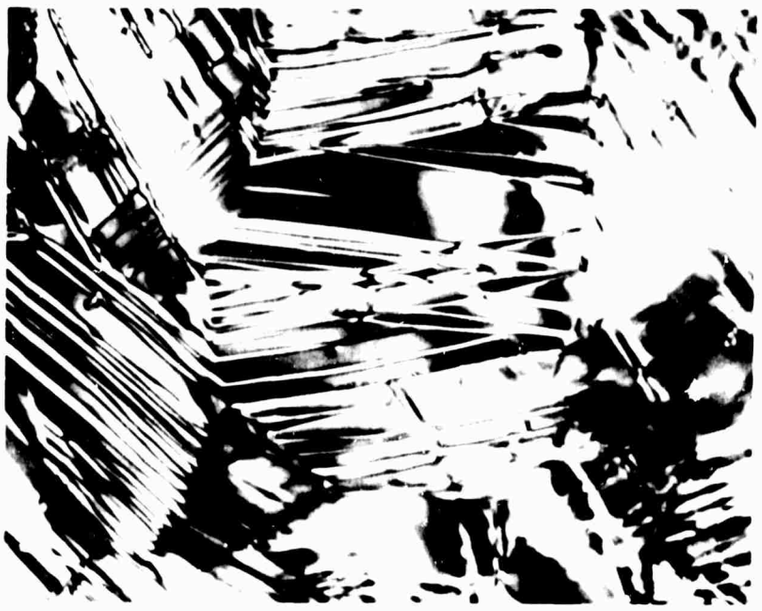

Fig. A-13 - Twins formed during 10% uniform elongation; bright field. × 750

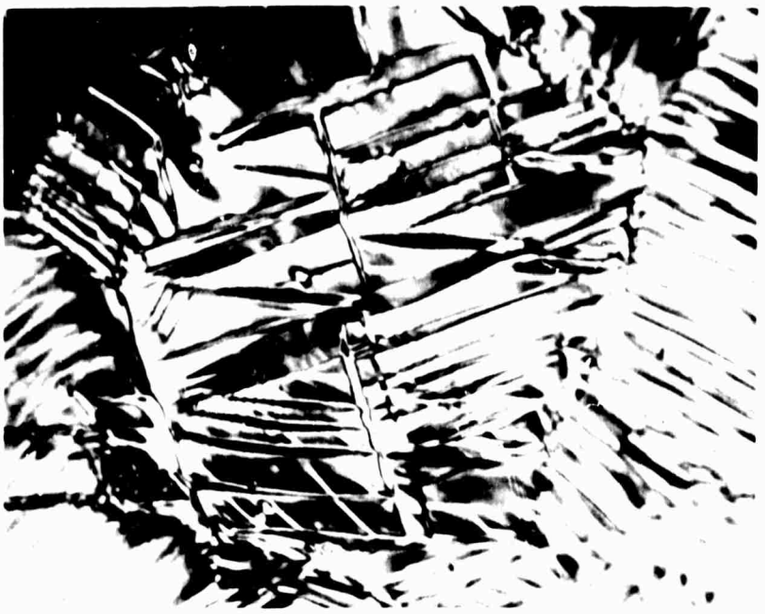

Fig. A-14 - Twins formed during 10% uniform elongation; Normarski interference contrast. × 750

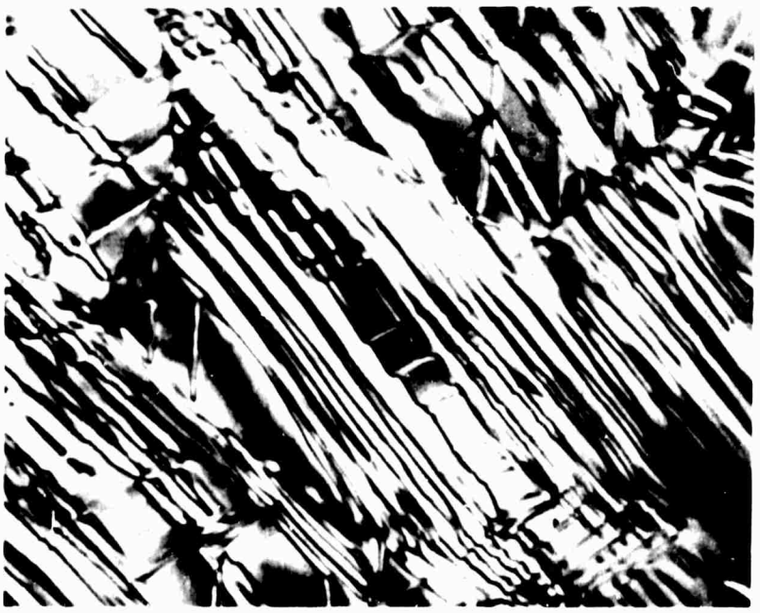

Fig. A-15 - Twins formed during 15% uniform elongation; Normarski interference contrast. × 750

Fig. A-16 - Bright-field electron micrograph of a twin formed during 2% uniform elongation

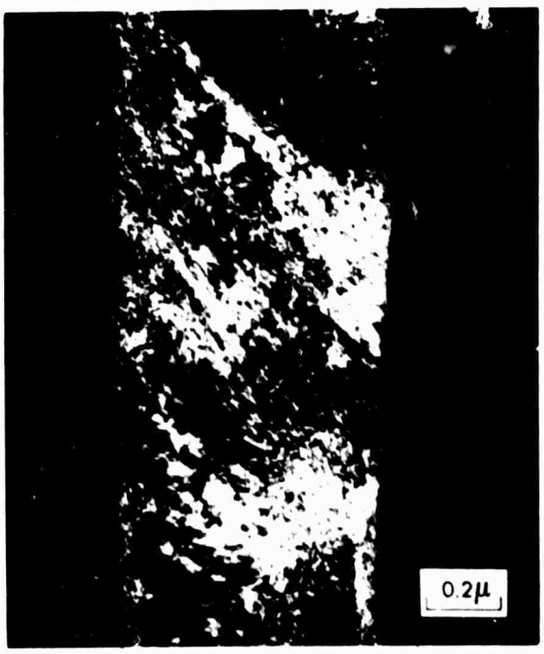

Fig. A-17 - Dark-field electron micrograph imaging on a twin reflection, twin formed during 2% uniform elongation.

Fig. A-18 - Bright-field electron micrograph of twins formed during 10% uniform elongation

Fig. A-19 - Bright-field electron micrograph of twin formed during 10% uniform elongation

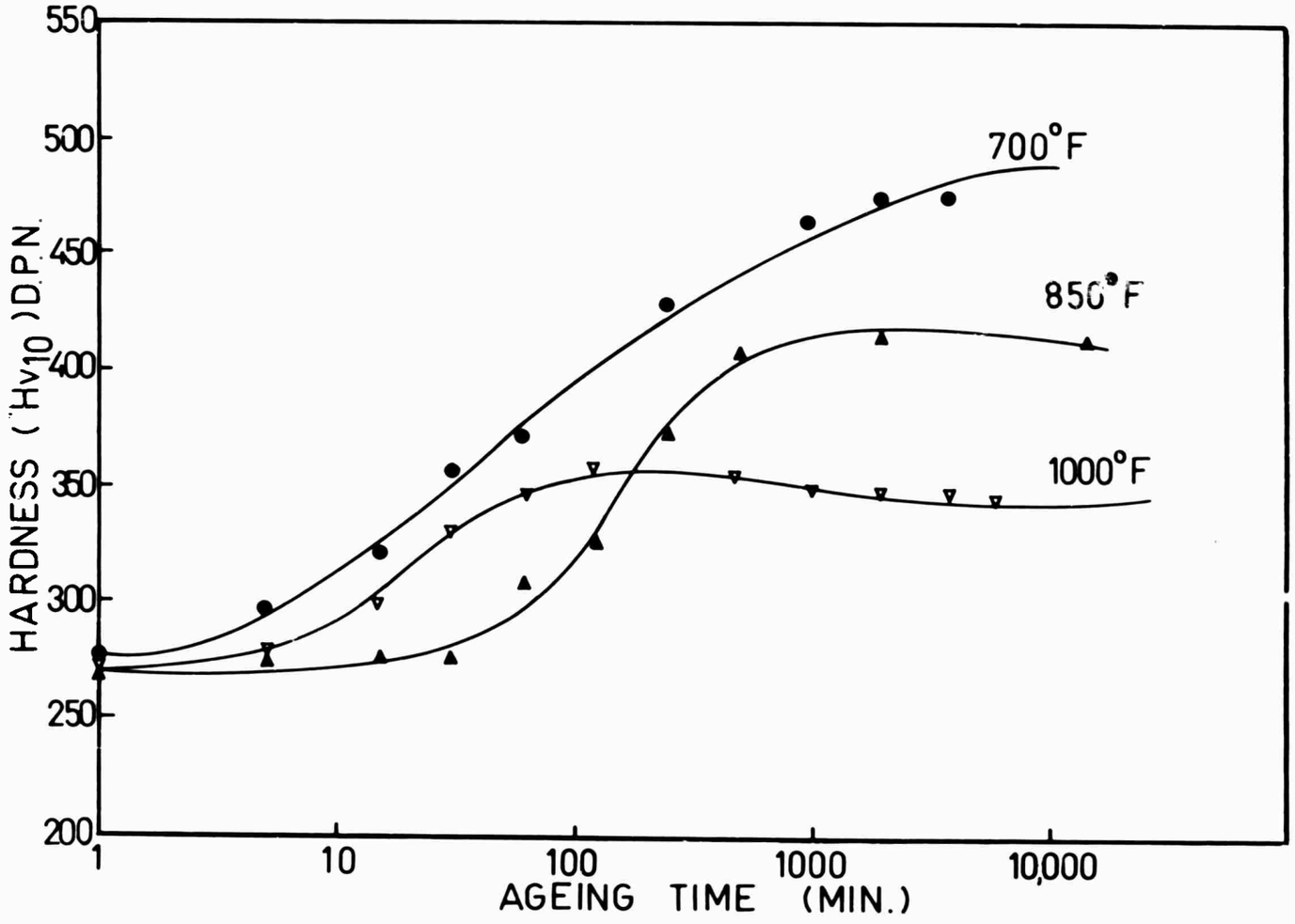

Fig. A-20 - Aging characteristics of Beta III at 700°F, 850°F, and 1000°F in absence of prior strain

Fig. A-21 - Dark-field electron micrograph of omega formed during aging at 700°F for 500 hr.

Fig. A-22 - Bright-field electron micrograph of Widmanstatten alpha formed during aging at 850°F for 64 hr.

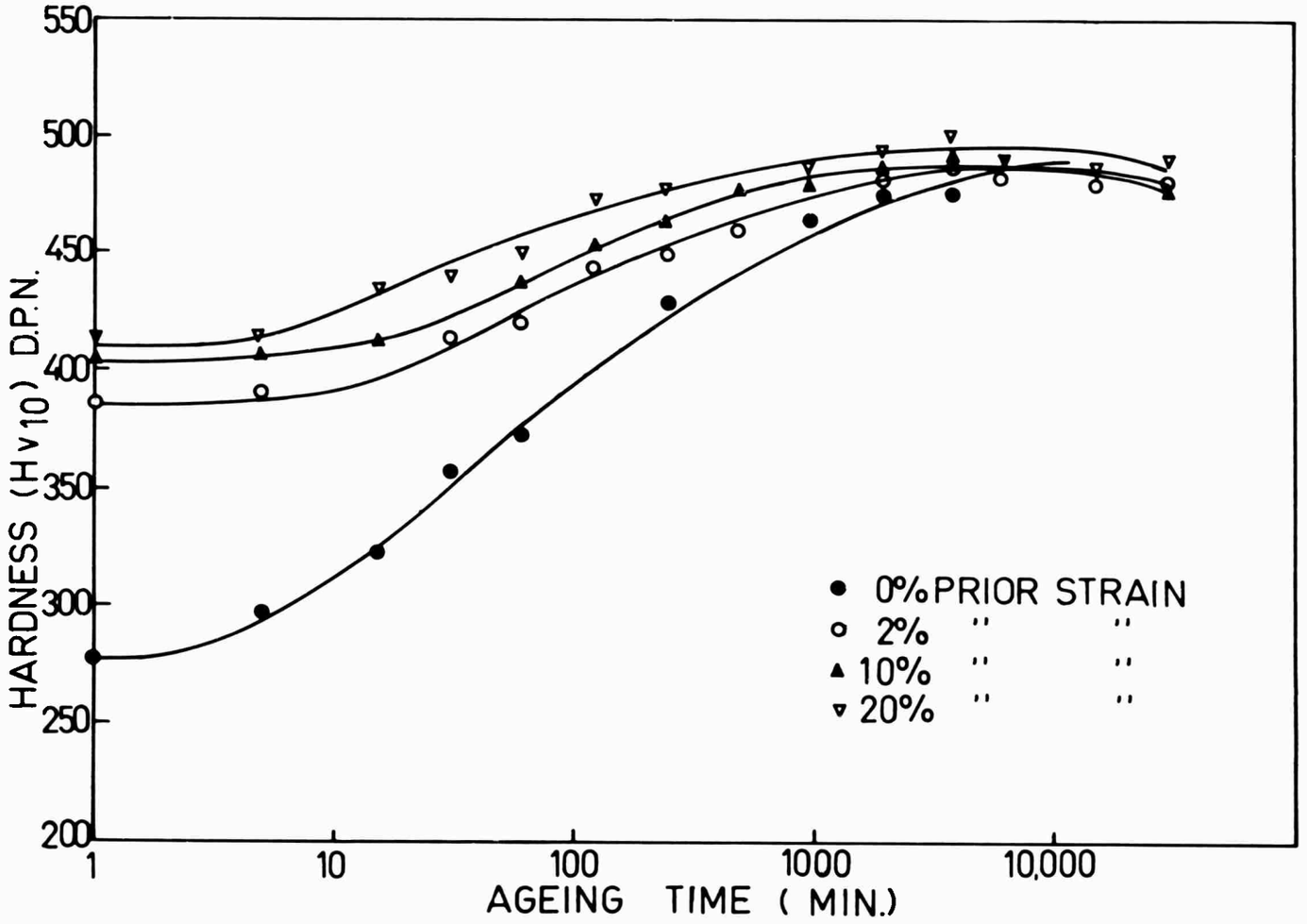

Fig. A-23 - Aging characteristics of Beta III at 700°F after 2%, 10%, and 20% prior strain

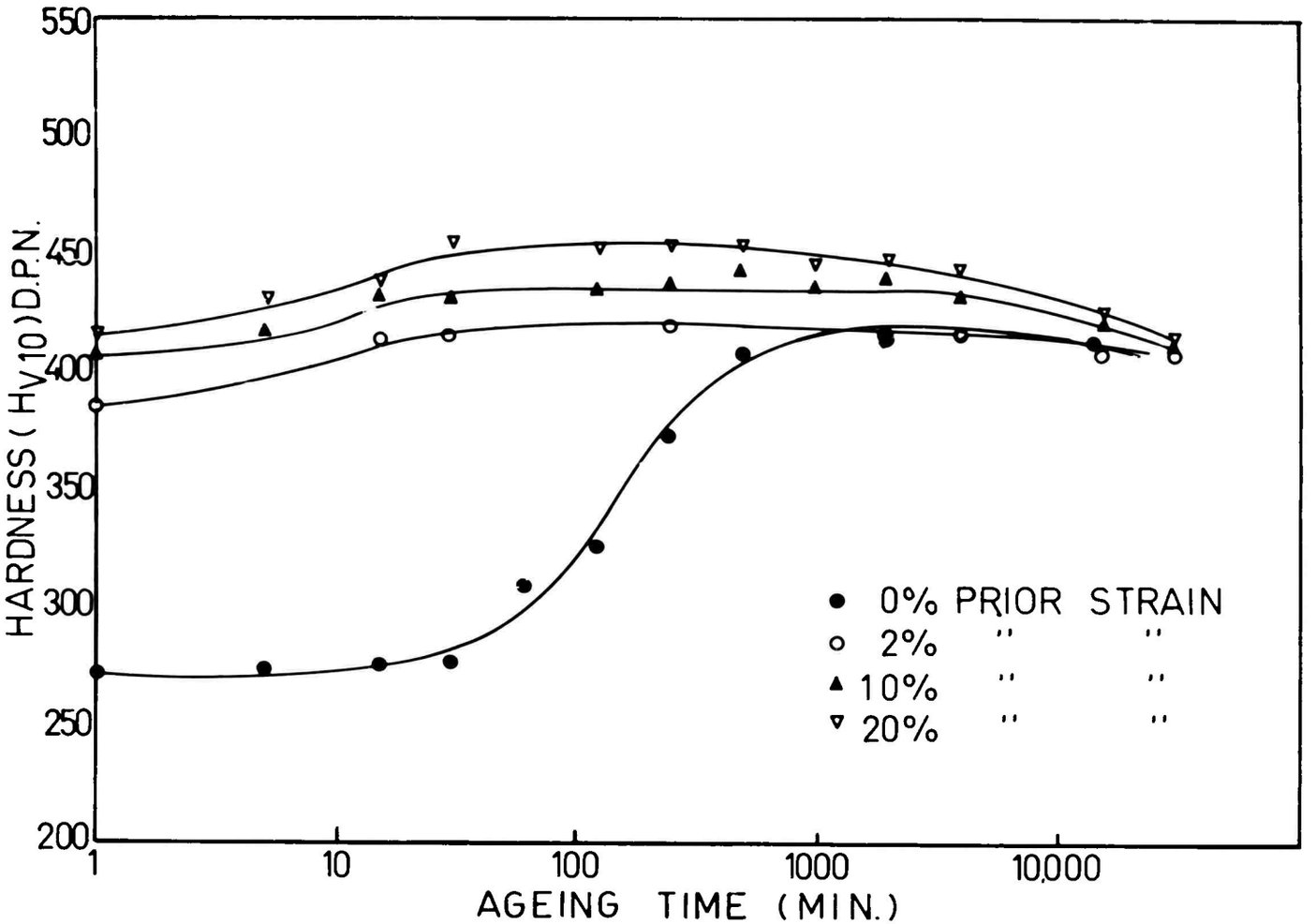

Fig. A-24 - Aging characteristics of Beta III at 850° F after 2%, 10%, and 20% prior strain

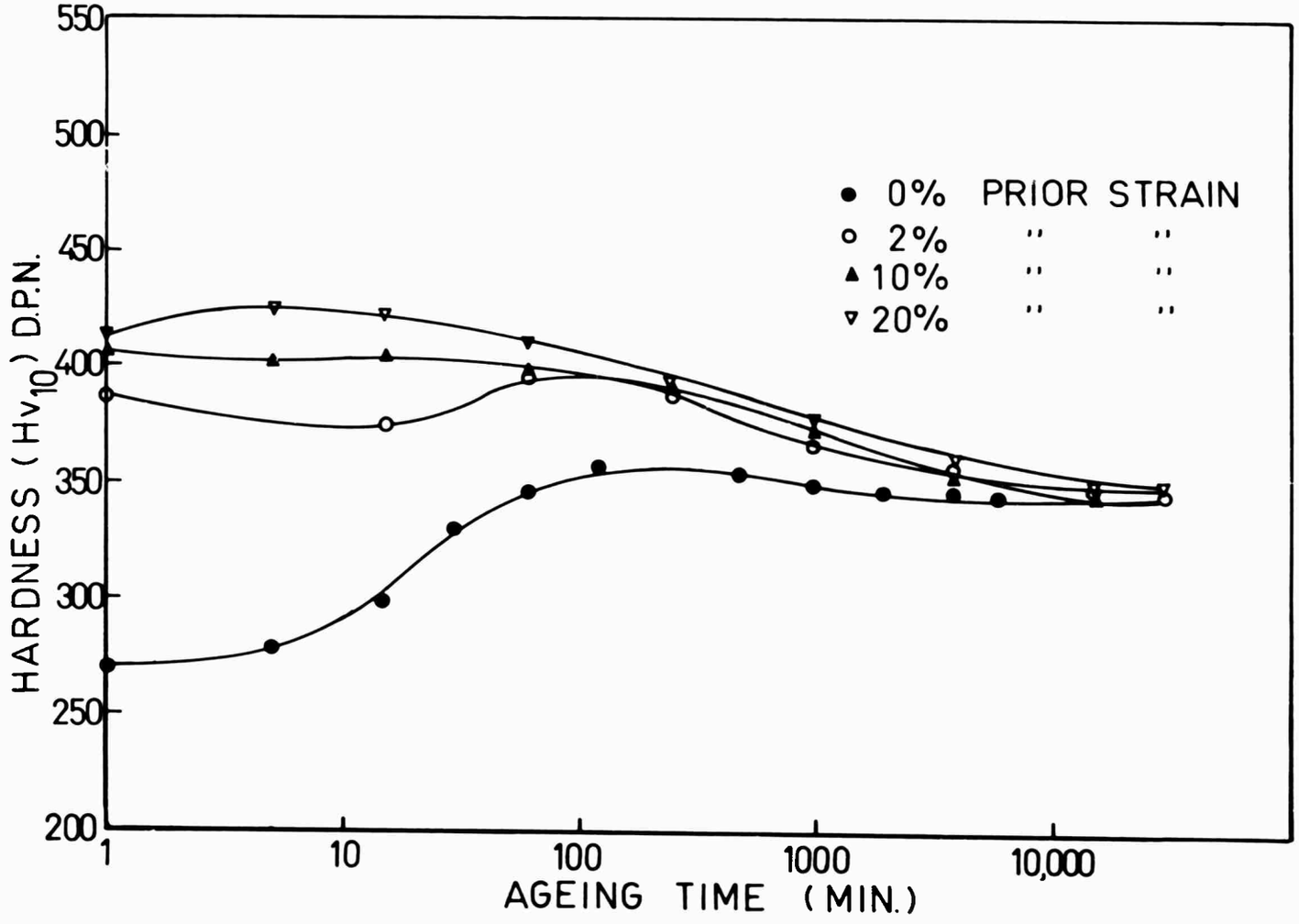

Fig. A-25 - Aging characteristics of Beta III at 1000°F after 2%, 10%, and 20% prior strain

Initial investigations have included a study of the effect of heat treatment on the precipitate morphology in B120VCA. The heat treatments examined to date have consisted of samples aged from 250° to 500°C at intervals of 50°C for periods up to 500 hours following solution treatment. The main interest of this study at this point is to explore the existence of a possible transition phase or phases: in particular, the presence of omega, which has been reported as a probable transition phase by other investigators. Electron microscopy and X-ray diffraction analyses have failed to reveal the presence of omega. However, an unidentified precipitate was detected during electron microscopic examinations in samples aged from 300° to 450°C for up to approximately 15 hours. This precipitate, which had no specific shape or preferred orientation, produced no effects in either electron or X-ray diffraction patterns. Hence, the identification of its crystal structure and the orientation relationship has been so far unsuccessful. The presence of denuded zones in the vicinity of the grain boundaries suggests that some vacancy mechanism may be operative in its formation.

Aging for longer periods of time resulted in the precipitation of needles of alpha phase with Widmanstätten morphology. The orientation relationship of this phase has been found to be in agreement with the Burgers relation On continued aging, the intermediate compound $TiCr_2$ appeared in the microstructure intimately mixed with alpha in samples aged at 450°C for 500 hours, while in samples aged at 300°C, no $TiCr_2$ was observed. More X-ray work is currently being planned to confirm the $MgCu_2$-type fcc structure reported for this phase

The mechanical property studies included measurement of microhardness and tensile properties on samples aged at 350°, 450°, and 500°C for up to 150 hours Although hardness measurements did not yield any valuable information regarding the phase transformations, the tensile properties showed significant changes with changes in aging temperature and time. An interesting observation made was the presence of a well-defined yield point in the stress-strain curve of samples aged at 350° and 450°C for short periods (up to 15 hours). These samples showed the presence of the unidentified precipitate in their microstructure. The fact that at longer aging times this yield point failed to occur suggests that these precipitates may be responsible for this mechanical behavior There is a general increase in yield and ultimate strengths with an increase in aging time at all temperatures, with little reduction in ductility during the early stages. However, at high strength levels, the ductility falls off rapidly. The alloy is relatively insensitive to strain rate variations. Additional work is being performed to correlate microstructure and mechanical properties in this alloy.

3. Simplified Research Alloys

(i) Physical Metallurgy

Work is continuing at Georgia Tech on a further series of titanium-aluminum alloys. Part of this work is to investigate the validity of the model of SCC presented at the annual meeting. This model attempts to explain SCC of the alpha phase in titanium-aluminum alloys containing 6% aluminum or above in methanol or 3.5% sodium chloride solution It has been found by other investigators (23) that, in hydrogenated specimens, titanium hydrides form and impede slip on the $\{10\bar{1}0\}$ and $\{10\bar{1}1\}$ slip planes In addition, others (14) have found in alloys containing above 6% aluminum that slip is seldom observed on the (0001) plane It is therefore postulated that in such all-alpha alloys, saturated with hydrogen from

the surface reaction, a less frequently observed slip system would become dominant. Such a slip system is $\{11\bar{2}2\}\ <11\bar{2}3>$. These $1/3\ <11\bar{2}3>$-type dislocations will pile up against the titanium hydride platelets, causing a stress field around the head of the dislocation pileup. According to Stroh (24), cleavage should then occur on a plane 70.5 deg from the operative slip plane as a result of the stress field of the pileup. This predicted cleavage plane is approximately 15 deg to the basal plane, which is the SCC cleavage plane observed in these alloys.

The high-temperature, inert-atmosphere quench furnace has now been completed. Its function is to grow large grains in several high-purity Ti-Al binary alloys. A comparison will then be made of 2.5%, 5%, and 8% binary alloys; one set of specimens will be hydrogenated and the other stress-corrosion cracked in 3.5% sodium chloride solution. The comparison will be made by determining the fracture habit plane and fracture surface topography for each set. The effect of hydrogen on deformation mode will also be studied in a similar series of alloys. Hydrogenation will be performed in a Sievert's apparatus.

(ii) Surface Studies

The primary objective of low energy electron diffraction (LEED) studies at Georgia Tech is to provide a fundamental understanding of surface reactions.

The need for LEED surface studies within a program of SCC investigations is based on the assumption that the mechanism, in part, deals with the chemical reactivity of clean surfaces. Such an assumption is realistic in that, during crack growth, fresh (clean) surfaces are exposed to the corrosion environment. In fact, it has been proposed that selective adsorption of gases or ions at the tip of the crack can induce variations in the strength of the metal-to-metal bonds. Consequently, the magnitude of the tensile fracture stress of the bond will be changed. The energy of the chemical reaction in the immediate vicinity of the crack tip can contribute to the propagation of the crack. The energy of the reaction can affect the specific surface energy such that the force required to advance the crack is altered significantly.

To make LEED studies of metals and alloys in the environments of interest to the SCC program, a special LEED vacuum system has been designed and constructed. The vacuum system is capable of pressures in the 10^{-10} torr range and has manifolds for handling highly corrosive, organic, and ultrapure, noncorrosive gases. Surfaces that are prepared in ultrahigh vacuum can be exposed to corrosive gases by means of a valve that isolates (*in situ*) the sample from the high-vacuum chamber.

Presently, studies are being done on the (0001) surface of pure (99.97%) titanium. This surface has been successfully cleaned by argon ion bombardment and annealing. The reaction of hydrogen with the clean titanium surface has been studied extensively. It has been found that hydrogen adsorbs with unit sticking probability and that one hydrogen atom is adsorbed for every surface titanium atom. This adsorbed hydrogen is slowly absorbed, at room temperature, into the surface. The absorption of hydrogen is accompanied by a 5% to 6% increase of the lattice in the c direction.

The fact that clean titanium readily adsorbs and absorbs hydrogen is not surprising. The observed expansion, on the other hand, was not expected, because there is sufficient volume in the octahedral interstices to accommodate hydrogen. A hydrogen-induced surface expansion of Ti-Al alloys has previously been reported, wherein the expansion was attributed to hydrogen going into the tetrahedral interstices.

Extension of the studies described above will be conducted. The following investigations will be accomplished: (1) the factors that may accelerate or inhibit hydrogen adsorption will be determined - for example, a monolayer of adsorbed oxygen may prevent the absorption of hydrogen; (2) the surface chemistry of titanium for a number of environments including oxygen, nitrogen, carbon monoxide, hydrogen chloride, chlorine, ethylene, and methyl alcohol will be studied; and (3) after the chemical reactions have been well characterized for pure titanium, studies will be undertaken to determine the effect of aluminum alloying on surface chemical properties.

The failure of materials that are susceptible to SCC is initiated at the surface of the material and proceeds with exposure of new material to the environment. Evidence, such as the rate and manner that cracks extend and the brittle character of the failures, indicates that the crack propagation is primarily mechanical. Consequently, to obtain an understanding of the fundamental mechanism responsible for stress-corrosion cracking, it is desirable to make mechanical property-environment correlations on materials sufficiently thin so that surface-dislocation interactions and mechanical property changes leading to crack initiation and subsequent stress-corrosion cracking failures are not completely masked by the bulk properties of the remaining unaffected material. There is good evidence that dislocation-surface interaction may be a particularly important process in the failure of materials in corrosive environments. Observations have indicated that dislocation arrangements in susceptible materials are essentially coplanar, whereas in less susceptible materials they appear as tangled networks. Surface coatings, such as oxide films as well as grain boundaries, provide barriers to dislocation motion, resulting in pileups. There are several mechanisms causing the oxide films to repel dislocations. One of these is attributed to the oxide film having a larger elastic modulus than the substrate material. Recent studies on the Al-Al_2O_3 system have shown that the elastic modulus of the oxide may be altered sufficiently by exposure to certain environments to change the dislocation-oxide interaction from one of repulsion to attraction. Additional factors of importance are the coherency of the surface coating, thickness of the coating, and the relative lattice constants.

Studies are now under way at Georgia Tech to investigate the surface-film dislocation interactions under various environmental conditions in an effort to elucidate the initiation of SCC. A micromechanical facility capable of precise measurements on very thin samples (0.01 micron to 100 microns) has been developed. This facility includes instruments for bending, tension, torsion, and fatigue measurements. The bending apparatus has been used for measurements on unsupported aluminum oxide films, thin aluminum and titanium foils, and thinned high-strength titanium alloy samples. Many of these measurements have been conducted under various liquid environments. The torsion device is presently being tested, and the microtension and fatigue instruments should be ready for initial tests shortly. Emphasis is now being placed on sample preparation

Future work will aim at subjecting the surface of thin samples of both titanium-aluminum alloys and pure titanium to carefully controlled chemical reactions to form adherent oxide coatings. Micromechanical tests on these samples will be made in various environments (air, salt water, methanol, etc.). These tests will include bending, tension, fatigue, and both static and dynamic torsion. Each sample is then analyzed to determine the microstructural aspects of the deformation or failure. The analytical techniques include electron microscopy, X-ray techniques, and scanning electron microscopy for, respectively, dislocation observation, structure and thickness studies, and fracture characterization. Mechanical-property measurements will therefore be correlated with deformation mode observations on well-characterized samples to differentiate between the possible surface-dislocation mechanisms and fracture initiation that may lead to SCC. The tensile properties of the oxides prepared under various conditions will be studied using techniques developed previously for unsupported aluminum oxide films.

Interactions with a clean surface of titanium by hydrogen, water, and some organic materials important to SCC of titanium alloys relate directly to the interactions of these materials with the clean metal at the tip of a crack in titanium or titanium alloys. The purpose of studies at Lehigh is to determine the interaction of hydrogen, water, and several organic materials with a clean titanium surface under ultrahigh vacuum conditions.

A titanium wire is cleaned by combined thermal treatment and argon ion bombardment until the residual pressure is of the order of 10^{-10} torr. The adsorption and desorption of gases is followed by monitoring the pressure at room temperature and upon resistance heating of the titanium wire. Rapid heating of the wire after argon ion bombardment leads to the evolution of argon in three distinct stages. Based on work by other investigators studying the same phenomenon in tungsten, it appears that the argon is trapped within the metal near the surface and is released upon thermal treatment with definite activation energies.

Hydrogen adsorption or absorption on the clean titanium surface is rapid both at room temperature and at 860°F. The amount of hydrogen sorbed at room temperature at pressures of 2-3 x 10^{-8} torr increased regularly with increase in time. The gas released on thermal treatment was exclusively hydrogen, as shown by mass spectrometric measurements of the released gas. These studies show the extreme reactivity of a clean titanium surface such as might be exposed during SCC.

Preliminary experiments have been performed on the field ion microscope (FIM) at Georgia Tech using various imaging gases on pure titanium, Ti-2.5Al, Ti-8Al, and Ti-16Al (the latter is approximately Ti_3Al). Images have been obtained using hydrogen. This imaging indicates hydrogen adsorption that changes the imaging potential and decreases the surface adherence. This is in keeping with the theory of Dr. Muller: hydrogen on the surface actually gains electrons from metal atoms, making the metal more susceptible to field evaporation. It appears that this can be correlated with the effects of hydrogen on the decreased strength and hydrogen embrittlement of alloys. A major contribution to this and a related program has been the symposium on "Field Ion Microscopy in Physical Metallurgy and Corrosion" presented at Georgia Institute of Technology, May 15, 16, and 17, 1968.

The program will be further developed to provide a structure analysis of titanium and titanium alloys. Later, it will be expanded to commercial alloys when the techniques dealing with simple binaries have been improved. The FIM technique will be used in conjunction with field emission microscopy (FEM) and surface reaction studies to characterize surface structure. Techniques developed by Ralph on IrO_2 to study features of the surface oxide, and the work of Muller and Rendulic on corrosion characteristics of metals in the FIM will be used to determine the effect of environment on these metals and alloys. The effect of hydrogen and chlorine on clear surface oxide films will be examined. This information will then be correlated with the surface and bulk characteristics of iron and titanium alloys. It will also be related to the physical metallurgy and stress-corrosion susceptibility of these materials.

4. References

1. H. R. Smith, D. E. Piper, and F. K. Downey, *A Study of Stress-Corrosion Cracking by Wedge-Force Loading*, D6-19768, The Boeing Company, June 1967 (also *Engineering Fracture Mechanics*, 1968, Vol. 1, p. 123)

2. *ARPA Coupling Program on Stress-Corrosion Cracking*, Second Quarterly Report, April 1967, p. 27

3. *ARPA Coupling Program on Stress-Corrosion Cracking*, Second Quarterly Report, April 1967, p. 26

4. C. S. Carter, *Terminal Fracture of Titanium Alloys Containing Stress-Corrosion Cracks*, D6-19771, The Boeing Company, May 1968

5. W. F. Brown and J. E. Srawley, "Plane Strain Crack Toughness Testing of High-Strength Metallic Materials," ASTM-STP 410, 1967

6. N. M. Lowry, D. R. Mulkey, J. M. Kuronen, and J. W. Bieber, *A Method of Measuring Crack Propagation Rates in Brittle Materials*, D6-60072, The Boeing Company, May 1967

7. R. W. Judy, Jr. and R. J. Goode, *Stress-Corrosion Cracking of Alloys of Titanium in Salt Water*, NRL Report No. 6564, 1967

8. *Titanium Development Program*, D6A10065-1, The Boeing Company, March 28, 1966

9. P. T. Finden, *Evaluation of Ti-6Al-2Mo and Ti-5Al-3Mo-1V-2Sn*, D6-19765, The Boeing Company, March 13, 1967

10. P. T. Finden, *Comparison of Titanium Alloys 6Al-6V-2Sn and 7Al-4Mo*, Engineering Report 6-7620-13-PMR3, The Boeing Company, February 16, 1967

11. P. T. Finden, *Environmental Crack Growth Susceptibility of Titanium EX 684*, Engineering Report No. 6-7620-13-PMR2, The Boeing Company, February 2, 1967

12. A. T. Churchman, Proc. Roy. Soc., 1954, A226, p. 216

13. A. J. McEvily, Jr. and T. L. Johnston, *Proc. of First International Conf. on Fracture*, Japanese Soc. for Strength and Fracture of Materials, Japan, 1966, p. 515

14. J. C. Williams, *Some Observations on the Stress-Corrosion Cracking of Three Commercial Titanium Alloys*, D6-19553, The Boeing Company, September 1967 (also *ASM Transactions Quarterly*, Vol. 60, No. 4, December 1967, p. 646)

15. F. C. Holden, H. R. Ogden, and R. I. Jaffee, *J. Metals*, May 1956, p. 521

16. D. N. Fager and W. F. Spurr, *Some Characteristics of Aqueous Stress Corrosion in Titanium Alloys*, D6-60083, The Boeing Company, September 1967 (also *ASM Transactions Quarterly*, Vol. 61, No. 2, June 1968, p. 283)

17. R. E. Curtis and W. F. Spurr, *ASM Transactions Quarterly*, Vol. 61, No. 1, 1968, p. 115

18. D. A. Meyn, "Effect of Crack Tip Stress Intensity on the Mechanism of Stress-Corrosion Cracking of Titanium-6Al-4V in Methanol," *Corrosion Science*, 7, 1967, p. 721

19. T. R. Beck, *Stress Corrosion Cracking of Titanium Alloys*, NAS 7-489, Progress Report No. 3, The Boeing Company Scientific Research Laboratory, March 1967

20. T. R. Beck and M. J. Blackburn, *Stress Corrosion Cracking of Titanium Alloys*, Progress Report No. 4, The Boeing Company Scientific Research Laboratory, June 1967

21. M. J. Blackburn and J. C. Williams (accepted for publication by ASM)

22. A. P. Young, R. I. Jaffee, and C. M. Schwartz, *Acta Met.*, 1963, 11, p. 1097

23. G. Sanderson, D. T. Powell, and J. C. Scully, "Fundamental Aspects of Stress-Corrosion Cracking," Paper presented at Columbus, Ohio, September 1967 (to be published in Proceedings of Conference)

24. A. N. Stroh, *Advances in Physics*, 1957, 6, p. 418

B. STEEL

B.1 INTRODUCTION

The organization of material in this section reflects the revised procedure of maintaining a primary division by alloys and a secondary division by disciplines. Organization of contributions from the various disciplines represented in this program by this procedure would permit ready access to all available information on a single alloy system. The primary sections are designated as:

B.2 Commercial Alloys: Alloys that are of current DoD interest and that are produced commercially.

B.3 Simplified Experimental Project Alloys: Alloys that are specifically prepared to represent basic composition of commercial alloys for study by most of the disciplines involved.

B.4 Simplified Research Alloys: Usually pure iron, or one of principal alloying elements (such as nickel), or simple binary alloys (such as Fe-C, Fe-Cr, etc.) used for metallurgical investigations and surface studies pertaining to stress-corrosion cracking.

These sections are subdivided into sub-sections entitled Characterization Studies, Test Techniques, Physical Metallurgy, and Surface Studies. Further sub-division by alloy systems (such as, Stainless and Precipitation-Hardening Steels, Maraging Steels, and Martensitic Steels) and by individual alloys (such as 17-4PH Stainless Steel, 18Ni(250) Maraging Steel, AISI 4340 Steel) are made when appropriate.

A number of alloys have been procured and designated as "project alloys". These alloys are available for distribution to the Coupling Program partners; in this way relevant information will be generated on a single source material. The current "project alloys" are as follows:

Commercial Alloys:
17-4PH Stainless Steel

18Ni(200) Maraging Steel
18Ni(250) Maraging Steel
AISI 4340 Steel
Simplified Experimental Alloys:
Fe-C-X Alloys

B.2 COMMERCIAL ALLOYS

B.2.1 Characterization Studies
B.2.1a Stainless and Precipitation-Hardening Steels
B.2.1b&c Maraging and Martensitic Steels

The Boeing Company

The stress-corrosion-cracking (SCC) characteristics of steel forgings of selected composition have been studied at the Materials Research Laboratory. This program was coordinated by Boeing under sponsorship by ARPA Order 878. The materials studied were 18Ni(250) Maraging, silicon-modified AISI 4340, and 9Ni-4Co-0.45C steel. Heat treatments and mechanical properties are given in Table B-1.

TABLE B-1

Heat Treatment and Mechanical Properties of Three Steels

Material	Heat Treatment	0.2% Offset Yield Strength, (ksi)	Tensile Strength (ksi)	Elongation in 1 in. (%)
18Ni(250) Maraging Steel	1600°F/1hr air cooled; 900°F/3hrs.	245.6	255.1	7
AISI 4340 M Steel	1550°F/1hr; quench in oil at 150°F; 550°/2hrs.	232.5	280.6	11
9Ni-4Co-0.45C steel	1550°F/1hr; air cooled, 1475°F/1hr; quench in salt at 460°F and held for 6 hrs air cooled	200.1	290.0	10

Tapered double-cantilever-beam (DCB) specimens (constant K specimens) were used for the SCC studies. Tests were performed by dead-weight loading these specimens in 3.5% NaCl solution and measuring the crack growth-rates at

several constant K-levels. Test results are given in Figures B-1 to B-3. The set of data points on the left-hand side of each graph correspond to K-levels at which "no crack growth"occurred (i.e. da/dt was less than about 10^{-2} microinch per second). An estimate of K_{Iscc} may be made from these data points.

B.2.2 Test Techniques

The Boeing Company

The stress-corrosion-cracking characteristics of steel forgings of selected composition have been studied at Materials Research Laboratory using the double cantilever beam (DCB) test. This program was coordinated by Boeing under sponsorship by ARPA Order 878. The materials studied were 18Ni(250) Maraging, silicon-modified AISI 4340, and 9Ni-4Co-0.45C steels. The heat treatment conditions and mechanical properties of these steels are shown in Table B-1. Tapered DCB specimens were prepared with the angle of taper being such that the stress intensity factor, K, remained constant as the crack length, a, increased.

Tests were performed by dead weight loading these specimens in 3.5% NaCl solution and measuring crack growth rates at several constant K-levels. K_{Iscc} was then estimated by extrapolating the rates to zero. Crack growth rates were monitored by a linear differential transformer extensometer calibrated to automatically register crack length on a constant speed recorder. Specimens were side grooved to radii of 0.125 in. in an attempt to restrict crack propagation to a plane normal to the direction of applied load. In spite of the side grooves, the stress corrosion cracks tended to propagate out of plane causing arms to break off the specimens in all the materials tested. Prior to this, however, sufficient data was generated to accurately characterize the crack growth rate as a function of K for each material. These are presented in Figures B-1 through B-3. The form of these curves can be used to explain the crack branching phenomenon. Each curve contains a portion over which crack growth rate appears to be independent of K. For the 4340M steel, this occurred at a rate of 30 microinches per second; for the 9Ni-4Co-0.45C steel, it was 15 microinches per second; and for the 18Ni(250) Maraging steel, it was 0.5 microinches per second. When a crack tended to branch at these "plateau" speeds, the lower K-value at the branch tip did not result in a lower growth rate and therefore the main crack did not outdistance the branch. In this circumstance and in this type of specimen the branch soon becomes unstable and the arm breaks off.

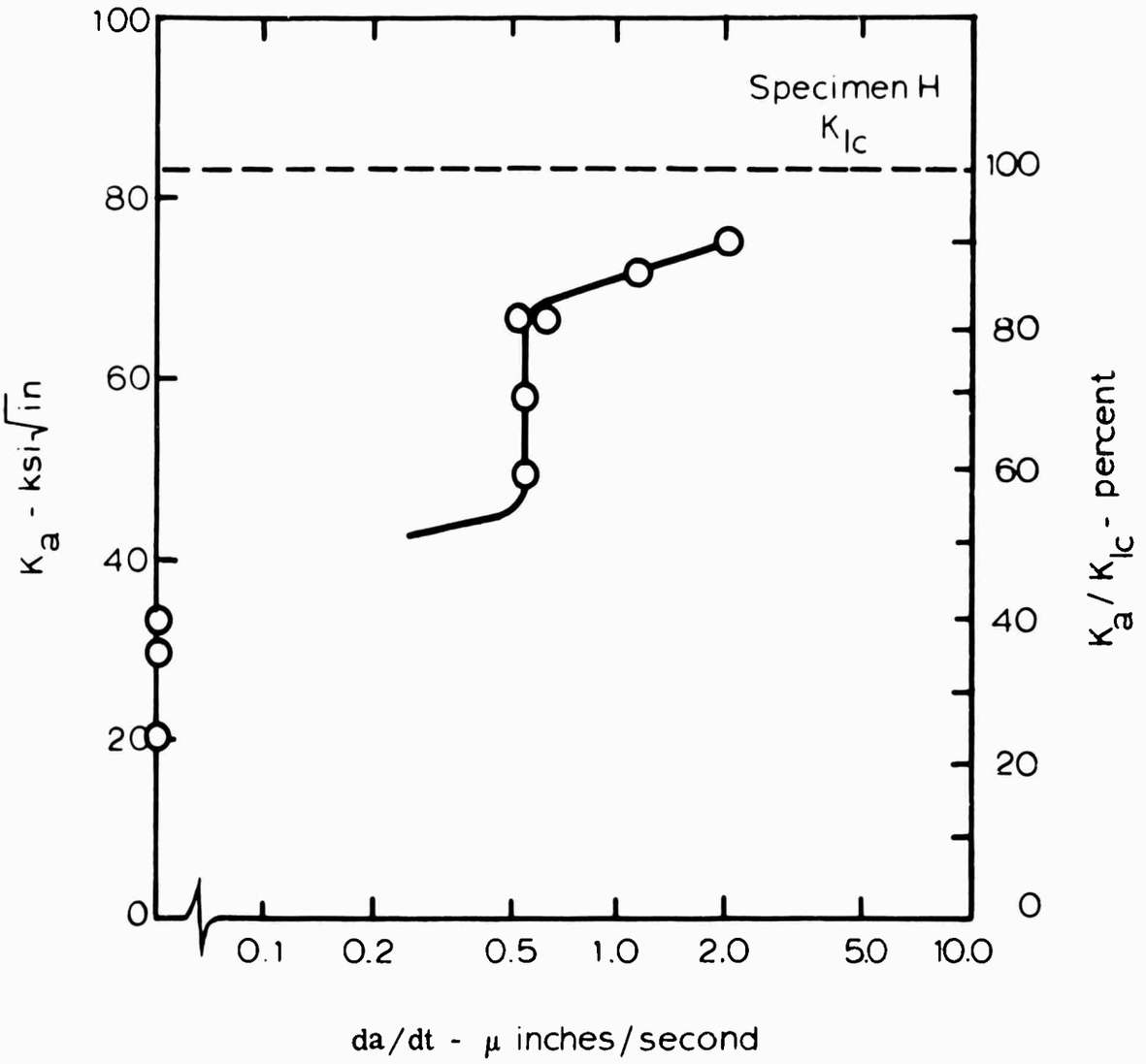

Fig. B-1 - Crack Growth Rate, da/dt, versus Applied Stress Intensity Factor K_a, and Ratio of K_a to K_{Ic} for 18Ni(250) Maraging Steel; Fully Heat Treated. Specimen Immersed in a 3-1/2% NaCl Solution at Room Temperature. Specimen with 25 percent Total Face Grooves (1/8 inch Cylindrical Grooves).

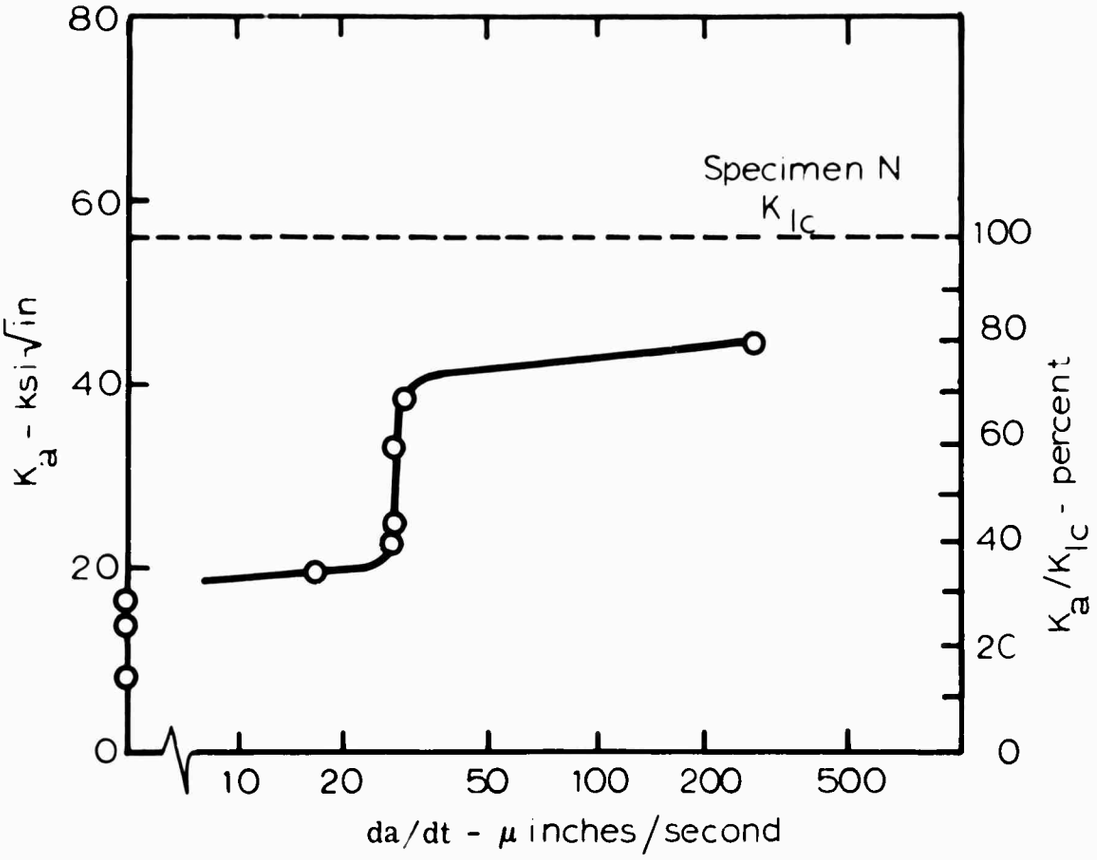

Fig. B-2 - Crack Growth Rate, da/dt, versus Applied Stress Intensity Factor, K_a, and Ratio of K_a to K_{Ic} for AISI 4340 M Steel, Tempered for 2 hours at 550°F. Specimen Immersed in a 3-1/2% NaC1 Solution at Room Temperature. Specimen with 50 percent Total Face Grooves (1/8 inch Cylindrical Grooves).

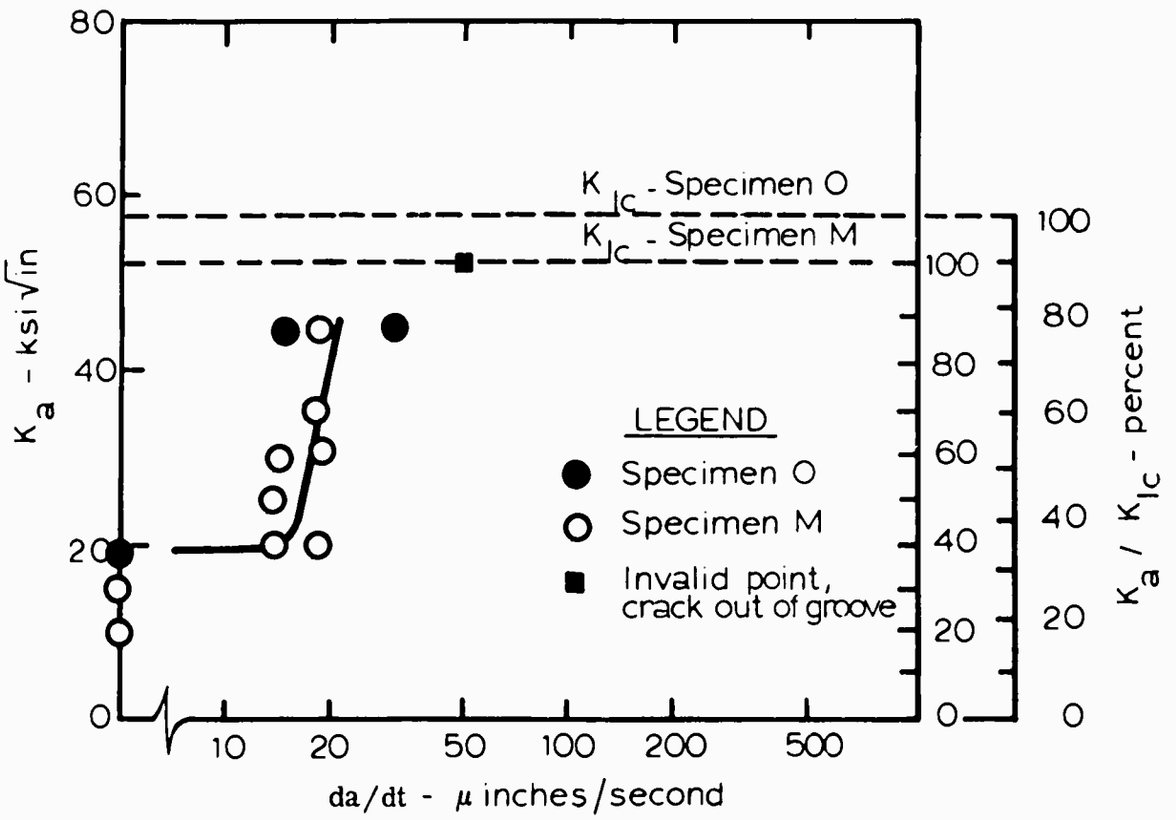

Fig. B-3 - Crack Growth Rate, da/dt, versus Applied Stress Intensity Factor, K_a, and Ratio of K_a to K_{Ic} for 9Ni-4Co-45C Steel. Specimen immersed in a 3-1/2% NaCl Solution at Room Temperature. Specimen M with 25 percent and Specimen O with 50 percent Total Face Grooves (1/8 inch Cylindrical Grooves).

This specimen and technique appear to be well suited for experiments involving the determination of the effect of variables (e.g., pH, environment, alloy composition, heat treatment) on stress-corrosion-crack growth-rate because the K-factor remains constant as the crack grows. However, as used in this program, it appears to be inefficient and too costly to be used in large scale determinations of the simple K_{Iscc} property.

A variation in technique can be employed so that the DCB specimen may be used to advantage in finding K_{Iscc} values for steels. A specimen can be loaded to a level between K_{Ic} and K_{Iscc} and the deflection at this level can be kept constant. When the crack extends due to stress corrosion, the load and related K-value decrease. The crack growth should arrest when K_{Iscc} is reached. The fixed deflection can be obtained by means of a screw threaded through one arm and bearing against the other. Because this technique requires a decreasing K versus crack length relationship, there is obviously no need to taper the specimen. If the technique is successful, K_{Iscc} may be determined several times on one specimen provided the crack stays in plane. The only serious drawback to the technique is the long times involved in obtaining crack growth arrest in materials where the rate is extremely slow as well as being nearly independent of K (see Figure B-1 for the da/dt versus K, for the 18Ni(250) Maraging steel).

B.2.3 Physical Metallurgy

B.2.3a Stainless and Precipitation-Hardening Steels.

B.2.3b Maraging Steels

18Ni Maraging Steels

Carnegie-Mellon University

A detailed investigation of the kinetics of aging (i.e. precipitation and reversion) in the 18 Ni maraging steels is being undertaken to study the reversion mechanism and the effect of overaging on the mechanical properties of 18Ni maraging steels. The primary experimental technique being employed in this project is the continuous monitoring of electrical resistivity at the aging temperature; this permits isothermal resistivity curves to be compiled for different aging temperatures. Such plots are significantly different from the corresponding curves obtained from room-temperature resistivity measurements; these latter

show only a single inflection during reversion while the present work indicates that multiple inflection points occur during overaging. Data from tensile and Charpy tests indicate that severe overaging may result in a decrease in yield strength of the order of only about 5% while the corresponding Charpy values may increase by as much as 50%. Two models have been proposed for the multiple stage reversion or overaging process; current and future work is aimed at deciding if either of these models is correct. This work will involve further electrical resistivity measurements, transmission electron microscopy. yield strength and fracture toughness measurements on specimens in selected over-aged conditions, hot hardness measurements and measurement of activation energies.

12 Ni Maraging Steels

Carnegie-Mellon University

An electron microscopic investigation of stress-corrosion in maraging steels is being conducted. The base material being used in this project is commercial 12 Ni-5Cr-3Mo (180 grade) maraging steel in the form of 1-inch-thick plate. The objective is to undertake a detailed electron microscopic study (using both transmission and extraction replica techniques) of the microstructure of this alloy after different heat treatments. Attempts will then be made to correlate such microstructural differences as are observed with differences in stress-corrosion susceptibility after similar heat-treatments. A jet-polishing technique has been developed to prepare thin foils of the 12Ni maraging steel for transmission electron microscopy; these are now being used in preliminary studies of the effect of various heat-treatments on the microstructure. The stress-corrosion behavior of these steels will be studied using self-stressed, plane-strain, double-cantilever-beam specimens, with an environment of 3.5% Na Cl; either fatigue or pop-in will be used to obtain a pre-crack. This phase of the work will be underway in the near future.

Naval Research Laboratory

The crystallography of fracture is being studied at the Naval Research Laboratory. A specimen of 12Ni-5Cr-3Mo maraging steel of 178 ksi yield strength was cracked as a cantilever bar in 3 1/2 percent salt solution. The part of the fracture surface arising from stress-corrosion cracking had a thin dark coating on it typical of maraging steels. This part of the fracture surface, when examined

in the scanning electron microprobe, was found to have been created mainly by intergranular separation. The remainder of the fracture surface was made up of dimples and other evidence of mechanical fracture. A systematic analysis of the film showed only that the oxygen content in it was higher than on the part of the fracture surface made up of dimples. No other element was found to be enriched in the stress-corrosion cracking area. The elements investigated were B, C, N, O, Mo, Al, Si, P, S, Ni, Cr, and Mo.

Georgia Institute of Technology

A high strength maraging stainless steel, Almar 362 has been the subject of a thorough study under environment-stress conditions. Typical analysis of this steel is C-0.035%, Cr-14.09%, Ni-6.70%, Ti-1.14%, Mn-0.24%, P-0.016%, S-0.004%, Si-0.10%. Table B-2 gives the mechanical test data for a range of heat treatments of this material.

TABLE B-2

Tensile and Yield Strengths for Almar 362 after Various Aging Treatments
(Austenitized at 1500°F)

	Unrolled		50% Reduction After Austenitizing	
Heat Treatment	Tensile Strength (ksi)	0.2% Offset Yield Strength (ksi)	Tensile Strength (ksi)	0.2% Offset Yield Strength (ksi)
Aged 8 hrs. at 900°F	188	182	240	228
Aged 4 hrs. at 950°F	177	172	234	215
Aged 3 hrs. at 1000°F	165	160	228	200
Aged 2 hrs. at 1050°F	152	144	220	180
Aged 1 hr. at 1150°F	140	115	182	144

Material aged at the high temperatures was found to be less susceptible to stress-corrosion cracking based on time to failure data, as compared with material aged at the lowest aging temperature. Almar 362 had very good resistance to cracking when aged at about 1150°F.

When the Almar 362 was austenitized, cold rolled and then directly aged, a significant increase in tensile strength, up to 240 ksi after an eight hour age at 900°F, was achieved. However, this was accompanied by the highest susceptibility for hydrogen embrittlement cracking. There were numerous indications that this susceptibility diminished with decreasing strength.

Potential-time curves have shown that when stress cracking occurred in a chloride solution containing acetic acid or SeO_2, an impressed anodic current of a few mA markedly increased the life of the material, whereas an impressed cathodic current decreased the time to failure. Therefore, there is strong evidence supporting the conclusion that in such media the steel fails by hydrogen embrittlement cracking. These corrodents were also found to play an important role in reducing the notch strength of the Almar 362. Metallographic examinations and transmission electron microscopy did not show any major differences between anodic and cathodic fractures. The complete data obtained in this work will soon be available in a thesis by P. Kalafonos in the metallurgy program at the Georgia Institute of Technology.

B. 2. 3c Martensitic Steels

AISI 4340 Type Steels

Carnegie-Mellon University

The effect of prior-austenite grain size on the stress-corrosion susceptibility of AISI 4340 steel is being studied. Published data indicates that rapid, short-time, repeated austenitizing and quenching heat treatments can result in the development of prior-austenite grain-sizes as small as ASTM 14 in many steels. It has been established that the yield strength of the quenched and tempered steels bears a Hall-Petch type relationship to the prior-austenite grain size and that in some cases the plane strain fracture toughness of the steels may be improved. Thus the development of ultra-fine prior-austenite grain sizes may offer the possibility of increasing the effective yield strength of an alloy steel without the usual concomitant decrease in K_{Ic} and K_{Iscc} values. Furthermore, stress-corrosion crack propagation occurs along the prior-austenite grain boundaries in many cases and it has been suggested that this may be due to grain boundary segregation or precipitation. Decreasing the prior-austenite grain size increases the total grain boundary area and thus for a given steel results effectively in "cleaner" grain boundaries; in this case an increase in stress-corrosion resistance of the

steel could be expected. Using both conventional and non-conventional austenitizing heat treatments six alloys having prior-austenite grain sizes covering the range ASTM 6-11 have been developed; these alloys were subsequently oil-quenched and tempered 1 hr. + 1 hr. at 400°F. Hardness data indicate that the yield strength of these steels increases with decreasing prior-austenite grain-size, over the range 220-260 k. s. i. Preliminary results indicate that the prior-austenite grain size does not affect the K_{Iscc} values (all lie within the range 15-17 ksi$\sqrt{\text{in.}}$ but that decreasing the prior-austenite grain size decreases somewhat the rate of stress-corrosion crack propagation (i. e. the initial stress intensity vs. time to failure curves are shifted increasingly to the right, toward longer failure times at a given K_{Ii} value, with decreasing prior-austenite grain size). The K_{Iscc} data for these AISI 4340 steels are being generated using fatigue-precracked, plane-strain, dead-weight-loaded cantilever-beam specimens; this technique will also be used to generate valid K_{Ic} data. An environment of 3.5% NaCl, fully aerated and controlled at 40°C is being used.

Lehigh University

An investigation of the nature and origin of K_{Iscc} in steels is being undertaken using AISI 4340 steel as the model material. Mr. A Sheinker, who is affiliated with this program, is working on a related project at the Boeing Company this summer to enhance the coupling characteristics of the ARPA program.

The Boeing Company

The influence of five levels of silicon (0.09, 0.54, 1.08, 1.58, 2.15 wt. %) on the stress-corrosion resistance of a 4340 base composition alloy is being investigated. Preliminary heat treatment studies have been completed and the tempering conditions necessary to obtain yield strength levels of 245 ksi and 200 ksi selected for each alloy. The 245 ksi strength level could not be achieved with the two alloys having the lowest silicon content, and the highest strength obtainable was used. Cantilever bend tests have been conducted on specimens heat treated to the highest strength level. Sodium chloride solution (3.5% NaCl) was dripped into the precrack in these tests rather than by the usual immersion technique.

Silicon appeared to have a small effect on K_{Iscc}; this increased from approximately 13 ksi $\sqrt{\text{in.}}$ to 18 ksi $\sqrt{\text{in.}}$ as the silicon was raised from minimum to maximum content. However, there was a marked effect on crack growth rate

which was significantly reduced with increased silicon content. This has been tentatively attributed to the retardation of hydrogen diffusion by silicon which has been demonstrated by other workers.

Tests have also been conducted on a commercially prepared 300M (1.6% Si) billet and results compared with the laboratory heat of similar composition. The K_{Iscc} values were similar but the crack growth rate in the commercial steel was slower than in the laboratory heat. This has been attributed to the larger grain size of the laboratory heat.

Stress-corrosion tests are now being conducted on the alloys heat treated to the lower strength condition.

B.2.4 Surface Studies

B.2.4a Electrochemistry
Martensitic Steels - AISI 4340 Steel

Carnegie-Mellon University

Anodic polarization measurements have been made at 25°C in the usual manner (see previous Quarterly Reports in this series) using five different types of AISI 4340 steel electrodes. These types were (1) As-received, no heat treatment (2) Heat-treated and quenched, number 4340-0 (3) Heat-treated, quenched and tempered at 400, 800, and 1200°F, numbers 4340-400, 4340-800, 4340-1200 respectively. The first series of measurements were made using an Armco iron reference electrode, an electrolyte of saturated aqueous $FeCl_2$ solution, and a purified N_2 atmosphere. Current densities used ranged from 5 to 50 microamperes per sq. centimeter. The anodic polarization measurements made on this alloy are not very reproducible either in making successive measurements (24 hour or greater time intervals) on the same electrode or in setting up the experiments with different electrodes. Each individual experiment was found to obey the equation,

$$\gamma_s = \frac{AI}{1+BI}$$

In this equation, γ_s is the steady state overvoltage in millivolts corresponding to the current, I, in milliamperes. The active electrode area was kept constant at about 20 sq. centimeters in all experiments. A and B are constants.

Although from day to day the values of A and B fluctuated it was found that they were related linearly. In other words high values of A were always accompanied by high values of B. In the following table are given the equations relating A to B and an average value of -B designated as $\overline{B}$.

TABLE B-3

Anodic Polarization Data - $FeCl_2$

Alloy	A (ohms)	$\overline{B}$ (milliamps^{-1})
4340 - untreated	0.0 - 69.2B	-7.2
4340 - 0	12.0 - 32.3B	-0.07
4340 - 400	32.3 - 38.7B	-0.7
4340 - 800	13.0 - 19.8B	-0.5
4340 - 1200	38.0 - 30.2B	-1.7

It will be noted that heat treatment causes considerable change in the anodic polarization and that as the alloy is tempered at the highest temperature, 1200°F, it is starting to approach the value of γ_s for the original as-received AISI 4340 steel. In attempting to account for the lack of reproducibility of AISI 4340 steel in anodic polarization measurements it was considered possible that the anode reaction was not simply the formation of ferrous ions but in addition the formation of ions of the metallic alloying elements present in this alloy (Ni, Mo, Mn, and Cr). Accordingly electrographic tests were made on all AISI 4340 steel electrodes. In these tests the electrode is made the anode, the electrolyte is a sheet of filter paper moistened with 1 molar aqueous $CaCl_2$ solution, and the cathode is aluminum. The current density used was equal to the maximum current density employed in the polarization experiments, 50 microamperes per sq. centimeter. Electrolysis is carried out for time periods of 0.5 to 1.0 hours. Following electrolysis the cell is disassembled and the filter paper cut into strips and tested for the various metallic elements. There is no good spot test for small amounts of Mo. Tests for Ni and Mn were negative and in all cases the tests for Cr and Fe were positive. To check this result two series of tests were made. Samples of AISI 4340 steel were immersed in 1.0 molar aqueous NaCl solution and tank N_2 bubbled through the solution. Tank N_2 contains about 0.5% or less of O_2. Checks on the corrosion products showed that chromium was present. In the second test sufficient (2ml.) of an aqueous solution of $CrCl_3$ was added to the saturated $FeCl_2$ solution so that the concentration of $CrCl_3$ was 0.01 molar. The results of the anodic polarization measure-

ments are given in Table B-4. The cells were not more reproducible but A was found as before to be a linear function of B.

TABLE B-4

Anodic Polarization Data - $FeCl_2$, 0.01M$CrCl_3$

Alloy	A (ohms)	$\bar{B}$ (milliamps^{-1})
4340 - 400	15.9 - 7.3B	+0.04
4340 - 800	8.1 - 6.4B	+0.04
4340 - 1200	177.8 - 73.9B	-0.70

The presence of chromic ion has had a considerable effect on the anodic overvoltage, raising it in one case and lowering it in the other two cases. It is not certain how the chromium ion appears in solution under the oxygen free conditions of the polarization measurements. It might be formed directly by the process $Cr \rightarrow Cr^{++} + 2e$ or indirectly by the reaction $2\,Fe^{++} + Cr \rightarrow 2Fe^{+++} + Cr^{++}$ ($\Delta G°298.1 = -6.8$ k cal). It should be noted that the reduction of Cr^{+++} by Cr is spontaneous, $2\,Cr^{+++} + Cr \rightarrow 3Cr^{++}$ ($\Delta G°298.1 = -23.3$ k cal) as is the reduction of Fe^{+++} by Fe, $2Fe^{+++} + Fe \rightarrow 3Fe^{++}$ ($\Delta G°298.1 = -55.8$ k cal.) The above reactions are written for elemental chromium. However, according to Richardson's data, none of the chromium carbides are sufficiently stable to reverse the sign of $\Delta G°$. Also neglected is the formation of complexes of chromium ions with chloride ions which would make the above reactions even more spontaneous.

B.2.4b Macroscopic Surface Studies

Stainless and Precipitation-Hardening Steels

Naval Research Laboratory

Adsorbed films of carbon-14 tagged stearic acid have been deposited on highly polished surfaces of iron, nickel, and alloy steel (Types 304 and 416) by retraction from a 0.1 percent solution of stearic acid in nitro-benzene. Contact angle and radioactivity measurements indicate that the nickel and alloy steel surfaces acquire a stearic acid film equivalent to about 85 percent coverage, whereas that on Armco iron approaches 95 percent of that expected for a highly compacted monolayer.

Thermal desorption of these films at temperature ranging from 80 to 110° C indicated that about 25-30 percent of a stearic acid monolayer is strongly (chemically) adsorbed on iron and Type 416 steel (12-14% Cr), but only 13-18 percent is strongly bonded to nickel or Type 304 stainless steel (18 Cr, 8Ni). It is felt that this difference is significant. However, the data were insufficient to permit any estimate of the bonding energies to be made.

Since a generally linear relationship between contact angle (methylene iodine) and surface coverage (as determined from radioactivity measurement) has been found, it was possible to compare the surface roughness of the polished metal samples with that of fire-polished glass reference surfaces. Surfaces of all four metals after machine lapping and polishing showed a roughness factor of about 1.07 relative to the glass reference. This compares with earlier studies on iron in which a hand polish gave roughness factors of about 1.38.

To learn more about the nature of the reactive sites on the metal surfaces, techniques are being developed for depositing films of octadecyl amine by the retraction technique. In spite of a variety of surface treatments, it has not been possible to date to produce highly compacted films of this material on either glass or metal surfaces. Methylene iodine contact angles of 55-60° on the metals and no more than 65° on Pyrex glass have been obtained, which suggest that the metal surface is barely half covered. A determination as to whether this behavior is due to a difference in the number of acidic and basic adsorption sites or is merely due to deficiencies in the experimental technique must await completion of desorption studies of C^{14}-tagged octadecyl amine films.

Martensitic Steels - AISI 4340 Steel

Naval Research Laboratory

One of the important areas of research effort on stress-corrosion cracking phenomena deals with the effects of oxide films; these films can be oxides grown in situ by the interaction of the metal alloy with its environment or they might be artifically applied. At any rate, evidence has accumulated in the literature supporting the hypothesis that the physical and chemical make-up of naturally occurring oxides have a bearing on the subsequent corrosion behavior of the substrate metal structure. Stainless steels derive their chemical inertness from films of magnetite (Fe_3O_4) in which cations derived from the alloy have

been substituted into the crystal lattice with resultant increase in stability through elimination of ferrous ions as part of that crystal is sharply reduced. Whether this is beneficial or detrimental remains to be determined.

The first experimental attack on the problem involved use of the Bloom hydrogen effusion technique to see whether a superior film could be generated from a caustic aqueous solution containing cobalt ions at 300° C. Specimens were removed from the apparatus at various times up to 150 days. The negative results of this experiment were attributed to deposition of cobalt metal on the oxide film after a short period of normal behavior. This metal acted as a cathodic depolarizer and served to maintain a relatively high corrosion rate. Cobalt was detected by spectrographic analysis in the outer part of the oxide film, but the innermost part was free of cobalt.

Since it appeared infeasible to try further to generate a substituted spinel by this technique, it was decided to proceed immediately with planned experiments using a substituted spinel generating procedure available in the literature to coat specimens designed to employ the cantilever beam testing technique. This would involve heating specimens at 100-125°C while submerged in oxygen-free solution of either cobalt or manganese (as sulphates) in 50 percent caustic soda. The heating temperature was not considered high enough to alter the metallurgical characteristics of the specimens.

It was proposed to use type 4340 high strength steel for a total of 18 specimens; six were to be fatigue cracked and then coated, six coated and then fatigue cracked and tested as blanks. The corrosion environment would be immersion in a 3 percent NaCl aqueous solution, air saturated, at room temperature.

The design and preparation of these specimens involved some departure from the routine of this type of test and has proven unexpectedly difficult. It was desirable to keep specimen size at a minimum. This and various other considerations involving mutual interplay of the preparation and test parameters resulted in specimens that would not demonstrate the stress-corrosion cracking phenomena unequivocally in blank tests. Thus it became necessary to re-orient the specimen preparation using a larger specimen and different metallurgical procedures.

An alternate approach to the unsucessful hydrogen effusion experiment with cobalt is available and some work has started. The steel tubing used for these experiments can be pre-coated by the same method proposed for the cantilever beam experiments. Then it can be fabricated into the usual type of capsule, but this time containing a solution appropriate for evaluation of a protective film without regard for further film growth. The problem here will be to work out a method of removal of the oxide at the end areas required for spot welding. A manganese-doped film has been prepared and its electrical conductivity is apparently low enough to prevent spot welding without its prior removal. An alternative to stripping the oxide for spot welding might be to torch weld, but this will be avoided if possible.

Some work has been conducted on effects of the chloride ion during corrosion of steel exposed to aqueous systems. A mechanism has been developed postulating a catalytic effect that tends to throw iron into solution to an extent that, although magnetite is eventually formed, it is non-adherent. Acid conditions are required for the mechanism, but the point is made that even in the presence of an alkaline solution, it may be possible to generate acidic conditions under a partially formed film or deep within a stress-corrosion crack.

B.3 SIMPLIFIED EXPERIMENTAL PROJECT ALLOYS

Naval Research Laboratory

A series of ternary alloys designated Fe-C-X have been made by vacuum-induction melting and deoxidizing with carbon. "X" represents Mn, Cr, Ni, and Mo. The macroscopic stress-corrosion characteristics will be determined and compared with the structure and substructure.

The precipitation-hardening steel designated 13-8 Mo has outstanding stress-corrosion resistance in neutral 3½% NaCl solution at yield strength levels up to about 200 ksi. If the solution becomes strongly acid, as at a site undergoing crevice corrosion, the resistance to stress-corrosion cracking plummets. It was found by direct methods that this decrease in stress-corrosion resistance requires that the pH be less than 2.

A modified method has been developed for automatically arresting a stress-corrosion crack in a cantilever-loaded specimen. This equipment consists of

a container of water which is the stressing medium, a dial gage which senses motion of the stressing arm, and microswitches which continue to pump water out of the system incrementally until no more motion is detected.

The macroscopic stress-corrosion characteristics of a large number of commercial and near-commercial steels have been determined in seawater and in salt water. This work has essentially completed the phase of surveying the characteristics of existing commercial high strength steels at NRL. A topical summary is in preparation. Future work on steels at NRL will concentrate on the research steels (Fe-C-X alloys) and on selected emerging developmental steels.

The freeze method of retaining the corrodent in place in the stress-corrosion crack, originally developed using aluminum alloys, will be applied in order to learn more of the electro-chemistry of the cracking process.

B.4 SIMPLIFIED RESEARCH ALLOYS

B.4.1 Characterization Studies

B.4.2 Test Techniques

B.4.3 Physical Metallurgy

Carnegie-Mellon University

At temperature below about 250° C, the activation energy for diffusion of hydrogen in iron increases by a factor of 2 to 3; this increase has been attributed to "trapping" of hydrogen atoms. In an attempt to identify the nature of these trapping-sites, the activation energy will be accurately measured and the effects of cold work and carbon content on the diffusion coefficient and the activation energy determined. Hydrogen is introduced into one side of the thin disc specimen by controlled under-water abrasion; the hydrogen diffusing through the specimen into the high vacuum (10^{-8} torr) at the other side is measured with a mass-spectrometer (see previous Quarterly Reports in this series for details of materials and apparatus). After a considerable number of experimental difficulties the apparatus is now working very satisfactorily; to date, however, only pure iron in the full-annealed condition has been in-

vestigated. The diffusion coefficient for H in this material in the range 10-100°C was found to be given by $D=2.3 \times 10^{-3}$ exp (-3, 100/RT) while the corresponding permeability is given by $P=7.2 \times 10^{-2}$ exp (-13,000/RT). It was observed that the degree of abrasion and the hydrogen ion concentration of the environment did not affect D although both increased the effective hydrogen concentration at the entry surface.

B. 4. 4 Surface Studies

B. 4. 4a Electrochemistry

Naval Research Laboratory

During this year, the elaborate high-purity experimental procedures which were set up for the electrochemical studies of the behavior of iron in alkaline solutions were in good working order. This permitted .. number of definitive polarization studies of the iron/alkaline system. Studies of the Pt electrode were carried out simultaneously so that comparison with this much better understood system could be made. The data obtained showed that the electrochemical behavior of pure iron under the rigorously controlled conditions used is entirely different from that recorded in the literature. The iron electrode behaved as an inert electrode material very similar to Pt. Significant corrosion was not found. Upon the addition of impurities to the system, results in accord with literature findings were obtained.

The results clearly showed that the electrochemical behavior of iron was strongly dependent on impurities in the environment. Meaningful studies of such electrochemical systems do demand rigorously controlled environments so that the contribution of each of the various components in a total system can be understood.

The potentiostatic polarization studies are being supplemented with transient pulse techniques in order to determine the surface species on iron and other electrodes in alkaline solutions. In addition, these transient methods should yield kinetic parameters so that both reaction mechanisms and kinetics can be determined. Effects of sorbed species and oxide layers on the electrode material, both on passivation and on reaction rates are to be investigated.

B. 4. 4b Macroscopic Surface Studies

Lehigh University

The stresses in ultrathin, ultraclean evaporated nickel films have been studied as a function of the environment. Films were formed by evaporation on very thin glass slides under conditions where the residual gas pressure was less than 5×10^{-10} torr. Film thickness ranged from 50 to 250 Å and evaporation rates of 2-20 Å /minute were utilized.

Films as prepared were under compressive stresses of $5\text{-}10 \times 10^{10}$ dyne/cm.^{2}, which is near the yield point of nickel. The stresses were estimated from ferromagnetic resonance studies carried out with the sample under vacuum. The changes in the stresses were determined as small amounts of foreign gases were added.

Admission of pure hydrogen, oxygen, water, carbon monoxide, and nitrous oxide caused the disappearance of the intrinsic stresses. The effect took place at measurable rates in the 10^{-7} torr range. Admission of pure nitrogen to pressures as high as atmospheric had no effect on the intrinsic stress, in conformity with the view that nitrogen does not interact with a clean nickel surface.

Deposition of the films on slides maintained at temperatures up to 335°C resulted in a smaller residual compressive stress. Admission of oxygen resulted in a decrease in the stress.

The experimental observations are in sharp contrast to observations reported in the literature. No effect of gases on stresses has previously been reported. Observations of compressive stresses in evaporated films is also rare; tensile stresses are generally detected. The major difference between the present work and the work reported in the literature is the ultrahigh vacuum utilized in the present work. Most of the reports in the literature are on systems maintained at 10^{-7} torr, where reactive gases are present in the system during evaporation.

Studies of adsorption on clean ferromagnetic metals is being carried out. The purpose of these studies is to improve our knowledge of the interaction of compounds with a clean metal surface since stress-corrosion cracking leads to the formation of fresh metallic surfaces.

Work on (100) and (110) single crystals of nickel has been completed and the research is being written up for publication. Research has begun on (100), (110), and (111) single crystals of iron.

Nickel single crystals, exposing surface areas of the order of 2 sq. cm., were cleaned under ultrahigh vacuum conditions by alternate electron bombardment and argon ion bombardment. Residual gas pressures of the order of 10^{-10} torr were obtained. Adsorption of $C^{14}O$ at 10^{-8} torr occurs rapidly at all temperatures from -100° to room temperature. This rapid adsorption is excellent proof that the surface is clean. At all temperatures, the carbon monoxide is adsorbed to the equivalent of a monolayer. If the surface is contaminated in various ways, the amount of $C^{14}O$ which is adsorbed is directly related to the amount of clean surface available. $C^{14}O$ did not adsorb on surfaces contaminated by prior exposure to water vapor or oxygen.

Exchange between adsorbed $C^{14}O$ and non-radioactive $C^{12}O$ in the gas phase occurs rapidly above 0° and very slowly below 0°. The kinetics of this reaction are now being analyzed.

Section C ALUMINUM ALLOYS

1. INTRODUCTION

The work on aluminum alloys is divided into two main parts; one concerned with commercial alloys and the other with simplified research alloys. In each case the major effort is concentrated on alloys of the 7075 and 2024 type which thus provide a common project series for investigation. Hopefully, the work on commercial alloys will provide better understanding of the influence of process variables and the effect of hitherto untried environments on stress-corrosion cracking. In addition, new and improved techniques for the rapid evaluation of the stress-corrosion performance of an alloy are being investigated. Perhaps the most significant progress in this direction is the development at N. R. L. of a self stressed double cantilever beam specimen. Not only does this specimen have the advantage of freedom of cumbersome stressing apparatus, a luxury previously confined to U-bend type devices, but it also incorporates a well defined stress state and thus has all the advantages of conventional precracked specimens. The reports from Boeing and N. R. L., contained in the following pages, illustrate some of the ways in which this type of specimen may become a powerful tool in the study of stress-corrosion cracking.

The work on the simplified research alloys is most advanced at Carnegie-Mellon but both Boeing and N. R. L. are moving into this area. This work is aimed at providing a greater understanding of the mechanisms which control stress-corrosion cracking, a desirable prerequisite to the development of new and improved alloys. The basic philosophy behind this research is to test specimens with well defined microstructures while keeping all other parameters constant and in this way attempt to isolate those structural features which are important in controlling the susceptibility to stress-corrosion cracking.

2. COMMERCIAL ALLOYS

(1) Characterization and Testing Techniques

A self-stressed double-cantilever beam specimen which is currently being developed and used at the Naval Research Laboratory to evaluate stress-corrosion cracking characteristics of high strength commercial aluminum alloys is shown in Figure (C1). The load is applied by means of a set screw located in one leg of the specimen. The specimens are 3-1/2 in. long and 1 in. wide and generally are cut from one-inch plate material. Stress intensity levels, for particular crack opening displacements (δ) at the point of load application, can be obtained from previously measured compliance determinations. The load screw is electrically insulated from the corrodent by a coating of paraffin and the entire specimen immersed in 3-1/2 percent NaCl solution or other environments. The crack length as a function of time can be determined by measurements usually made daily with a traveling microscope. Since this is a constant displacement test, at least for short crack lengths, the stress intensity will decrease as the crack grows.

The results for two alloys - 7075-T6 and 7079-T651 - are shown in Figure (C2). Crack growth rate (da/dt) is plotted on a log scale against K level. The figure shows the great difference between growth rates for the two alloys and also shows the difference in K_{Iscc} level.

It has been observed that for long deep cracks, approximately 2-1/2 in., the stress intensity values increase for increasing crack length. Such results complicate the analysis, and this tendency is currently being analyzed.

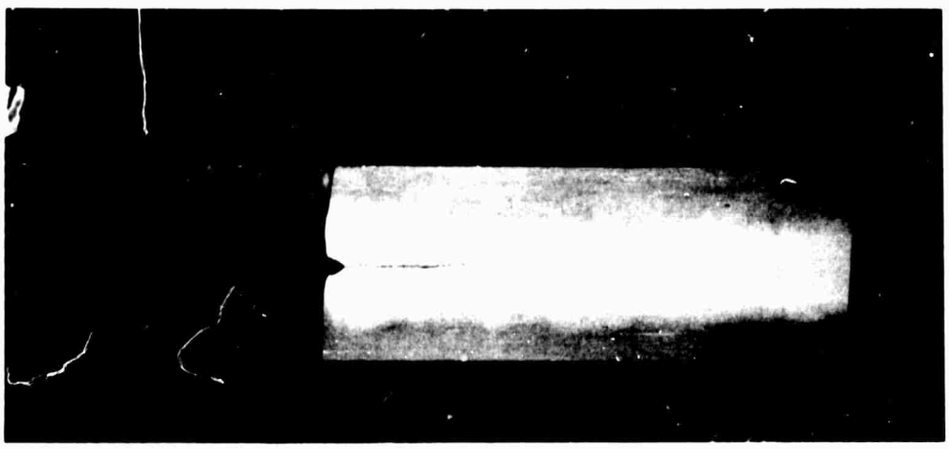

Fig. C-1 - Self-stressed uniform double-cantilever beam specimen with stress-corrosion crack. Dark region at left is paraffin used to insulate the loading screw from the crack area.

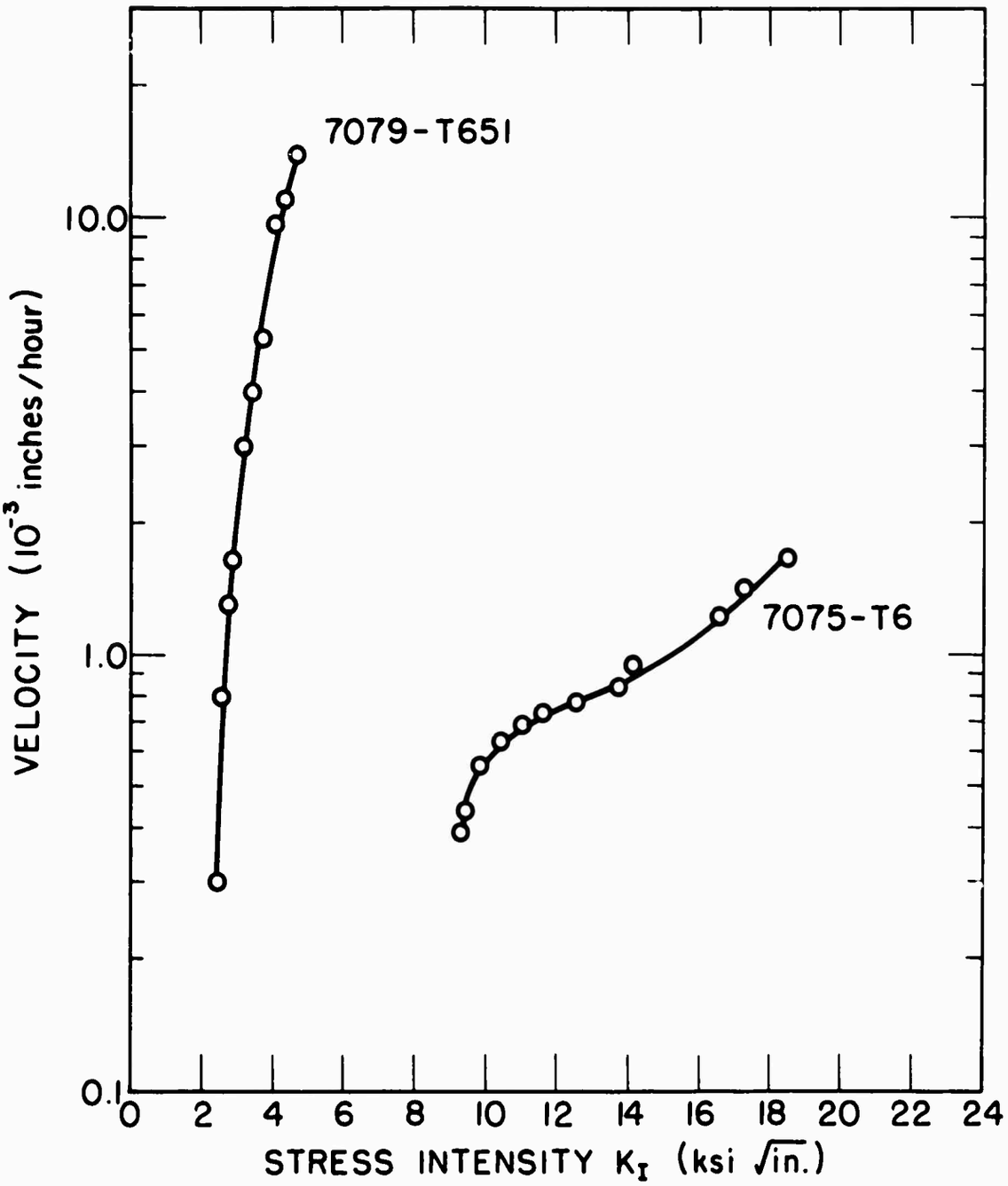

Fig. C-2 - Crack growth rate data for two aluminum alloys as a function of stress intensity level (K) tested in 3.5% NaC1 solution

Of critical importance in understanding the nature of stress-corrosion cracking in any alloy system is the characterization of the local environment in the region of the growing crack tip. The application of Pourbaix diagrams (1) to problems of stress-corrosion cracking requires understanding of the electrochemical potential and the pH condition at the advancing crack tip. The problem of characterizing the potential and pH at an advancing crack tip is very difficult. The region of interest is small and is embedded deep in the interior of a test sample. The self-stressed double-cantilever beam specimen is particularly well suited for use in developing techniques for measuring pH and potential at a crack tip because the specimen is small, portable, and can be handled without the restriction of a tensile machine. A technique for measuring the pH at a growing crack tip, using this specimen, has been developed as follows: A double-cantilever beam specimen of 7079-T6 aluminum alloy was precracked, loaded to an initial stress intensity of 14 ksi$\sqrt{\text{in.}}$ and placed in a 3.5% NaCl solution for 3 hours. During this time the crack grew 0.36 in. The final stress intensity was 7.4 ksi$\sqrt{\text{in.}}$ In a glove box in an atmosphere of dry nitrogen the sample was removed from the salt water solution and placed partly submerged in a Dewar flask of liquid nitrogen. The solution in the stress-corrosion crack was quickly frozen. The sample was removed from the liquid nitrogen, broken open, and the pH of the layer of frozen solution measured at various distances from the crack tip.

Two methods were used to measure the pH of the frozen solution, both involving pH indicator paper. The first method was to chip small pieces of ice from the fracture surface and allow them to melt on the indicator paper. The second was to place strips of indicator paper on the frozen solution in lines parallel to the crack front. After a short time, the solution melted on the fracture face and was absorbed into the indicator paper.

The results of these measurements showed that the pH of the solution within the propagating crack varied from 6.5 of the initial salt water solution to 3.5 at the tip of the crack along the fracture centerline.

Similar tests are presently being conducted on high purity Al-Zn-Mg, Al-Zn and Al-Cu alloys supplied by Carnegie-Mellon University.

(Naval Research Laboratory)

Self stressed double-cantilever beam specimens are being used also at Boeing to determine the dependence of stress-corrosion crack growth rate on stress intensity (K) for several commercial and experimental alloys. Specimens (1 in. by 1 in. by 5 in. and 1 in. by 0.25 in. by 5 in.) from 1 in. and 0.25 in. thick plate are being used. These are slotted to a depth of 0.6 in. with the slot in the rolling plane of the material. They are then loaded to a constant deflection using a 0.25 in. diameter bolt to push against one face of the slot causing the crack to propagate in the short transverse or TR direction. The 1 in. thick specimens are loaded initially until "pop-in" occurs, thus allowing K_{Ic} to be calculated and causing a sharp crack to be present at the start of stress-corrosion testing. The 0.25 in. thick specimens are not loaded to "pop-in" since plastic bending of the arms occurs before "pop-in" in these thin specimens. A fatigue precrack at the tip of the notch in these specimens or a lower toughness in the short transverse direction would eliminate this problem.

An equation relating stress intensity (K) and crack length (a) was obtained using beam theory and the equation for the crack extension force G. An empirical correction factor was introduced into the compliance (reciprocal stiffness) equation to account for the deflection due to rotations at the assumed "built-in" end of the beam. Using this specimen and constant deflection loading, K decreases as crack length increases.

Three times each day (except on weekends) several drops of 3.5% NaCl solution are applied to the crack tip of each specimen. Thus, no attempt was made to control pH and values of pH as high as 9.5 have been measured at the crack tip area of some specimens by noting color changes in a mixture of Agar, water, and Gramercy Universal Indicator applied to the sides of the DCB specimens. It should be emphasized that these readings were made in the bulk solution adjacent to the specimen at the crack tip and are not necessarily in conflict with the observation of N.R.L. that the pH in the center of the specimen at the crack tip may be in the range 3-4. In fact subsequent similar experiments at Boeing have confirmed the N.R.L. result.

Stress intensity versus crack growth rate data for the specimens tested are shown in Figures (C3-C6). Alloy composition and heat treatment of the alloys being tested are also indicated in these figures. 7079-T651 shows the fastest growth rates of any alloy tested to date. When 7079-T651 is first placed in test, audible "Pops" are heard periodically during the rapid growth period when K is still high (slightly below K_{Ic}), indicating a discontinuous crack growth.

Some specimens seem to show a growth period where rate is independent of K. However, it is possible that a particular combination of decreasing K and increasing pH is leading to this situation.

One specimen of 7075-T651 was immersed in a solution of 1% NaCl-2%$K_2Cr_2O_7$ (pH = 4) after a previous exposure to the daily triple wetting cycle with 3.5% NaCl solution. The K-level had decreased to about 8 ksi$\sqrt{in}$. when the specimen was placed in the NaCl-$K_2Cr_2O_7$ solution. As shown in Figure C4, the growth rate in this solution increased about a factor of two. Hopefully, a solution of this type will eventually allow more rapid accumulation of meaningful test data.

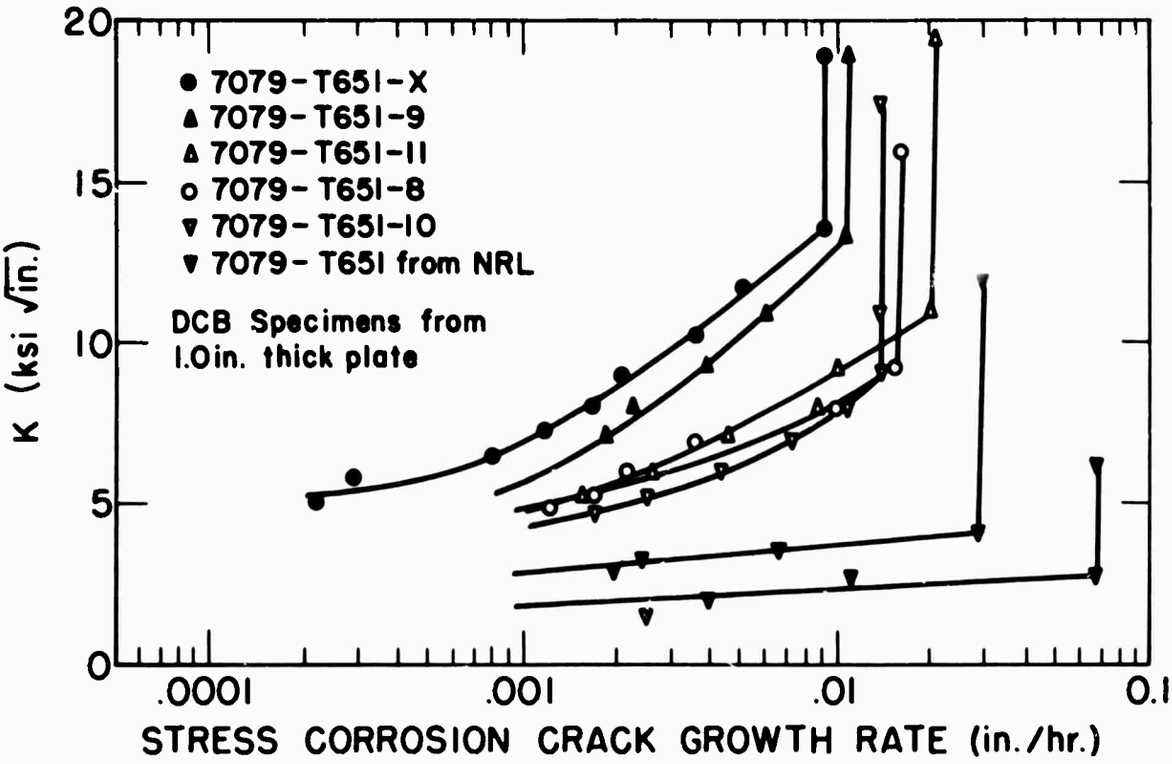

Fig. C-3 - K vs SCC Growth Rate Curves for 7079-T651 subjected to intermittent wetting in 3.5% NaCl solution, except as noted

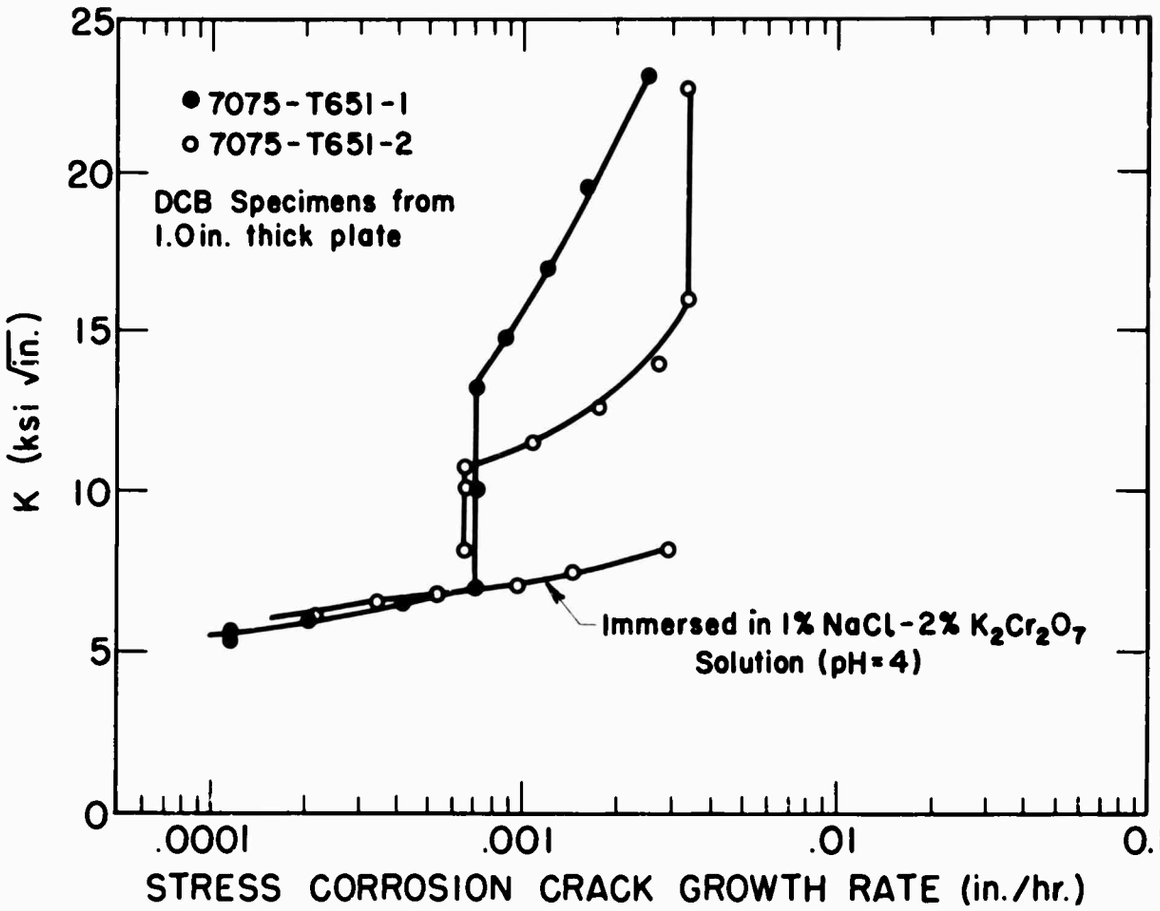

Fig. C-4 - K vs SCC Growth Rate Curves for 7075-T651 subjected to intermittent wetting in 3.5% NaCl solution, except as noted

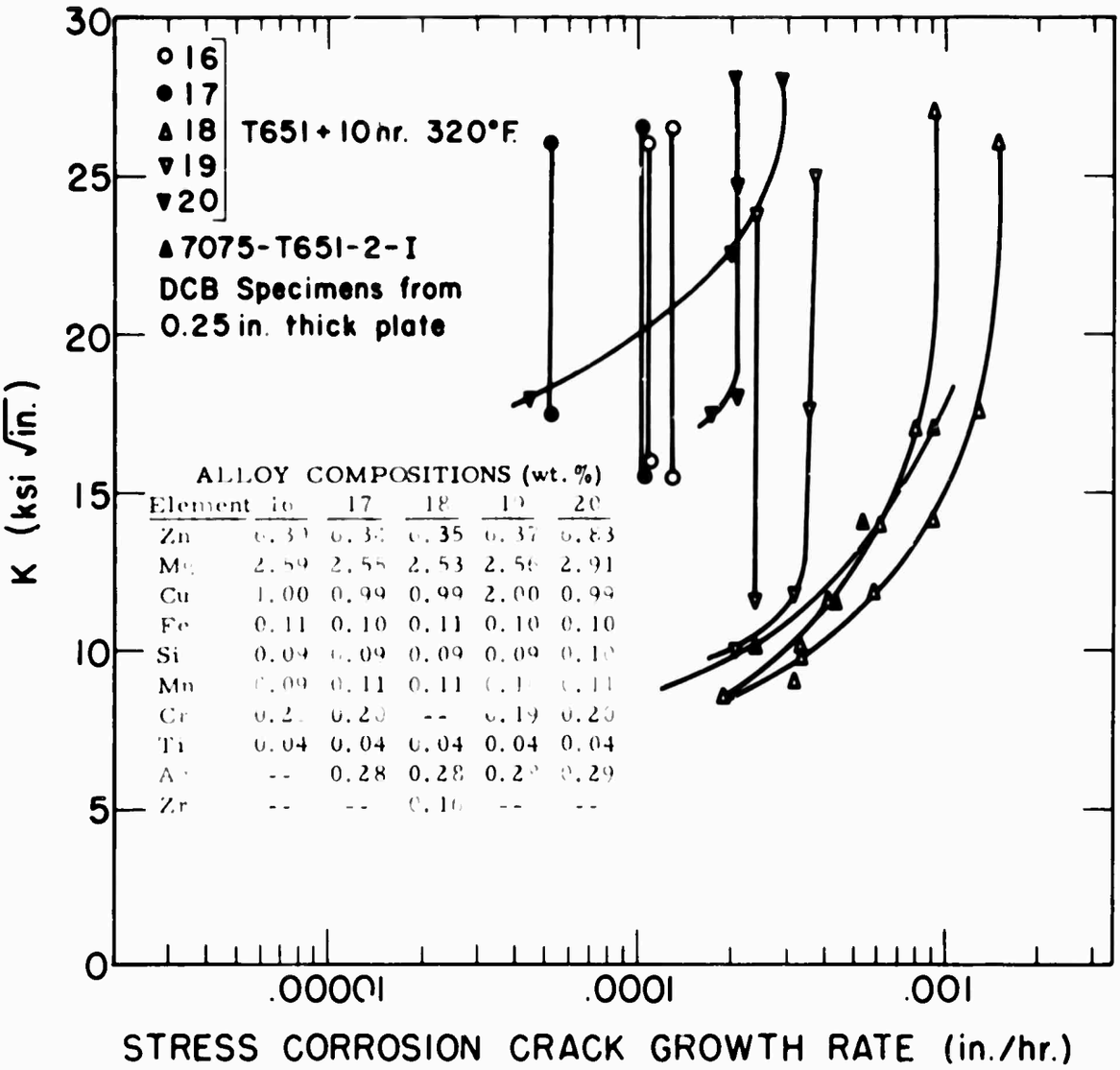

Fig. C-5 - K vs SCC Growth Rate Curves for 7075-T651 and Experimental 7000 Series Alloys subjected to intermittent wetting in 5% NaCl solution

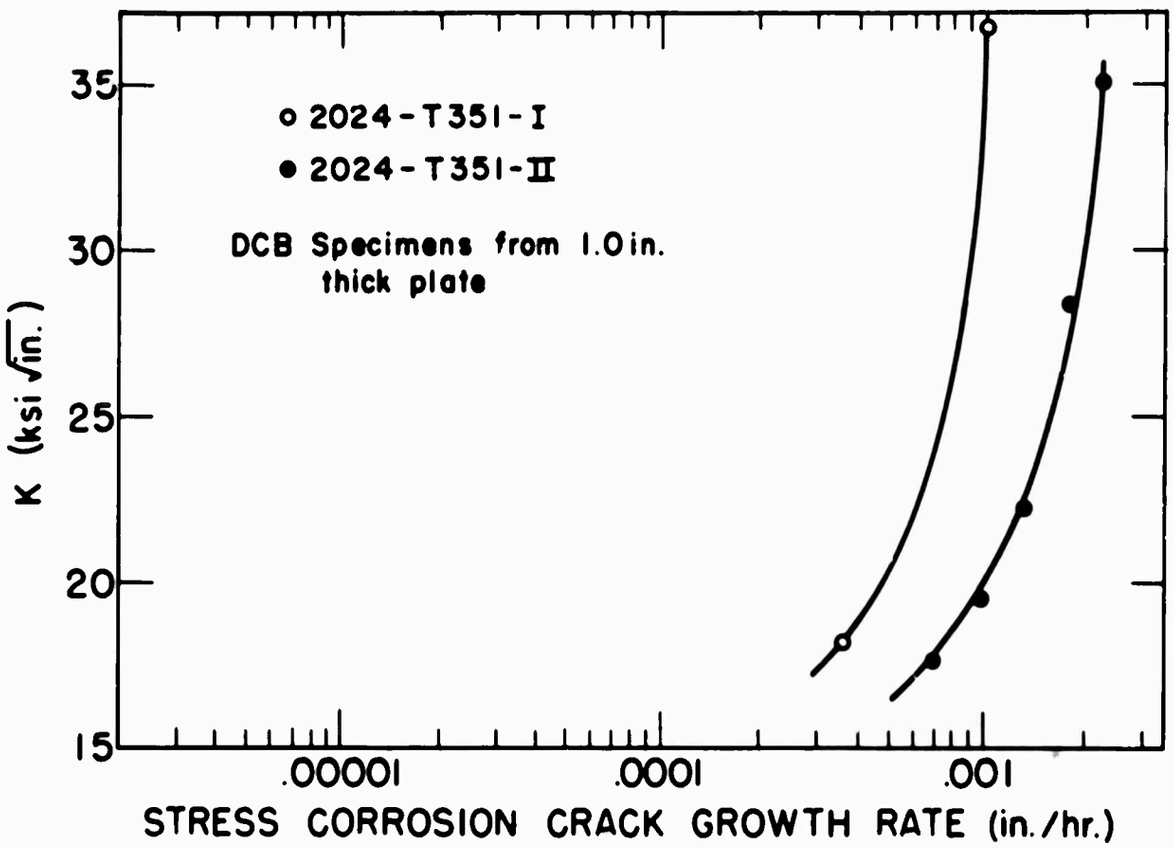

Fig. C-6 - K vs SCC Growth Rate Curves for 2024-T351 subjected to intermittent wetting in 3.5% NaC1 solution

In addition to obtaining K-rate data, several DCB specimens of 7075-T651 are being used to determine the minimum degree of overaging required to provide complete resistance to crack growth. This is being done in two ways: first, a 1 in. by 1 in. by 5 in. specimen of 7075-T651 was overaged various amounts along its length by heating one end in a Bunsen flame while the other end was being cooled with running water. Temperature readings on the specimen ranged from about 375°F at the hot end to 135°F at the cold end. After 16 hours of such treatment, a hardness survey was made along the length of the specimen. Rockwell B hardness ranged in a smooth manner from 91 at the cooled end to about 50 at the heated end. A 4 in. long DCB specimen was then cut from the 5 in. long sample in the hardness range of interest. This specimen is being bolt loaded to "pop-in", wet with 3.5% NaCl three times a day until growth of about 0.2 in. occurs, loaded to "pop-in" again and wet three times a day until another 0.2 in. of growth occurs. This process has been repeated four times to date and the crack now appears to be slowing down appreciably. The hardness, electrical conductivity, and temperature during heat treatment at the place where the crack stops growing should give a measure of the minimum amount of overaging required to provide immunity to stress-corrosion cracking. It should also be possible to determine the minimum amount of overaging required to provide any given rate of stress-corrosion crack growth rate.

The second method being used is to heat treat individual DCB specimens of 7075-T6 for various times (10, 15, 20, 30, 40 hours) at 320°F. These specimens are then loaded to "pop-in" as before and wet three times a day with 3.5% NaCl solution. These specimens will also allow determination of the minimum amount of overaging required to provide immunity to stress-corrosion cracking. In addition, it will be interesting to compare the K-rate curves for those specimens where growth does occur.

Another technique used in an attempt to obtain K-rate and K_{Iscc} data was to test a 7075-T6 forging parting plane (short transverse direction) which had been electron beam welded into a center cracked panel configuration equipped for wedge force loading. The entire specimen was reheat treated to the T6 condition to remove residual stresses from the welding operation. When the specimen was loaded in 3.5% NaCl solution, crack growth arrest was anticipated when the K-level decreased to about 7 ksi $\sqrt{in}$.. However, the crack continued to grow at lower K-levels and, in fact, grew a considerable distance ($\approx$1 in.) in the complete absence of load. This behavior probably resulted from the fact that during quenching after solution heat treatment the edges of the panel cool more quickly since three cooling surfaces are exposed. This can leave the entire thickness around the edges of the panel in residual compression whereas only the surfaces are in residual compression on the remainder of the panel. This residual compression around the edges of the panel (window-frame effect) means there is a residual tensile stress around the inside of the compression area. This tensile stress added to the regular residual stress pattern on the remainder of the panel is probably what caused the crack growth on the unloaded panel. This effect indicates the importance of residual stresses in trying to evaluate crack growth rate data at supposedly "known" K-levels. Testing specimens from stretcher straightened plate (TX51) will remove the residual stress pattern from quenching but if any re-heat treatment is necessary or if different specimen geometries are quenched or different quench rates on the same geometry used, then the residual stress patterns will be different and the test results will be affected.

(The Boeing Company)

(2) Physical Metallurgy

Stress-corrosion cracking of titanium alloys in a variety of non-aqueous environments is well established and in some cases is a severe practical problem; these phenomena are being actively studied by a number of groups. It has also been reported in the literature that some high-strength steels are susceptible to stress-corrosion in organic environments. However, no information was available on the behavior of high-strength aluminum alloys when stressed in non-aqueous liquids. This project was designed to investigate whether stress-corrosion occurs under these circumstances and to give a preliminary insight into the phenomenology and mechanism of any such stress-corrosion. The alloy 7075-T651 was chosen as a typical, moderately susceptible high strength aluminum alloy. Initially longitudinal plane-strain cantilever-beam specimens containing an RW-type fatigue-precrack were tested; these specimens were exposed to fresh reagent methanol, ethanol, ethylene glycol and isopropanol. In all cases the precrack propagated a short distance transgranularly as an RW-type crack and then spread laterally as intergranular WR-type cracks. These experiments were carried out at a stress intensity of 60-90% K_{Ic}. Exposure of unstressed specimens to the same environments produced no crack blunting or propagation whatsoever and it was concluded from these results that some stress-corrosion phenomena was occurring. The lateral spreading of the cracks is accompanied by a decrease in stress-intensity at the crack tip; this latter soon falls below the relevant K_{Iscc} so only limited spreading occurs before a stable situation is reached (in about 4000 minutes). Secondly, long-transverse, plane-strain, double-cantilever-beam specimens containing a WR-type fatigue-precrack were investigated; in both cases dead-weight loading was used. The latter specimens were exposed to the above reagents and in addition to acetone, heptane, carbon tetrachloride and benzene. In all cases intergranular stress-corrosion crack propagation occurred although there were wide variations in the rates of propagation. However, even

the growth rates in ethanol and carbon tetrachloride, which were the most rapid and were consequently chosen for a more detailed investigation, were considerably slower than the growth rates commonly observed in 3.5% aq. NaCl. There is evidence that the crack growth is not due to traces of water in the environments or adsorbed on the oxide film at the fatigue-precrack tip:

(a) One of the most aggressive environments, CCl_4, has a maximum water solubility of 0.0078 w/w% at 15°C.

(b) There was no significant difference in the crack growth rates observed in benzene saturated with water (0.051 w/w% at 15°C) and benzene dried with sodium.

(c) When stressed in laboratory air, cracks propagated at a negligibly slow rate (as measured by the loading arm deflection): addition of a liquid environment caused an immediate significant increase in crack growth rate.

U-bend specimens of the sheet material failed within 20-30 days (depending on surface preparation) when exposed to 3.5% NaCl solution containing 3.5% tetrasodium ethylene-diamine - tetracetate; similar specimens exposed to C_2H_5OH and CCl_4 have not failed after approximately 5 months. Thus, there is preliminary evidence that the stress-corrosion cracks will not initiate on smooth specimens. Using the DCB specimens curves of crack growth rate against applied plane-strain stress-intensity were generated for both CCl_4 and C_2H_5OH. This was done by fatiguing a specimen, allowing a stress-corrosion crack to propagate a short distance (≃1/100 in. - 1/10 in.) over which range K_I is essentially constant, for a measured time, then refatiguing the specimen and repeating the procedure at a different K_I value. On completion of the test, the specimen was broken open and a series of crack growth rates and corresponding K_I values calculated. In the case of both environments it was found that the crack growth rate increased more or less linearly with applied stress intensity; for example, for C_2H_5OH, the growth rate varied from 0-7μ in./min. when K_I

varied from 8-16 ksi $\sqrt{in.}$. Extrapolating these experimental curves back to zero growth rate gives an estimate of K_{Iscc}; for C_2H_5OH this was placed at 8-10 ksi $\sqrt{in.}$ while the preliminary estimate for $C Cl_4$ is 10-12 ksi $\sqrt{in.}$. Excellent fractographs have been obtained from the fracture surfaces and a detailed fractographic analysis of these is currently being undertaken. The results will be correlated with the results of a transmission electron microscopy characterization of the alloys which has already been carried out. Qualitative microanalyses of the C_2H_5OH and $C Cl_4$ environments after stress corrosion had occurred revealed traces of Al in both; this Al was not present in the original solvents and was not present in solvents exposed to unstressed specimens of the alloy for a period of 2 months. Furthermore, the $C Cl_4$ was discolored slightly (yellowish) and the stress-corrosion fracture surfaces were blackened slightly in $C Cl_4$ These observations are in agreement with the published data on the chemical reaction between pure Al and boiling $C Cl_4$, which was shown to be electrochemical in nature and may be represented as: $Al + C Cl_4 \rightarrow Al Cl_3$ (complexed) + C_2Cl_6 + 2 unidentified high molecular weight polymers (responsible for the discoloration and the surface blackening). This reaction is reported not to occur at room temperature in unstressed specimens. The fact that $Al Cl_3$ is complexed accounts for the fact that no Cl^- ions were detected in the $C Cl_4$.

(Carnegie-Mellon University)

(3) Corrosion Fatigue

Initial tests of fatigue crack propagation rates for 7075-T6 aluminum alloy in the TR fracture orientation(parallel to the rolling direction and in the rolling plane) in air and NaCl solution using the double-cantilever beam specimen have been carried out. The results from these initial tests are

shown in Figure (C7). All the data represent growth rates measured from the same specimen at frequencies which varied between 1 and 5 cycles per second. The amount of scatter is believed to have resulted from two sources: first, some alignment and gripping problems were encountered in this initial test, and second, the testing sequence often involved testing at a high K level followed by testing at a low K level. These difficulties are being corrected in future tests. The data show significant increases in growth rate for salt water tests for all levels of stress intensity.

(Naval Research Laboratory)

Corrosion Fatigue of commercial alloys continued on page 94.

3. SIMPLIFIED RESEARCH ALLOYS

(1) Physical Metallurgy

The role of microstructure in controlling the susceptibility of aluminum alloys to stress-corrosion cracking has been the subject of wide controversy. At the center of this controversy is the actual role played by the precipitate free zones(P. F. Z.s) which occur adjacent to the grain boundaries. Several authors (2, 3, 4,) have expounded the view that such P. F. Z. s have a deleterious effect on stress-corrosion cracking while others (5, 6) consider these regions to play no part in the phenomenon.

The first objective of this investigation was to elucidate the effect of the P. F. Z. on the mechanical properties and the susceptibility to stress-corrosion cracking by varying the width of such zones by suitable heat treatments. The alloy being studied is high purity Al-6. 8% Zn-2. 3% Mg with a probable G. P. zone solvus temperature of $170 \pm 5^{\circ}C$ (7).

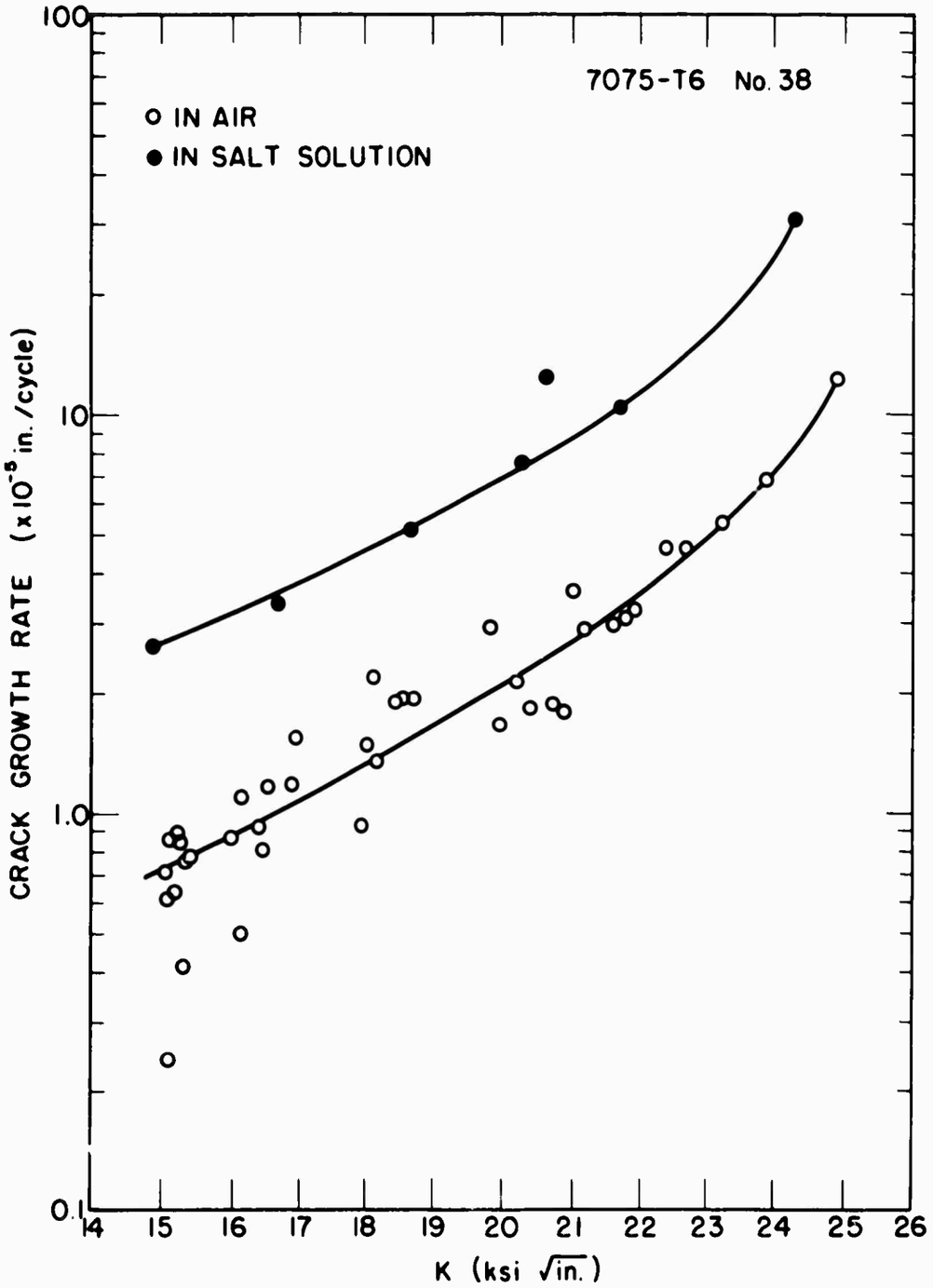

Fig. C-7 - Crack growth rate data for 7075-T6 aluminum alloy fatigue cracked in air and salt water at 1-5 cycles per second

Aging temperatures of 180°C and 130°C have been chosen for this investigation so that the response to aging above and below the G. P. solvus on the stress-corrosion resistance could be evaluated. For both aging temperatures an attempt was made to vary the P. F. Z width by employing the following heat treatments with different sets of specimens:

Solution Anneal for 1 Hour at 465°C

Oil Quench to Room Temperature

Age at 180° or 130°C (P. F. Z. s characteristic of the aging temperature) (Type 1 specimens)

Age for 1 Hour at 100°C

Age at 180°C or 130°C (P. F. Z. s narrower than type 1 specimens due to growth of G. P. zones at 100°C within the vacancy depleted region) (Type 2 specimens)

Specimens given these two treatments and aged at 130°C (below the G. P. zone solvus) showed almost identical aging responses as determined by standard room temperature tensile tests. At maximum yield strength both types of specimen were extremely brittle showing little or no elongation beyond the elastic limit. The tensile strengths agreed well with values determined by Varley et al. (8) and in all cases fracture was intergranular. Stress-corrosion tests were performed on types 1 and 2 specimens aged to give the same yield strength. These tests were performed on smooth specimens loaded to 70% of the 0.2% proof stress with aerated 3.5% NaCl at 30°C used as the environment. In the underaged condition both types of specimen were extremely susceptible to stress-corrosion cracking since the mean time to failure was 17 minutes. However, unstressed specimens which had been exposed to the salt solution for the same time showed no degradation of mechanical properties. Transmission electron microscopy has not been performed on these specimens as yet but thin foils of the overaged structures have been prepared

and examined. These foils revealed no P. F. Z. in either type of specimen except that due to solute denudation near the grain boundary precipitates.

Aging at 180°C (above the G. P. zone solvus) caused greater differences between specimens given the two types of treatment. Type 2 specimens showed improved tensile strength but lower ductility at all times, except in the overaged condition. At maximum strength type 1 specimens showed 2% elongation while type 2 showed essentially no elongation beyond the elastic limit. However, the microstructures, Figures C8 and C9 , obtained from these treatments in the underaged condition, although showing a narrower P. F. Z. with the type 2 treatment also showed that this treatment resulted in a much finer dispersion of η particles within the grain interiors. Since it is desirable, when comparing the effect of different P. F. Z. widths on the stress-corrosion susceptibility, that all other features of the microstructure be as constant as possible, a further heat treatment was adapted. This consisted of:

Solution Anneal for 1 Hour at 465°C

↓

Oil Quench to Room Temperature

↓

An Age at 180°C for 20 Minutes

↓

An Age at 100°C for 1 Hour

↓

A Reage at 180°C

(Type 3 specimens)

Fig. C-8 - Type 1 specimen underaged.
×60,000 0.2% Proof Stress = 40,000 p.s.i.

Fig. C-9 - Type 2 specimen underaged.
× 100,000 0.2% Proof Stress = 40,000 p.s.i.

In this treatment, the 20 minute anneal at 180°C established a P. F. Z. width and an η' distribution within the grain interiors characteristic of type 1 specimens. The treatment at 100°C then allowed G. P. zone formation within the original P. F. Z. which on reaging at 180°C caused formation of η' particles thus narrowing the P. F. Z. The resultant microstructure in the underaged condition is shown in Figure (C10) from which it can be seen that the η' distribution within the grain interiors is very close to that of type 1 specimens. In the overaged condition, the microstructures obtained from all three treatments were very similar. Figure (C11) is typical of the structures obtained showing a very coarse η and η' dispersion; the only difference with previous treatment was the width of the P.F. Z.s noted in table C1.

Stress-corrosion tests were conducted on specimens subjected to all three treatments in the underaged and in the overaged conditions; all specimens were aged to give the same 0.2% Proof Stress. The results of these tests are shown in table C1:

Table C1

Specimen	Time to Failure (mins. *)	P. F. Z. Width	Precipitate Distribution in Grain Interior
Type 1 (underaged)	561 ± 50	0.5μ	Coarse
Type 2 (underaged)	48 ± 10	0.06μ	Fine
Type 3 (underaged)	490 ± 50	0.1μ	Coarse
Type 1 (overaged)	2470 ± 200	0.5μ	Very coarse
Type 2 (overaged)	2440 ± 200	0.06μ	Very coarse
Type 3 (overaged)	2100 ± 200	0.1μ	Very coarse

* Each time an average of 6 determinations

Fig. C-10 - Type 3 specimen underaged.
× 80,000 0.2% Proof Stress = 40,000 p.s.i.

Fig. C-11 - Type 1 specimen underaged.
× 60,000 0.2% Proof Stress = 40,000 p.s.i.

Again unstressed specimens exposed to the salt solution for the same times showed no degradation in their mechanical properties.

From these results it is tentatively concluded that the P. F. Z. plays only a minor role in determining the stress-corrosion susceptibility of this alloy and that the major microstructure feature controlling the stress-corrosion behavior is the size, type and distribution of precipitates within the grain interior.

(Carnegie-Mellon University)

The correlation between microstructure and stress-corrosion behavior is being studied also with a high purity Al-15% Zn alloy. Susceptibility is measured by means of the elastic energy released during crack propagation in a double-cantilever specimen. At present, this technique is being applied to two different types of specimens: (a) polycrystals with equiaxed grains, approximately 1mm. in size, and (b) bicrystals with crack propagation confined to the grain boundary. Testing of bicrystals offers a well-defined crack path as compared to the arbitrarily orientated grains in the polycrystalline specimens. Thus, intergranular cracking in the equiaxed structure exhibits an average crack growth rate while bicrystals show a crack propagation rate characteristic of a single well-defined grain boundary with a specified misorientation. The kinetics of the crack propagation at a given stress level can be monitored by measuring load relaxation with time, as the crack advances under fixed-grip conditions. The continuous nature of this data enables one to determine discontinuous changes in velocity during crack growth quite easily.

Tentative results favor a discontinuous cracking mechanism, with points of zero velocity and with periodic increases and decreases in crack growth rate. This mechanism of cracking is also indirectly suggested by the observed topographic features of the fracture surface: light microscopy and replica techniques

indicate that the Zn-rich precipitate in this alloy borders the periphery of regions which change elevation during the crack propagation. These preliminary results tend to indicate that the density and distribution of precipitates in the grain boundaries strongly influences the crack path and the kinetics of crack propagation.

(Carnegie-Mellon University)

The work of Dix[9] has shown that the susceptibility of age-hardened Al-Cu alloys to intergranular corrosion and stress-corrosion cracking is due in part to the formation of a solute depleted zone adjacent to the grain boundaries which is anodic with respect to the grain boundary precipitates and the grain interiors. However, the active sites for cathodic reaction have not as yet been established and furthermore the exact role of stress in influencing the electrochemical processes is not known. The object of the present investigation is to clarify these areas of doubt. Since the active cathodic sites and the role of stress may well depend on the particular cathodic reaction taking place, the effect of pH on corrosion and stress-corrosion cracking is being studied initially. The effect of pH on the time to failure of samples of Al-4% Cu aged for 24 hrs. at 180°C has been investigated. U-bend samples were immersed in solutions of 3.5% NaCl whose pH had been adjusted to 0, 1, 3, 5 and 6.5 by additions of HCl. The condition of the specimen surfaces was observed by means of a low powered microscope. Some of the specimens immersed in the solution of pHl had only one grain boundary, running completely across the specimen, exposed; the grain interiors were masked by Gyptol. Decreasing the pH of the solution increased the susceptibility to stress-corrosion cracking indicating that suppression of the hydrogen reaction is responsible for the slow rate of attack in near neutral solutions. It was also noted that masking off the grain interiors decreased the rate of cracking; this would seem to indicate that the hydrogen reaction occurs both on the grain boundary precipitates and

within the grain interiors. This work is soon to be extended to different aging times at 180°C.

(Carnegie-Mellon University)

Corrosion Fatigue (Continued from page 83).

In a previous study the effect of water, dry hydrogen, and dry oxygen on the rate of fatigue-crack propagation in an aluminum-zinc-magnesium-copper type alloy (bare 7075-T651) was determined, over a range of test temperatures (approximately 25 to 100°C), to elucidate the possible mechanism for water-enhanced crack growth in high-strength aluminum alloys (10). The results of this study suggested that (a) a pressure mechanism of hydrogen embrittlement (suggested by Broom and Nicholson [11]), requiring a water-metal surface reaction, is responsible for the increase in the rate of fatigue-crack propagation by water, and (b) the rate-controlling process, for the range of growth rates from 1 to 10 micro-inch per cycle, to be the mechanical process of creating fresh crack surfaces. At higher rates of crack growth the rate-limiting process may become that of transport of environment to the crack tip, or that of diffusion of hydrogen into the crack-tip region, as suggested by Bradshaw (12) and by the results of Wiederhorn for glass (13). To verify this possibility further experiments, at room temperature, have been conducted which extend the rate of crack growth to about 100 micro-inch per cycle. In addition to dehumidified high-purity argon and distilled water, D_2O (99.98% purity) was also used. These experiments were carried out under zero-to-tension loading at 5 cycles per second, in a MTS Systems Corporation testing machine, compared to 143 cycles per second employed in the previous study. Data for the different test environments are shown in Figure C-12 along with corresponding data from the previous study (10). The results show that the the factor of ten increase in growth rate is maintained up to a growth rate of about 100 micro-inch per second, and that the effect of D_2O on this alloy

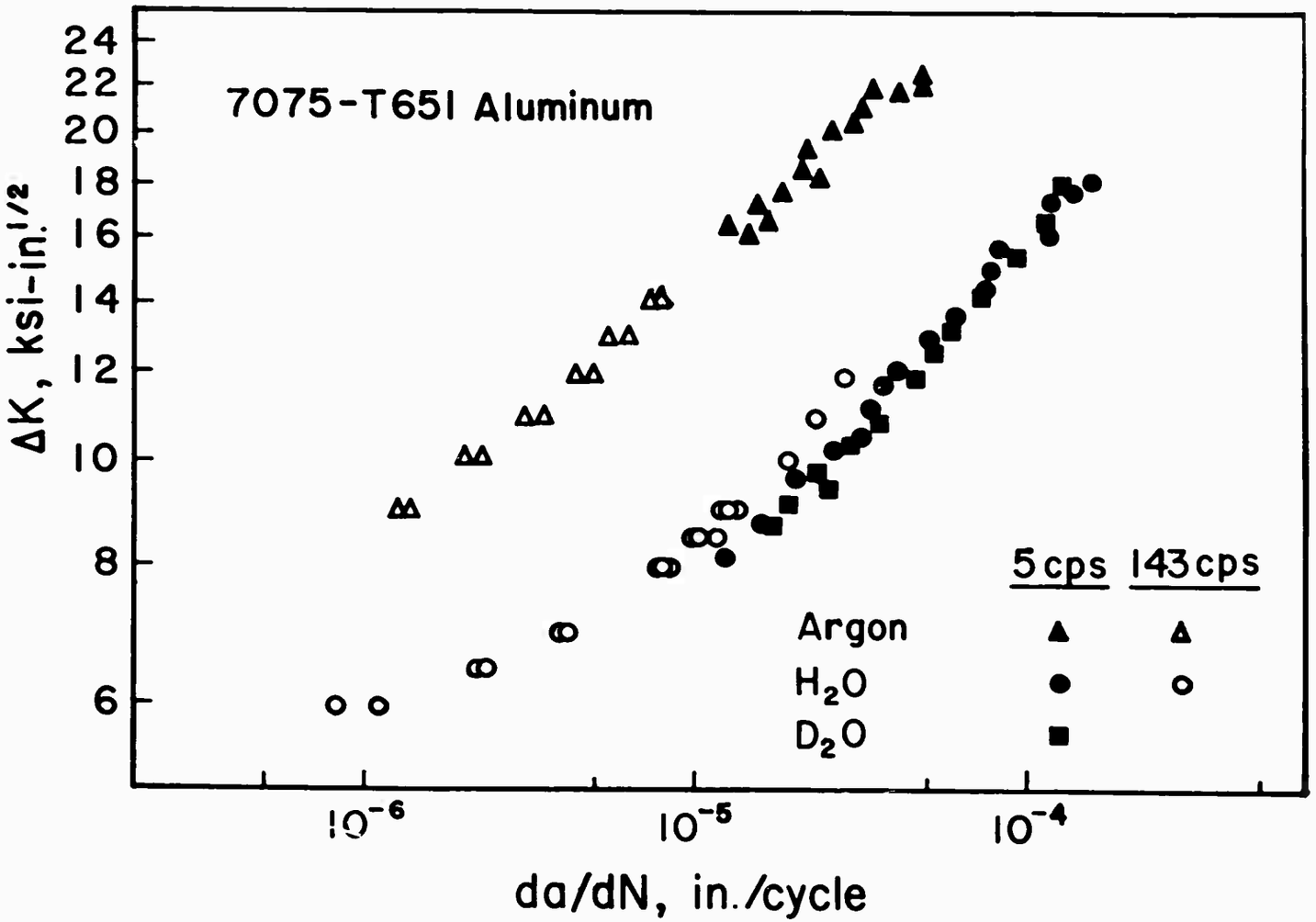

Fig. C-12 - Crack growth rate as a function of ΔK for 7050-T651 aluminum for various environments and frequencies

is essentially the same as that of distilled water. These findings suggest that environment transport and hydrogen (or deuterium) diffusion are not the rate-limiting processes, and lends further support to the previous observation that the rate-controlling process (at rates below 100 micro-inch per cycle) is the mechanical process of creating new surfaces.

The small difference between the rates of fatigue-crack growth in the water at the two cycling frequencies (5 cps and 143 cps) is attributed, principally, to "stress-corrosion cracking," i.e., environment-enhanced crack growth under sustained loads.

(Lehigh University)

REFERENCES

1. Marcel Pourbaix, "Atlas of Electrochemical Equilibrium In Aqueous Solution," Pergamon Press, CEBELCOR, 1966

2. G. Thomas, J. Nutting, J. Inst. Metals 88, 1959-60, 81

3. E. N. Pugh and W. R. D. Jones, Metallurgia, 63, 1961, 3

4. A. J. McEvily, Jr., J. B. Clark and A. P. Bond, Trans. ASM, Vol. 60, 1967

5. M. O. Speidel, Ohio State Stress-Corrosion Conference, 1967

6. H. A. Holl, Corrosion, 23, 1967, 173

7. I. J. Polmear, J. Inst. Metals, 87, 1958-60, 24

8. P. C. Varley, M. K. B. Day and A. Sandcock, J. Inst. Metals, 86, 1957, 337

9. E. H. Dix, Trans. A.S.M., 42, 1950, 1057

10. R. P. Wei, Int'l. J. Fracture Mechanics, 4, 1968

11. T. Broom and A. J. Nicholson, J. Inst. Metals, 89, 1960

12. F. J. Bradshaw, "The Effect of Gaseous Environment on Fatigue Crack Propagation," Tech. Memo. MAT 26, Royal Aircraft Establishment, Farnborough, England, March 1968

13. S. M. Wiederhorn, Int'l. J. Fracture Mechanics, 4, 1968

D. DIARY OF EVENTS

The summer quarterly ARPA program meeting, covering stress-corrosion cracking of aluminum, was held at Lehigh University on 20 June 1968. Arrangements were made by Dr. J. D. Wood of Lehigh University. Eleven persons from various industries, five from universities, and five from Government laboratories made technical presentations at the meeting. This group represents most of the research in the country on the subject of the stress-corrosion cracking of aluminum alloys.

The American Society for Testing and Materials held its fall conference in Atlanta, Georgia, 2-4 October 1968. Six technical sessions at this conference were devoted to problems of stress corrosion. ARPA personnel from each coupling institution helped with the planning and presentations for these technical sessions.

Professor M. Pourbaix conducted a lecture-discussion seminar on the subject of the Solution Chemistry of Stress-Corrosion Cracks at the Naval Research Laboratory on 20 September 1968. Over 30 people from NRL and laboratories in the Washington area attended.

UNCLASSIFIED

Security Classification

DOCUMENT CONTROL DATA - R & D

(Security classification of title, body of abstract and indexing annotation must be entered when the overall report is classified)

1. ORIGINATING ACTIVITY (Corporate author)	2a. REPORT SECURITY CLASSIFICATION
Naval Research Laboratory Washington, D.C. 20390	UNCLASSIFIED
	2b. GROUP

3. REPORT TITLE

ARPA COUPLING PROGRAM ON STRESS-CORROSION CRACKING
(Seventh Quarterly Report)

4. DESCRIPTIVE NOTES (Type of report and inclusive dates)

A progress report on the problem.

5. AUTHOR(S) (First name, middle initial, last name)

E. P. Dahlberg (General Editor)

6. REPORT DATE	7a. TOTAL NO. OF PAGES	7b. NO. OF REFS
November 1968	102	37

8a. CONTRACT OR GRANT NO	9a. ORIGINATOR'S REPORT NUMBER(S)
M04-08 b. PROJECT NO RR 007-08-44-5512 c. ARPA Order 878 d.	NRL Memorandum Report 1941
	9b. OTHER REPORT NO(S) (Any other numbers that may be assigned this report)

10. DISTRIBUTION STATEMENT

This document has been approved for public release and sale; its distribution is unlimited.

11. SUPPLEMENTARY NOTES	12. SPONSORING MILITARY ACTIVITY
	Department of the Navy (Office of Naval Research) and ARPA, Washington, D.C.

13. ABSTRACT

A progress report of the research investigations being carried out on the problem of stress-corrosion cracking of high strength materials under ARPA Order 878 is presented. Work at Carnegie-Mellon University, Lehigh University, Georgia Institute of Technology, The Boeing Company and the Naval Research Laboratory concerni g test techniques, materials characterization, physical metallurgy, surface studies, and corrosion fatigue is described. The report is divided into three main sections covering work on high strength titanium, steel, and aluminum.

DD FORM 1 NOV 65 1473 (PAGE 1)

S/N 0101-807-6801

UNCLASSIFIED

Security Classification

14 KEY WORDS	LINK A		LINK B		LINK C	
	ROLE	WT	ROLE	WT	ROLE	WT
Stress-corrosion cracking						
High strength steels						
Titanium alloys						
Aluminum alloys						
Electrochemistry						
Fracture mechanics						
Surface chemistry						